



UNIVERSITAT
POLITÈCNICA
DE VALÈNCIA



ESCUELA TÉCNICA
SUPERIOR INGENIEROS
INDUSTRIALES VALENCIA

TRABAJO FIN DE MÁSTER
TECNOLOGÍA ENERGÉTICA PARA DESARROLLO SOSTENIBLE

**“Energy assessment and optimization
of a novel dual-source heat pump
system in different climates in Europe”**

AUTOR: MILANOWSKI, MACIEJ

SUPERVISOR: DR. CAZORLA MARÍN, ANTONIO

CO-SUPERVISOR: DR. MONTAGUD MONTALVÁ, CARLA ISABEL

Curso Académico: 2020-21

07/2021

*“It is surely our responsibility to do everything within our power,
to create a planet that provides a home not just for us,
but for all life on Earth”*

David Attenborough

ABSTRACT

The following master thesis is a complementary investigation for the studies developed in the framework of the GEOTeCH project. The novelty of this master thesis lays in the individual approach for a Dual Source Heat Pump (DSHP) system simulation and assessment in three climatic conditions in Europe (cold, average, and warm climates), as the main component of the DSHP – the coaxial Borehole Heat Exchanger (BHE) – is designed independently for each representative city (Stockholm, Strasbourg, and Athens respectively). Furthermore, the source control parameters are analyzed in all locations to select the one that best enhances the system energy performance.

The master thesis has three main objectives. The first objective is to design the optimal length of the coaxial BHE for the DSHP system in Stockholm, Strasbourg, and Athens. For this purpose, the GEOTeCH Design Guide is used, and the obtained borehole sizes are verified using two different software: GLHEPro and TRNSYS. Once the BHE depth is determined for each specific case, the second objective is to assess the long-term energy performance of the DSHP during 25 years of operation. The energy assessment of the system in each city serves as a reference case for further analysis comprised of the application of the different source control strategies. Each location is characterized by a different climatology, meaning that the changes in the governing parameters of the control system might differ between the analyzed locations. Different control parameters are tested to select the one that best improves the performance of the DSHP system.

The results of the master thesis validate the use of the GEOTeCH Guidelines for the design of the BHE field. The BHE configuration selected for each city is the rectangular 2 x 2, with the total size of 170.6 m, 168 m, 131.3 m, in Stockholm, Strasbourg, and Athens, respectively. Although the yearly SPF4 values of the DSHP are fairly low ($SPF4_{STO} = 3.04$, $SPF4_{SXB} = 3.06$, $SPF4_{ATH} = 3.80$), the long-term energy assessment of the system indicates that the DSHP has the ability to maintain the efficiency during the 25 years of operation. Finally, the source control optimization method results only in small increase in efficiency of 0.11%, 0.12%, and 0.34% in Stockholm, Strasbourg, and Athens, respectively. On the other hand, using different control parameters has a stronger impact on the proportion of the use of the ground and air, which may be beneficial for reducing the BHE size, and therefore the cost of the installation.

Keywords: Ground source heat exchanger; Dual source heat pump; Energy assessment; Heating and cooling

RESUMEN

El siguiente TFM es una investigación complementaria a los estudios desarrollados en el marco del proyecto GEOTeCH. La novedad de este TFM radica en el enfoque individual para la simulación y evaluación de un sistema de bomba de calor dual (DSHP) en tres condiciones climáticas en Europa (climas frío, medio y cálido), como el componente principal del DSHP, el intercambiador enterrado coaxial (BHE), se diseña de forma independiente para cada ciudad representativa (Estocolmo, Estrasburgo y Atenas, respectivamente). Además, se analizan los parámetros de control del sistema, en todas las climatologías, para seleccionar el que optimice el rendimiento energético del sistema.

El TFM tiene tres objetivos principales. El primer objetivo es diseñar la longitud óptima del BHE coaxial para el sistema DSHP en Estocolmo, Estrasburgo y Atenas. Para ello se utiliza la Guía de Diseño GEOTeCH y se verifican los tamaños de pozo obtenidos mediante dos softwares diferentes: GLHEPro y TRNSYS. Una vez que se determina la profundidad de BHE para cada caso específico, el segundo objetivo es evaluar el desempeño energético del DSHP a lo largo de los 25 años. La evaluación energética del sistema en cada ciudad sirve como caso de referencia para un análisis más detallado de la aplicación de las diferentes estrategias de control de fuente. Cada ubicación se caracteriza por una climatología diferente, lo que significa que los cambios en los parámetros de control del sistema pueden diferir entre las ubicaciones analizadas. Deben probarse diferentes parámetros de control para seleccionar los que mejor optimicen el rendimiento del sistema DSHP.

Los resultados del TFM validan el uso de las Directrices GEOTeCH para el diseño del campo BHE. La configuración de BHE seleccionada para cada ciudad es la rectangular de 2 x 2, con un tamaño total de 170.6 m, 168 m, 131.3 m, en Estocolmo, Estrasburgo y Atenas, respectivamente. Aunque los valores anuales de SPF4 del DSHP son relativamente bajos ($SPF4_{STO} = 3.04$, $SPF4_{SXB} = 3.06$, $SPF4_{ATH} = 3.80$), la evaluación energética a largo plazo del sistema indica que el DSHP tiene la capacidad de mantener la eficiencia durante los 25 años de funcionamiento. Por último, el método de optimización del control de fuente da como resultado solo un pequeño aumento en la eficiencia del 0.11%, 0.12% y 0.34% en Estocolmo, Estrasburgo y Atenas, respectivamente. Por otro lado, el uso de diferentes parámetros de control tiene un mayor impacto en la proporción de uso del suelo y del aire, lo que puede ser beneficioso para reducir el tamaño del BHE y, por tanto, el coste de la instalación.

Palabras Clave: Intercambiador enterrado; Bomba de calor dual; Evaluación energética; Calefacción y refrigeración

CONTENTS

Abstract	iii
Resumen	v
Contents	vii
List of figures	ix
List of tables	xi
Acronyms	xiii
Chapter 1	1
1 Introduction.....	1
1.1 Motivation	1
1.2 State of the art	3
1.3 The objective of the study.....	6
1.4 Methodology	6
1.5 Structure of the study	7
Chapter 2	8
2 The plug and play DSHP system	8
2.1 Introduction.....	8
2.2 Plug and play system description	8
2.2.1 The main components of the system	9
2.2.2 The operating modes.....	11
2.2.3 The selection of the source/sink	12
2.2.4 The system efficiency	12
2.3 The system model in TRNSYS	13
Chapter 3	15
3 Thermal demand in different locations.....	15
3.1 Parameters in each location.....	15
3.1.1 Climatic conditions	15
3.1.2 The building description	16
3.1.3 Operating parameters	17
3.1.4 Thermal demands.....	18
Chapter 4	20
4 The design of the BHE field	20
4.1 Introduction.....	20
4.1.1 Methodology	20

4.2	BHE sizing with the Design Guide.....	22
4.2.1	The correction factors	23
4.2.2	The Design Guide BHE depth calculation	24
4.3	The design constraints.....	25
4.4	BHE sizing with GLHEPro	26
4.4.1	Defining the G-function parameters	27
4.4.2	Preliminary configuration analysis	29
4.4.3	Detailed configuration analysis in GLHEPro	35
4.5	BHE sizing with TRNSYS	36
4.5.1	Outlet temperature verification.....	37
4.6	Techno-economic analysis	43
Chapter 5	53
5	The energy assessment in different locations.....	53
5.1	Introduction.....	53
5.1.1	Methodology	53
5.2	The ground energy balance.....	53
5.3	The energy production analysis.....	54
5.4	The energy efficiency analysis.....	57
Chapter 6	60
6	The source control optimization	60
6.1	Introduction.....	60
6.1.1	Methodology	60
6.2	The optimization methods	61
6.2.1	Using different hysteresis bands	61
6.2.2	Testing different offsets	62
6.3	Results of the analysis	64
6.3.1	Stockholm.....	64
6.3.2	Strasbourg	65
6.3.3	Athens.....	66
6.4	Discussion of results	67
Chapter 7	69
7	Conclusions.....	69
References	72
Annexes	76
A.	Long-term energy assessment	76
A.1	Ground thermal balance and outlet temperatures.....	76
A.2	Energy production in different operating modes.....	78
A.3	The long-term SPF4 analysis.....	79

LIST OF FIGURES

Figure 2.1. Piping and instrumentation diagram of the GEOTeCH plug & play system [38].....	9
Figure 2.2. The DSHP unit developed within the GEOTeCH project [39].	10
Figure 2.3. Coaxial spiral BHE, GEOTHEX [®] ; a helical path of the fluid (left), axial view (right) [37]....	11
Figure 2.4. Selection of the source depending on the air and ground temperature [34].....	12
Figure 2.5. The main view on the system layout in TRNSYS.	13
Figure 3.2. Hourly DHW demand per one person in an office.	18
Figure 3.1. Thermal demand in kW, in Stockholm (a), Strasbourg (b), and Athens (c).....	19
Figure 4.1. Methodology for the BHE depth design.....	21
Figure 4.2. The GEOTeCH plug & play systems Design Guide consortium.....	22
Figure 4.3. The steps of the GHE design process.	23
Figure 4.4. Configurations: a) L-configuration 2 x 2; b) Rectangular 2 x 2; c) Rectangular 2 x 3; d) Line 1 x 4.	29
Figure 4.5. Steps of the process of load extraction.....	30
Figure 4.6. Heating and cooling maximum load profiles for Athens.....	30
Figure 4.7. Secondary ground loop parameters for Athens (DG depth, 2 x 2 configuration).	31
Figure 4.8. Heating and cooling day temperature response using the averaging method.....	32
Figure 4.9. Heating and cooling day temperature response using the maximum method.	32
Figure 4.10. Outlet temperatures for 2 x 2 DG depths in: (a) Stockholm, (b) Strasbourg, (c) Athens. .	39
Figure 4.11. Minimum fluid temperature evolution in Stockholm using different peak durations.....	40
Figure 4.12. Peak fluid temperature for 2 x 2 configuration in (a) Stockholm, (b) Strasbourg, (c) Athens.	42
Figure 4.13. Methodology flux for the comparative BHE depth analysis.	44
Figure 4.14. Depth-averaged drilling prices per meter for different borehole depths [55].	49
Figure 5.1. The energy produced in different operating modes (15th year of operation).	55
Figure 5.2. Percentage of energy production in each operating mode (year 15th).	56
Figure 5.3. Winter, summer, and yearly SPF4 in three analyzed cities (year 15th).	58
Figure 6.1. Deadbands used for the source control analysis: a) $\pm 1K$; b) $\pm 2K$; c) $\pm 3K$	61
Figure 6.2. Two different offsets adopted to a $\pm 2K$ deadband: a) offset -1K, b) offset 2K.	63
Figure 6.3. The sensitivity of the optimization method on the SPF4, with respect to the reference case in each city (overall sensitivity is the sum of efficiency gain and efficiency loss, both in absolute values).	67

LIST OF TABLES

Table 2.1. The DSHP system operating modes.....	12
Table 2.2. Main elements of the DSHP model developed in TRNSYS.	14
Table 3.1. Maximum, minimum, and average temperatures in Helsinki and Strasbourg [43].	16
Table 3.2. Location dependent parameters for Stockholm, Strasbourg, and Athens.....	16
Table 3.3. The building’s thermal parameters extracted from TABULA database.....	17
Table 3.4. Thermal energy demand in Stockholm, Strasbourg, and Athens.....	19
Table 4.1. Reference design (RD) for the two types of plug and play DSHP in different climates [38].	23
Table 4.2. Design correction factors for different governing parameters [38].....	24
Table 4.3. Site-specific parameters necessary for the correction factors determination.	24
Table 4.4. Selected design correction factors.	25
Table 4.5. Maximum drilling depths for different HE diameters according to drill rig capacity [38]. ..	25
Table 4.6. Reference outlet fluid temperatures [38].	26
Table 4.7. Ground loop parameters equal for every g-function.	28
Table 4.8. Design Guide depths per borehole for a field of 4 BHEs.	29
Table 4.9. Monthly loads (kWh) for the preliminary analysis.	33
Table 4.10. Peak monthly loads (kW), and peak durations (h) for the preliminary analysis.	33
Table 4.11. BHE depths corresponding to each configuration from the preliminary sizing analysis in GLHEPro.....	34
Table 4.12. Maximum and minimum outlet temperatures simulated in GLHEPro for the DG BHE depths.	35
Table 4.13. First iteration sizing results with GLHEPro.	35
Table 4.14. Total and per-borehole depth for two configurations using the Design Guide.	36
Table 4.15. Outlet fluid temperatures for 2 x 2 configurations from TRNSYS.	38
Table 4.16. Outlet fluid temperatures for 2 x 3 configurations from TRNSYS.	38
Table 4.17. Summary for the alternative BHE sizes.	43
Table 4.18. The summary of borehole depths from TRNSYS, and both iterations from GLHEPro.	43
Table 4.19. Percentage of operation of the DSHP out of the design temperature limits.....	45
Table 4.20. Data of the variable speed compressor of the DSHP unit [39].....	46
Table 4.21. The energy consumption of the HP components during 25 years of operation (in kWh). 47	
Table 4.22. Electrical energy and financial savings in reference to design guide result in 25 years.....	48
Table 4.23. Additional drilling costs related to the borehole depth increment.....	51
Table 4.24. The savings per meter generated in 25 years.	51
Table 5.1. Ground thermal balance in 15th year of the system operation.....	54
Table 5.2. Outlet ground loop temperatures in the 15th year of analysis.....	54

Table 5.3. Energy demand vs energy production (15th year of operation).....	55
Table 5.4. Percentage of ground and air used for each city (year 15).	56
Table 5.5. Useful heat and consumption of the DSHP in summer in the 15 th year (Strasbourg).....	58
Table 6.1. Efficiency gains and the rate of ground/air use for both seasons in Stockholm.	64
Table 6.2. Efficiency gains and the rate of ground/air use for both seasons in Strasbourg.	65
Table 6.3. Efficiency gains and the rate of ground/air use for both seasons in Athens.....	66
Table A. 1. Long-term outlet temperature and thermal balance results in Stockholm.	76
Table A. 2. Long-term outlet temperature and thermal balance results in Strasbourg.....	77
Table A. 3. Long-term outlet temperature and thermal balance results in Athens.....	77
Table A. 4. The energy produced (in kWh) in summer and winter modes for 3 different cities.	78
Table A. 5. SPF4 values calculated for different cities in each analyzed year.	79

ACRONYMS

Acronym	Description
ASHP	Air Source Heat Pump
B2G	Borehole-to-Ground
BHE	Borehole Heat Exchanger
BPHE	Brazed Plate Heat Exchanger
DHW	Domestic Hot Water
DG	Design Guide
DSHP	Dual Source Heat Pump
GSHE	Ground Source Heat Exchanger
GSHP	Ground Source Heat Pump
HE	Heat Exchanger
HP	Heat Pump
LSA	Line Source Approach
SPF	Seasonal Performance Factor

CHAPTER 1

1 Introduction

1.1 Motivation

According to the Intergovernmental Panel on Climate Change (IPCC), over the past 150 years, the average temperature has increased by almost 0.8°C worldwide and by around 1°C in Europe, whereas by the year 2100 global temperature could rise by a further 1.5 – 4.75°C [1]. In 2007, IPCC approved the estimate of a 2°C temperature raise threshold, above from which the risk of irreversible, catastrophic changes increases significantly [2]. Currently, many scientists claim that the approximation from 2007 was underestimated, and agree on a 1.5°C threshold which may be reached between 2030 and 2052 if the temperature continues to increase at the current rate [3]. One of the reasons for triggering such serious environmental problems is the worldwide increase in global energy consumption, primarily due to the emission of carbon dioxide and other toxic substances into the atmosphere.

In 2007, European Union (EU) responded to these alerting matters by setting three key targets for the year 2020, which were 20% greenhouse gas emissions reduction from 1990 levels, reaching 20% share of renewables in energy generation, and 20% improvement in energy efficiency [4]. The directive 2012/27/EU, adopted in 2012, enacted the 20% improvement in energy efficiency, and in 2014, this target was almost reached in the EU-27. Since then, both primary and final energy consumptions were gradually rising, until the COVID-19 crisis, which according to IEA, caused a significant 5% drop in global energy demand [5] possibly helping the EU to reach the 2020 targets. Moreover, before the Coronavirus crisis in December 2018 the Energy Efficiency Directive was amended, setting a target for 2030 of a minimum 32.5% improvement in energy efficiency compared to projections of the expected energy use in 2030 [6]. To reach the energy efficiency targets the EU determined the most relevant topics that identify the implementation areas for the energy efficiency measures, such as “Energy Efficient Buildings” or “Heating and Cooling” sector.

According to the International Energy Agency (IEA), in the global spectrum of energy consumption, about 30% corresponds to transport, roughly 29% is related to the industry, while the third great contributor is the residential sector with more than 21% of the total final energy consumption, the majority of which is associated with heating and cooling purposes [7]. In the past 20 years, such a high energy demand for buildings and the heating and cooling sector became a driving force for undertaking actions aimed at improving the functionality, durability, and quality of buildings and their thermal installations, which reflected in the appearance of EU legislation such as the Energy Performance of Buildings Directive 2010/31/EU and the Energy Efficiency Directive 2012/27/EU. These

improvements lead to many benefits, including significant financial, and energy savings. Additionally, a well-insulated building, producing low heat losses, requires a small amount of energy for heating and cooling so it will have a low environmental impact. Nowadays, buildings in many countries are insulated in accordance with standards that allow modern heating and cooling systems to provide the comfort conditions to the building while reducing the necessary power, resulting in significant energy gains compared to conventional solutions. Therefore, the first step for reducing the energy demand of a building is energy-efficient construction.

Further reduction of the energy demand may be achieved by installing efficient Heating, Ventilation, and Air Conditioning (HVAC) devices, responsible for distributing the Domestic Hot Water (DHW) and maintaining the comfort conditions inside the building, such as temperature, humidity, and airflow. According to Eurostat, in 2018, these systems accounted for 78,8% of energy consumption in European households indicating the great potential of the HVAC systems for energy reduction [8]. Moreover, heating and cooling for buildings and industry account for 50% of the EU annual energy consumption, whereas much of this supply comes from fossil fuels, causing significant greenhouse gas emissions, as the heating sector alone is responsible for about 38% of the overall EU emissions [9]. These two sectors combined correspond to 13% of oil consumption, and roughly 60% of the total EU gas consumption which equates to 68% of all gas imports [10]. In this context, the use of renewable, efficient, and contaminant-free HVAC technologies for heating and cooling purposes is not only the key to the reduction of pollutant emissions but also to decrease the dependency on fossil fuels as the primary energy source in European buildings. There is a wide variety of HVAC systems in the market among which the geothermal heat pump technology is considered the most efficient solution, as it is capable to extract and exchange heat from the ground taking advantage of a stable and relatively constant source temperature. Additionally, this geothermal-based technology requires electricity instead of conventional fuel for the operation which makes it a more environmental solution.

One of the possible solutions to fulfill the EU's climate and energy goals is to reduce the 50% share of the heating and cooling sector in EU energy consumption, and the best way to do so is to cut its use of fossil fuels. This can be achieved by developing innovative, energy-efficient, and environmental-friendly technologies for heating and cooling such as geothermal heat pumps. The main EU funding program aimed at promoting innovation in technology (among others) was Horizon 2020 with nearly €80 billion of funds between the years 2014 and 2020 available for the research and innovation projects [11]. Within the framework of the Horizon 2020 program 36 projects related to renewable energy sources and energy efficiency were co-funded [12]. By the end of 2018, €250 million of the funds has been allocated to projects related to the development of geothermal energy which allowed for launching projects such as "GEOthermal Technology for Economic Cooling and Heating" (GEOteCH), that aims to contribute to the deployment of the geothermal heat pumps in the market by reducing the investment costs [13]. One of the most efficient ways for investment cost reduction is to develop optimization and control strategies, as it may lead to significant energy, financial and environmental gains.

In this context, the following master thesis's main motivation is to contribute to the mitigation of climate change and at the same time, to develop innovative optimization methods that may lead to increasing the cost competitiveness of geothermal technologies in European countries.

1.2 State of the art

Currently, shallow geothermal applications commonly known as Ground Source Heat Pump (GSHP) systems are the most widespread geothermal heat pump technology in Europe [12]. According to European Geothermal Energy Council (EGEC) report, in 2014, the European shallow geothermal market was estimated by the capacity of at least 19,000 MW_{th} distributed over about 1.4 million GSHP installations [14]. Just a few years later, in 2019, EGEC reported that Europe reached the milestone of 2 million geothermal heat pumps installed, becoming a mainstream heating and cooling solution in some regional and national markets, primarily in countries with colder climates like Sweden, where a record number of 13 GSHPs accounts for 100 households on average [15]. The main advantage of the shallow GSHP systems is their high flexibility. They can be installed and used anywhere, regardless of geographical location or ground conditions, may be combined with many heat sources, and work in a reversible cycle, providing heat both in the summer and winter season. It is why in the past 20 years in the EU the number of shallow geothermal systems is gradually growing at an average rate of 3% and now can be found everywhere across Europe [12]. Nevertheless, it is the north and central European countries that account for most of the installed potential. In 2016, Sweden along with Germany, France, and Switzerland had the highest number of GSHP systems among all European countries, corresponding to 69% of the total installed capacity [14].

Often, to compare the feasibility of the GSHPs with other HVAC systems the conventional Air Source Heat Pump (ASHP) is used as a reference [16]-[18]. Due to the variation in external air temperature throughout the year, ASHPs are characterized by a variable energy performance which often leads to lower overall system efficiency, especially in cold climates. On the other hand, GSHPs take advantage of a more stable external heat source and thus significantly enhance the heat pump efficiency. Despite that, their application is not as widespread as the ASHPs mainly due to the high cost of the Ground Source Heat Exchanger (GSHE). GSHE, installed vertically or horizontally to exchange the heat with the soil, is the main component of a GSHP. Although the most energy-efficient GSHP configuration is achieved by coupling it with a vertical Borehole Heat Exchanger (BHE), the main drawback of BHE systems is their high investment cost compared to horizontal configurations. Avoiding the over-sizing of the BHE leads to a lower investment cost, therefore an accurate assessment of thermal loads is necessary. For this purpose, many simulation softwares are used, such as GLHEPro, EED, or TRNSYS. According to the European Technology and Innovation Platform on Renewable Heating & Cooling (RH CETIP), one of the key actions in the research and innovation on shallow geothermal energy foreseen in the new Horizon Europe program will be enhancing the use of simulation tools for optimization of the performance of geothermal systems by the integration of subsurface models into the building energy models, which may lead to a reduction in the length of the vertical heat exchanger. The detailed objectives, performance indicators, and the implementation timeline for the specified key actions can be found in the following reference [12].

The further reduction in the borehole length might be obtained by hybridizing the GSHP with an additional heat source, for instance, the air. In such a way the hybrid heat pump alternates between the air and the ground as external heat sources, potentially overcoming some of the limitations of the two most common ASHP and GSHP systems. For example, Grossi et al. concluded that a Dual Source Heat Pump (DSHP) that chooses between the air or the ground as an external heat source can work with up to 50% shorter BHE fields [19]. Furthermore, another recent study by Marinelli et al. compares the environmental impact of a DSHP air/ground system with conventional solutions, concluding, that

in humid climates, the dual-source technology is more environmentally friendly than ASHP. Moreover, in comparison with GSHP, using shorter geothermal probes for the BHE once again leads to a reduction in the environmental impact [20]. In terms of using the heat as an additional energy source for a hybrid GSHP system, another dual-thermal configuration is studied by Rayegan et al. where a BHE is coupled with a solar-assisted desiccant cooling system, and assessed in hot and humid climates [21]. In this configuration, the solar evacuated tube collectors are used to generate additional heat to store up any deficit from the geothermal heat pump. Both ground and solar systems are used for regenerating the desiccant wheel and a pre-cooling process, respectively. The authors conclude that in the simulations with the absence of the GSHE, the system cannot provide thermal comfort in extremely humid regions even with high regeneration temperatures, meanwhile for simulations with the BHE the established thermal comfort improves significantly.

Apart from coupling the GSHP system with a different external heat source, a hybrid configuration can be also achieved by using a supplementary electricity source, for example, solar photovoltaic energy. This configuration is particularly interesting from an economical perspective because the electricity necessary for running the compressor of the heat pump is supplied by means of the PV modules. Such a system is described in research work by Kaviani et al., where 3 different module types, with polycrystalline, monocrystalline, and thin-film cells are analyzed in order to determine the best system performance from the irreversibility and economic point of view [22]. Moreover, in this study, a single GSHP is compared with a hybrid PV/GSHP system, resulting in that apart from reaching lower values of the Levelized Cost of Electricity (LCOE), in the case of a DSHP, the hybrid system has a lower carbon footprint of around 30%. Another example of using solar energy for the hybrid GSHP system is the Photovoltaic/Thermal (PVT) module, which allows using waste thermal energy from photovoltaic panels as an inlet water source for the ground source heat pump system. Recent studies show that in this configuration not only the otherwise lost heat can be partially recovered, but it can be also used to cool the PV module and increase its electrical efficiency [23], [24]. Moreover, similarly to the PV/GSHP hybrid system, the authors anticipate many economic benefits, such as short Discounted Payback (DPB) period (5 – 6 years) for the most optimal configurations. A recent review of the solar-assisted heat pumps, including GSHPs, ASHPs, and others, can be found in the following reference [25]. Additionally, another review of hybrid heat pumps presents a higher variety of possibilities for the integration of the GSHP, such as cooling towers, gas boilers, biomass reactors, electric heaters, and chillers [26].

Many different factors influence the performance of the BHE in a GSHP system. A commonly known parameter for describing the efficiency of a heat pump is the Coefficient of Performance (COP), which in the case of heating mode can be described as the relation between the heat transfer in the condenser (or in the case of cooling mode as the relation between the heat transfer in the evaporator) and the total input power consumed by the device [27], and usually varies linearly with the carrying fluid outlet temperature [28]. A work by Tang et al. investigates the influence of 15 different factors (meteorological condition, hydraulic condition, the grout thermal conductivity, carrying fluid material, etc.) on the yearly average heat pump COP for the shallow BHE. The study concludes that the factor with the highest impact on the BHE performance is the meteorological condition (defined by 3 different climate conditions) where the measured COP values had up to 45.3% of difference [29]. The result of this study indicates the importance of energy assessment and optimization of GSHP systems in different climate conditions. Moreover, the economic feasibility of the GSHP systems in different

climates is also often a subject of research. For example, a work by Rivoire et al. compares the feasibility of GSHP and hybrid GSHP/gas boiler systems installed in different building types and under different climate conditions. The economic analysis results reveal that public subsidies are essential to ensure the profitability of investment, as far as the European energy prices are concerned [30]. Another result for the simulations with a single GSHP system is that in case of the absence of subsidies the only climate zone that reached the “feasible” or “almost feasible” status for every building type (house, office, and hotel) was the zone with moderate climate conditions (Madrid, Bologna, Thessaloniki). For such conditions, a balance between the heating and cooling operating hours is maintained, which is favorable in the case of reversible heat pumps because it reduces the thermal imbalance of the ground, and hence the required length of the borehole. Authors conclude that from an economic perspective, in colder climates, it is more beneficial to hybridize the GSHP with a conventional heat source, although it is achieved at expense of slightly lower CO₂ reduction [30].

One of the possible solutions to overcome the mentioned constraints is to couple the GSHP with a reverse cycle air conditioner. Recent work by Aditya et al., in which an exemplary building is simulated in ten different cities, compares the economic feasibility of such a hybrid air/ground heat pump with four other conventional systems. As a result, in 7 out of 10 analysed cities, the DSHP is considered the most cost-efficient solution [31]. Although the results of the study cover a significant number of climatic conditions as well as potential changes in key parameters, the analysis does not consider a wider range of building types and characteristics, and more importantly, the DSHP is not optimized nor properly modelled as an independent system component.

However, such an example of a novel air/ground source DSHP unit, installed in three demonstration facilities in Europe, can be found in the GEOTECH project, co-funded by the European Commission as a part of the H2020 program [13]. In the framework of this four-year project, several studies were developed. A novel “plug-and-play” DSHP, capable of working in eleven operating modes, was designed and modelled in TRNSYS, which is described by Corberán et al. in the following study [32]. Another work, by Cazorla-Marín et al., in which the integrated DSHP system has been adapted to three different locations in Spain (Valencia, Madrid, Bilbao) analyzed the percentage of operation of the DSHP under each of the selected working modes [33]. An extension to this study, where an office building with the DSHP unit is simulated for three different European cities with representative climates: Strasbourg (average climate), Athens (warmer climate), and Stockholm (colder climate), concluded that in warmer climates the use of DSHP is not as profitable as in cold climate, as the air is used to satisfy only 4% of the thermal energy demand [34]. Another work by Cazorla-Marín et al. consisted of the implementation of a coaxial borehole heat exchanger TRNSYS type into the previously developed DSHP model, which allowed for both short and mid-term simulations [35]. The most recent study regarding this novel heat pump unit, where different optimization strategies were tested using data from the demo site in Amsterdam, was presented at the 8th Iberian-American Congress of Refrigeration Science and Technology [36].

The following master thesis is a complementary investigation for the studies developed in the framework of the GEOTECH project. Although the previously mentioned papers [33], [34] analyze in detail the energy performance of the modeled DSHP in different climates, the BHE length was not designed for each specific location, but it was considered the same for all of them. Additionally, the energy performance of the DSHP was assessed only for one year of the system operation, excluding the long-term approach analysis. Moreover, the most recent study, where different DSHP optimization

strategies are tested [36], analyzes the system performance in only one climatology, lacking in the system performance analysis in warmer climates. Additionally, although in the previously specified work by Aditya et al. [31], the DSHP is assessed for a significant number of cities with diversified climates, the building for which the simulations are executed is characterized by the same insulation parameters for each climatic condition, and the typical building constructive typology for each location was not considered. The novelty of the study lays in the individual approach for the system simulation in each climatic condition (cold, average, and warm climates), as the main component of the DSHP – the coaxial BHE – will be configured independently for each representative city (Stockholm, Strasbourg, and Athens respectively). Furthermore, the energy performance of the DSHP will be assessed in a long-term period of 25 years. Finally, the source control optimization strategies will be adapted to the DSHP in all the climatologies and simulated for the corresponding building characteristics to find the best solution for each specific case.

1.3 The objective of the study

The objectives of the master thesis are presented in the following:

1. Design the optimal length of the coaxial BHE for the DSHP system in 3 different locations (Stockholm, Strasbourg, Athens), considering the different ground properties, climatic conditions, and building typology.
2. Assess the long-term energy performance of the DSHP during a 25-year operation in three different locations.
3. Optimize the source control by analyzing different parameters in order to select the best configuration for each location.

1.4 Methodology

The methodology is carried out in three consecutive stages. The first stage is dedicated to the design of the BHE depth for the three cities selected to represent different climatologies encountered in Europe. The tool developed for that purpose in the course of the GEOTECH European project was the Design Guide for the plug and play DSHP systems. This stage aims to verify the accuracy of the results of the BHE depths obtained by following the Design Guide instructions. The main tool used for that purpose is the DSHP model, developed in the TRNSYS simulation program, similarly as part of the GEOTECH project. It is used for carrying out the energy simulations necessary for the system performance evaluation under different climatic conditions. Moreover, another GSHP simulation program, GLHEPro, serves as a tool for the sizing of the BHE. However, due to higher precision, the DSHP model developed in TRNSYS, is used for the validation of the final BHE depths obtained both, with the Design Guide, and in GLHEPro.

The second stage of the methodology analyzes the long-term energy performance of the DSHP system with previously selected BHE depths in the different locations. Here, the analysis is done by assessing: the energy efficiency of the system, ground thermal balance, and energy produced in each operating mode.

The last, third stage aims to verify and select the source control strategy, that would best enhance the energy performance of the system. A parametric study is carried out changing the values of two constants (the hysteresis band and the offset) that may influence the source selection, and therefore, the efficiency of the heat DSHP. Finally, the SPF4 and ground/air use are assessed comparing the results with the reference case for each city analyzed in chapter 5 with the energy assessment.

1.5 Structure of the study

The master thesis is organized in the following chapters:

- Chapter 2 *“The plug and play DSHP system”*, provides information on the main components of the DSHP. Additionally, includes a brief description of the system model developed in TRNSYS.
- Chapter 3 *“Thermal demand in different locations”*, identifies the thermal demands and the main input data for the project related to the building typology, three different locations, and their main governing parameters.
- Chapter 4 *“Design of the optimal BHE depth”*, describes the process of the BHE depth design for the selected locations. Each location has different governing parameters, meaning that the optimal BHE depth must differ between analyzed cities. In this section, the GEOTECH Design Guide BHE depths for the DSHP system are verified by comparing the results with the simulations executed in GLHEPro, and TRNSYS.
- Chapter 5 *“The DSHP energy performance assessment”*, evaluates the long-term system performance in three analyzed cities, using the simulation results obtained for the BHE depths selected in the previous chapter.
- Chapter 6 *“The analysis of the different control strategies”*, provides the analysis of the control strategies that best enhance the energy performance of the DSHP.
- Chapter 7 *“Conclusions”*, recaps the main results of the work and demonstrates the outcomes of the study.

CHAPTER 2

2 The plug and play DSHP system

2.1 Introduction

The following chapter identifies the main components of the GEOTeCH hybrid air/ground heat pump, and briefly describes the DSHP model previously developed in TRNSYS and used as a tool for this master thesis. One of the main objectives of the GEOTeCH project was to obtain a “plug-and-play” packaged solution, meaning that the heat pump and its main components could be easily sized (by following dedicated design guides) and installed to work in diversified climatic conditions. For this purpose, the prototypes of the DSHP unit were installed and tested in the following three demonstration facilities in Europe for at least 12 months:

- Amsterdam small-scale office building. Located at the offices of the company Groenholland BV, in Amsterdam (Netherlands).
- Tribano small-scale office building installed in the offices of the company HiRef S.p.A., in Tribano, province of Padova (Italy).
- Leicester small-scale household. Located in Leicester (United Kingdom).

One of the most versatile tools for reflecting the actual performance of transient energy systems is TRNSYS software. This energy simulation tool was used for the modeling of the DSHP system, and during this four-year European project, the developed model has been modified to enhance the theoretical performance of the system. The last modification in the TRNSYS model along with the detailed description of the system components can be found in [37], thus in this master thesis, only some of the main elements will be summarized in section 2.3.

2.2 Plug and play system description

The plug-and-play system incorporates a heat pump with a variable speed compressor. The system is reversible, meaning that it can be used both for heating and cooling. Additionally, the system can produce Domestic Hot Water (DHW) for the user. The heat pump is hybrid, meaning that it can use more than one source/sink. In the GEOTeCH plug-and-play solution, the hybridized thermal sources are the air and the ground. If the heat pump uses the air as the thermal source/sink, it behaves as a conventional air-to-water HP, exchanging the heat between the air and the internal fluid, which is water. On the other hand, when the ground temperature is more favorable, it injects or extracts the heat from the ground, behaving as a water-to-water heat pump. This dual-source concept allows the HP to alternate between both sources selecting the most favorable, depending on their temperature (warmer in heating and colder in cooling).

The heat that enters the DSHP unit is either distributed by the fan coils providing air-conditioning to the building or delivered to the DHW system to accumulate hot water in the DHW tank. In this plug and play system the DSHP unit connects with the following hydraulic loops:

- User side system (User loop).
- Domestic hot water system (DHW loop).
- Borehole heat exchangers system (Ground loop).

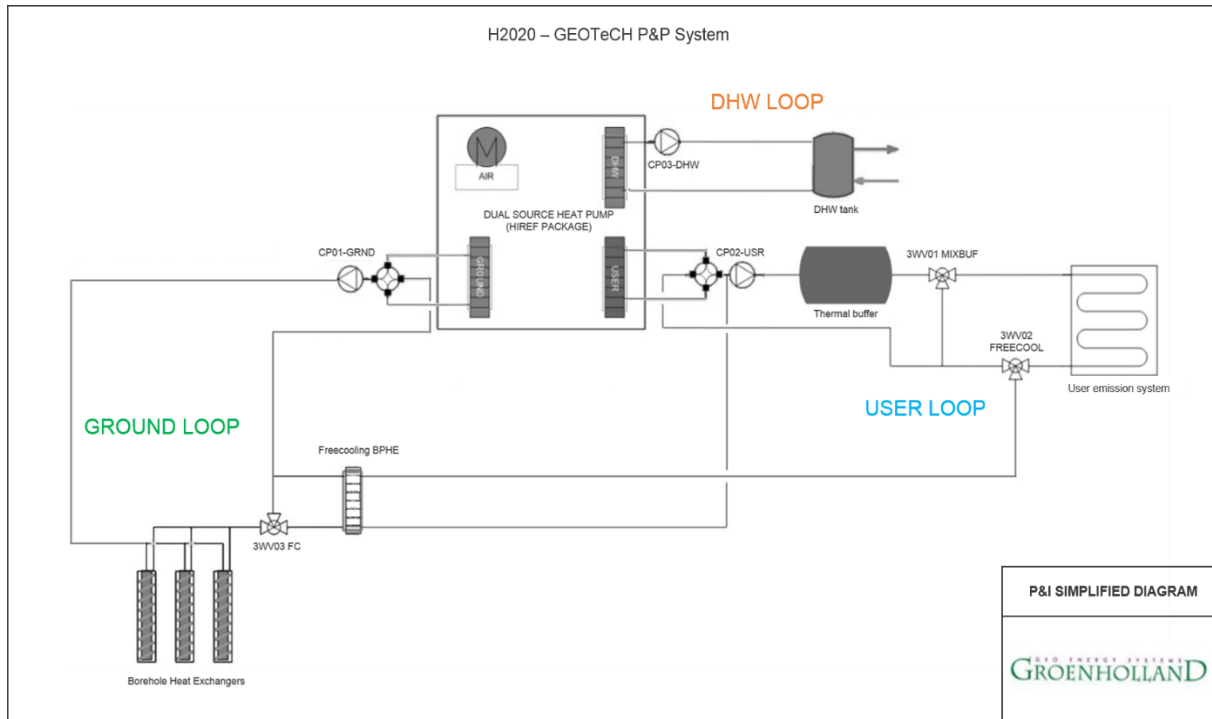


Figure 2.1. Piping and instrumentation diagram of the GEOTeCH plug & play system [38].

2.2.1 The main components of the system

- **The heat pump unit**

In the GEOTeCH project, two DSHP prototypes of different sizes (8kW and 16kW nominal heating capacity) have been constructed. The heat pump size selected for this study is the smaller, 8 kW unit. The heat pump is equipped with a variable speed compressor: XHV-25 (25 cc), by Copeland; which adapts the heat pump capacity to different operating conditions. The compressor, its operating temperatures, and main parameters are further described in section 4.6.1.2. The DSHP works with the refrigerant R32, which has a considerably low Global Warming Potential and complies with the current European F-gas regulation.

Apart from the heat exchangers of the air coil and the user (evaporator or condenser), the aerothermal heat pump has two Brazed Plate Heat Exchangers (BPHE). One BPHE is used for the ground loop, whereas the other produces the DHW for the user. All four heat exchangers are summarized below:

- The air coil: Round Tube and Plate Fin (RTPF) heat exchanger.
- User BPHE: Behaves as a condenser (heating) or evaporator (cooling), depending on the mode of operation. (Model: F80AS, by SWEP).
- Ground BPHE: It is used as an evaporator or condenser. (Model: F85, by SWEP).

- DHW loop BPHE. It is always used as a condenser. (Model: B26, by SWEP).

Figure 2.2 depicts the view from the side of the heat pump unit. The two-round elements on the side of the HP are the Electronically Commutated Motor (ECM) fans with continuous variable speed control. Together with the RTPF heat exchanger, they form a part of the air coil. It is an outdoor unit, meaning that it uses the ambient air as a thermal source/sink, exchanging the heat with the secondary fluid, which then is used in the vapor compression cycle, and distributed to the given loop.

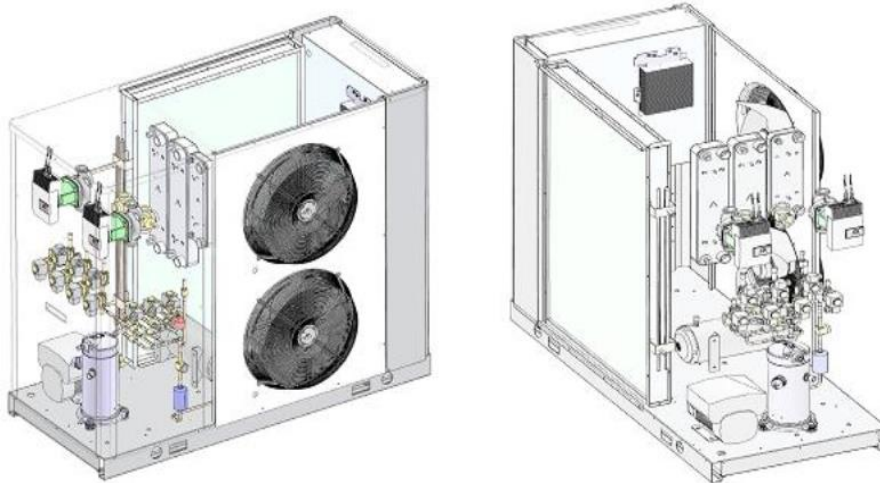



Figure 2.2. The DSHP unit developed within the GEOTeCH project [39].

- **Free cooling BPHE**

Apart from the four heat exchangers integrated within the DSHP unit, a free-cooling BPHE is adopted to the plug and play system. The main function of this heat exchanger is to directly cool down the water in the user loop (bypassing the heat pump) when the fluid coming from the ground loop is sufficiently cold to cover the cooling demand.

- **Circulation pumps**

The plug-and-play system incorporates three circulation pumps, one per hydraulic loop. One model is used for the three individual circuits. In Figure 2.1, the circulation pumps are represented with a  symbol and are labeled as CP01 (ground), CP02 (user), and CP03 (DHW).

- **Buffer tank**

The buffer tank has a total volume of 150 l. It is located in the user loop, before the user emissions system (fan coils), to provide thermal inertia to the system. Additionally, placing a temperature sensor after the thermal buffer (on the supply pipe) allows for better control of the supply temperature, as it prevents the compressor of the heat pump from instant starting or stopping.

- **DHW tank**

The main component of the DHW loop is the storage tank used to accumulate the domestic hot water. It is coupled indirectly with the BPHE to prevent the potable water from being polluted. The tank has a storage capacity of 300 liters.

- **The borehole heat exchanger**

The borehole heat exchanger integrated within the plug and play system is based on a coaxial spiral design developed in cooperation with GEOTHEX[®] company. During the course of the GEOTeCH project, the prototype has been innovated with a coextrusion of the internal spiraled pipe. The BHE

has two pipes of different diameters: an insulated inner pipe, and an outer pipe, whereas between them an additional spiral rib is located. The rib is attached to the inner tube leaving a gap thanks to which a helical flow of the fluid is achieved through the outer pipe.

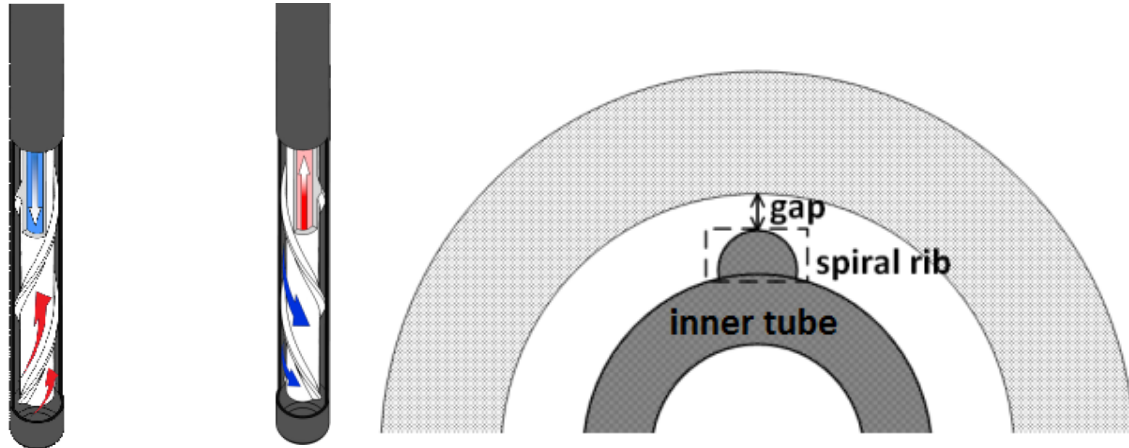


Figure 2.3. Coaxial spiral BHE, GEOTHEX®; a helical path of the fluid (left), axial view (right) [37].

The main advantage of the use of this coaxial spiral technology is the reduction of the borehole thermal resistance especially at laminar flow conditions of the circulation medium. Furthermore, as the DSHP hybridizes two energy sources, the load on the borehole is reduced, allowing for the use of shallower boreholes. For this reason, the coaxial spiral BHE is integrated with the new dry auger drilling technique, also developed in the GEOTeCH project. In comparison with other drilling methods, the dry auger technology is more suitable for shorter BHEs, meaning that the BHE field will be usually composed of multiple boreholes. The increase in the number of boreholes causes the reduction of the flow rate per borehole, therefore the system efficiency is enhanced by the decrease in the pumping energy needed for the circulation of the fluid (less pressure loss per borehole).

2.2.2 The operating modes

The DSHP is designed to provide air-conditioning or DHW, using 11 individual operating modes. Each operating mode is assigned to one of the two defined seasons:

- Summer season, where the heat pump operates as a chiller to meet the cooling demand, while at the same time produces the DHW in the corresponding schedule.
- Winter season, where the unit works as a heat pump, simultaneously producing the DHW.

In contrast to air-conditioning, the DHW production is therefore not affected by the currently defined season. Additionally, in both seasons the DSHP alternates between the ground or the air, summing up to 8 different modes (4 per season). Another, 9th operating mode allows to provide cooling to the building during the summer season and to produce DHW simultaneously. This mode is labeled as M3 and called “Full recovery”.

In addition, there are 2 different free-cooling modes defined for the summer operation. The first - M10 - is selected if the outlet borehole temperature is cold enough to cover the cooling demand. In this mode the thermal fluid bypasses the heat pump, sending the cool water directly to the user loop. The second free-cooling mode (M11) apart from providing the air-conditioning, allows producing the DHW with the air coil component.

Table 2.1. The DSHP system operating modes.

	Condenser	Evaporator	Operating mode
Summer	Air	User	M1-Summer Air
	Ground	User	M2-Summer Ground
	-	-	M10-Free cooling
	DHW	User	M3-DHW User "Full Recovery"
	DHW	Air	M6-DHW Air
	DHW	Ground	M8-DHW Ground
Winter	DHW	Air	M11-Freecooling +DHW Air
	User	Air	M4-Winter Air
	User	Ground	M5-Winter Ground
	DHW	Ground	M9-DHW Ground

2.2.3 The selection of the source/sink

The principle of the selection of the source or sink relies on the current season (heating or cooling) and the source temperature (of the air and ground). The season is defined manually by the user, depending on the local climatic conditions. Once the season is defined the thermal source is selected automatically by the controller. The controller compares the air and ground temperatures and chooses the most favorable (the colder in summer and the warmer in winter). Figure 2.4 shows the basic principle of the thermal source/sink selection.

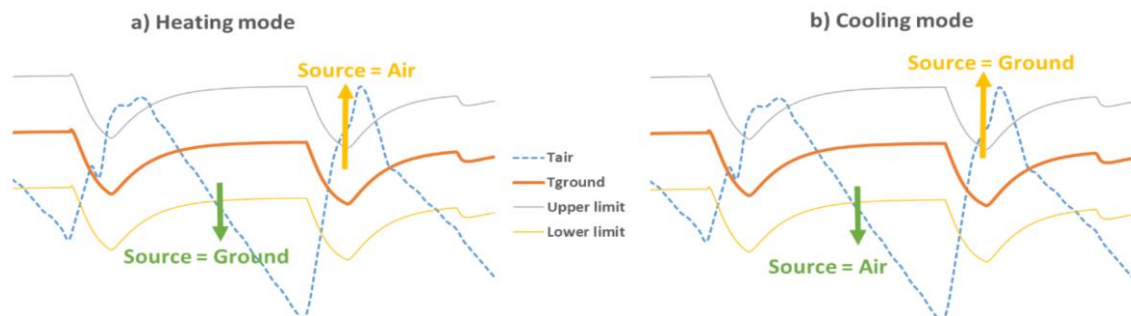


Figure 2.4. Selection of the source depending on the air and ground temperature [34].

The air source is measured using the ambient air temperature, whereas the ground source is evaluated using the temperature of the fluid that leaves the borehole field and enters the heat pump. As seen in Figure 2.4, a hysteresis band (upper and lower limit) is used to control the source selection, preventing the HP from switching the source too frequently. In this master thesis, the hysteresis band used for the source control is ± 2 K.

As stated before, the DHW is produced during the whole year. Although the scheduled production of the DHW is from 4 am to 6 am, the storage tank is sized to meet the DHW demand during the entire day. However, if the temperature in the storage tank goes below a specified value, the control system prioritizes the production of the DHW over the air-conditioning production.

2.2.4 The system efficiency

Following the methodology of the SEPAMO European project [40], four different Seasonal Performance Factors (SPFs) are defined to assess the efficiency of the system. Each SPF considers

different consumptions of the system components. The following equations describe the SPF's of the system.

$$SPF1 = \frac{\int_0^t (\dot{Q}_{USER} + \dot{Q}_{DHW}) \cdot dt}{\int_0^t (\dot{W}_{HP}) \cdot dt} \quad (1)$$

$$SPF2 = \frac{\int_0^t (\dot{Q}_{USER} + \dot{Q}_{DHW}) \cdot dt}{\int_0^t (\dot{W}_{HP} + \dot{W}_{FAN} + \dot{W}_{BHE}) \cdot dt} \quad (2)$$

$$SPF3 = \frac{\int_0^t (\dot{Q}_{USER} + \dot{Q}_{DHW}) \cdot dt}{\int_0^t (\dot{W}_{HP} + \dot{W}_{FAN} + \dot{W}_{BHE} + \dot{W}_{BACKUP}) \cdot dt} \quad (3)$$

$$SPF4 = \frac{\int_0^t (\dot{Q}_{USER} + \dot{Q}_{DHW}) \cdot dt}{\int_0^t (\dot{W}_{HP} + \dot{W}_{FAN} + \dot{W}_{BHE} + \dot{W}_{BACKUP} + \dot{W}_{USER} + \dot{W}_{DHW}) \cdot dt} \quad (4)$$

where \dot{Q} is the common numerator corresponding to the useful heat in the user loop and DHW loop (\dot{Q}_{USER} and \dot{Q}_{DHW} , respectively); and \dot{W} is the power consumption of each component of the system (heat pump \dot{W}_{HP} , fan \dot{W}_{FAN} , ground loop circulation pump \dot{W}_{BHE} , user circuit circulation pump \dot{W}_{USER} , DHW loop circulation pump \dot{W}_{DHW} , electrical consumption of the backup system \dot{W}_{BACKUP}). The integration period depends on the time of the simulation.

SPF4 represents the energy efficiency of the system as a whole, including all existing electrical consumptions. Thereby, it is the indicator used at the later stage of the master thesis to carry out the energy assessment of the DSHP system (section 5.4).

2.3 The system model in TRNSYS

The main tool used in this master thesis is the DSHP model developed in TRNSYS. In the course of the GEOTECH project, the model has been continuously updated with different features and components, which can be found in scientific and conference papers [32]-[35]. The extensive description of its final version, including the modeling of the different subsystems and control strategies, is presented in the Ph.D. dissertation by Cazorla-Marín [37].

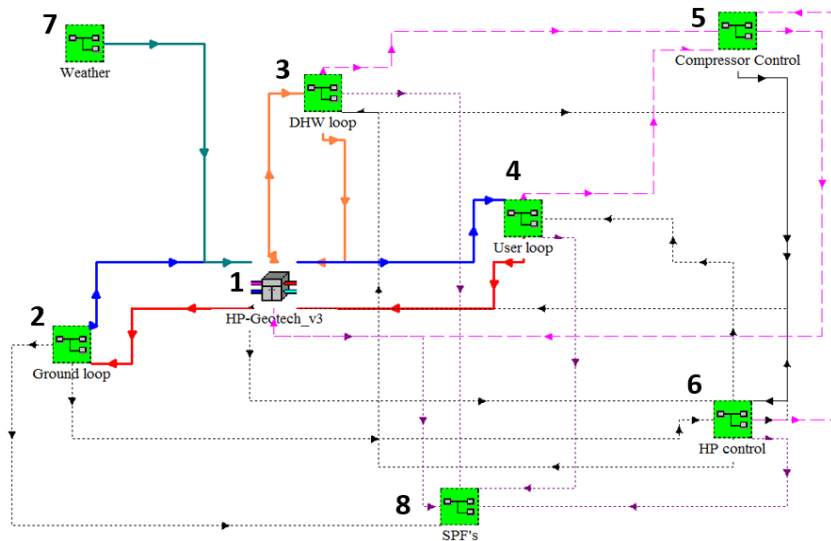
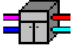
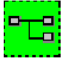
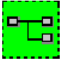
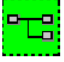
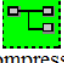
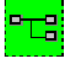
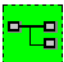
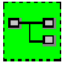


Figure 2.5. The main view on the system layout in TRNSYS.

As seen in Figure 2.5, the system designed in TRNSYS is modular and includes macros (green icons; 2 - 8) that describe in detail: three hydraulic loops (user loop, DHW loop, and the ground loop), two different control systems (PID and differential controllers), weather data, and the system efficiency. The governing element of the model is the heat pump (1) which sends and receives signals to the different systems, which depend on the defined equations and relations. Table 2.2 recaps the main elements of the DSHP model previously depicted in Figure 2.5.

Table 2.2. Main elements of the DSHP model developed in TRNSYS.

 HP-Geotech_v3	<p>HP-Geotech_v3 corresponds to the DSHP, defined as a black box in the TRNSYS model. The performance is calculated using polynomial correlations that depend on the operating mode, the selected source, distribution of temperatures, and flow rates.</p>
 Ground loop	<p>In the ground loop, the spiral coaxial BHE is defined, including the piping. A dynamic B2G model was developed by Cazorla-Marín et. al., to reproduce the behavior of the BHE [35]. Additionally, the long-term response of the ground is considered in the ground loop using the Line Source Approach (LSA) type.</p>
 DHW loop	<p>The DHW loop includes the storage tank, the control for the DHW production, and the DHW demand. The DHW demand profile is introduced as an external file, which is further described in section 3.1.4.2.</p>
 User loop	<p>The user loop includes the thermal buffer, circulation pump (with CP control system), piping, and user demand. The building model is not included in the DSHP model. However, the thermal demands of the building defined as hourly thermal loads are introduced as an input to perform the simulations.</p>
 Compressor Control	<p>In this macro, the frequency of the variable speed compressor is defined, depending on the temperature in the user circuit. The compressor speed control allows the heat pump to adapt the thermal capacity to the instantaneous demand.</p>
 HP control	<p>This macro defines the selection of the different operating modes (described in section 2.2.2), and the thermal source control (section 2.2.3).</p>
 Weather	<p>The weather conditions are defined by introducing an input file that corresponds to a given location. The ambient temperature at each time step is used as the air temperature in the DSHP model.</p>
 SPF's	<p>In this macro, the consumption of the different components is calculated, and system efficiency is analyzed using SPF's defined in section 2.2.4</p>

CHAPTER 3

3 Thermal demand in different locations

This chapter follows a methodology adopted in earlier studies [34], [37] and describes the necessary inputs for the analysis carried out in sections 4 and 5. The inputs are related to the building typology determined for each location analyzed in the study: Stockholm, Strasbourg, Athens. These three cities have been chosen to represent some of the different climatic conditions encountered in Europe, therefore each will be governed by different location-dependent parameters.

In previous studies, the building was properly modeled and simulated to retrieve the thermal demands. However, as stated in chapter 2, the DSHP model in TRNSYS has been modified to easily enter the thermal loads of the building in a form of an input file, and it is no longer necessary to develop a separate building model. The following sections of this chapter describe the thermal demands and all the necessary location-dependent inputs for the DSHP model used in this master thesis.

3.1 Parameters in each location

3.1.1 Climatic conditions

One of the main objectives of the study is to compare the DSHP system performance under different climatological conditions. Following the European regulation EU Reg. 811/2013 which establishes requirements for the energy labeling of the space heating devices, Strasbourg (France), Helsinki (Finland), and Athens (Greece) are defined as cities with representative climate conditions, namely: ‘average climate conditions’, ‘colder climate conditions’ and ‘warmer climate conditions, respectively.

Nevertheless, following the previous studies [34], [37], the three European locations selected to represent the distinctive climate types defined in the mentioned regulation (average, colder, and warmer conditions) are Strasbourg (France), Stockholm (Sweden), Athens (Greece), respectively. As it can be noticed, the only difference between the methodology used is in the EU Reg. 811/2013 and this work is the city that represents the colder climatic condition (Helsinki is replaced with Stockholm). This is due to the lack of data for Helsinki in the database of the European project TABULA (Typology Approach for Building Stock Energy Assessment) [45], where the information of the building construction type in different cities around Europe can be found, and which has been considered for modeling the building thermal loads in each representative climate. In addition, Finland shares a western border with Sweden thus, both have similar climate conditions. Table 3.1 represents the differences between the maximum, minimum, and average temperatures in those two cities.

Table 3.1. Maximum, minimum, and average temperatures in Helsinki and Strasbourg [43].

Location	Maximum temperature (°C)	Minimum temperature (°C)	Average temperature (°C)
Helsinki	24	-21	4.7
Strasbourg	28	-20	5.3

Following the methodology adopted in earlier studies [34], [37], the weather data (minimum, maximum, and average temperature) for each city were retrieved from the weather database Meteonorm [41]. Although factors such as moisture evaporation or solar radiation can affect the undisturbed ground temperature at shallow depths [42], for simplicity, the undisturbed ground temperature was assumed to be the local average annual. Moreover, at this shallow depth, it is also assumed that the geothermal gradient does not affect the undisturbed ground temperature. As previously described, the DSHP is reversible, thus can provide both, heating in winter, and cooling in summer to the building. The duration of the two defined seasons (winter and summer) was determined previously at the time when the building was simulated using the local meteorological data. As shown in Table 3.2, only in the case of Stockholm no summer period is considered. It means that the DSHP does not work in cooling mode, therefore the heat is continuously extracted from the ground. This will be further analyzed in the energy assessment in section 5.

Additionally, using the results obtained from a previous study [43] developed in the framework of the GEOTECH Project, the ground thermal properties such as ground thermal conductivity and ground volumetric heat capacitance were determined for the analyzed cities. Table 3.2 recaps the main location and climate dependent parameters.

Table 3.2. Location dependent parameters for Stockholm, Strasbourg, and Athens.

Parameter	Stockholm	Strasbourg	Athens
Minimum/Maximum/Average temperature (°C)	28(-20)/5.3	32(-11)/9.8	38/0/17.6
Summer period duration	-	18/6 - 10/9	2/5 - 22/10
Ground thermal conductivity (W/m·K)	3.75	2.25	3.75
Ground volumetric thermal capacitance (kJ/m ³ ·K)	1250	3000	1250

3.1.2 The building description

The building analyzed in the study belongs to the Department of Applied Thermodynamics and is situated on the campus of the Polytechnic University in Valencia, Spain. The building was built in the '70s, and in past, its thermal demand used to be partially covered by a GSHP system with a nominal capacity of 17 kW in heating and 14.7 kW in cooling, and a field of six 50 m deep U-tube BHEs. The old GSHP system was installed as a result of the European project "GeoCool", coordinated by the Polytechnic University of Valencia [44]. While the total air-conditioned area of the building is 250 m², which includes nine offices, a computer room, a printer room, and a corridor, in this study only a part (75 m²) of the building will be considered for the analysis. This is related to the size of the DSHP prototype selected for the study, which does not have a sufficient heating capacity (8 kW) to meet the

entire building's demand. The analyzed area is mainly dedicated to offices thus, the schedule of occupancy corresponds to the working office hours, further described in section 3.1.4.2.

Although the layout, area, and spatial distribution of the building are considered identical for each city (Stockholm, Strasbourg, Athens), the building partitions and windows materials (types, layers) and their corresponding properties (thicknesses, thermal transmittances) were chosen based on the specific construction typology for each location analyzed further in section 3.1.1. Following the methodology developed in previous studies [34], [37], the data used for each building typology identification was retrieved from the European project TABULA, which the main idea was to make an agreed systematic approach to classify building stocks according to their energy related properties [45]. The TABULA project provides an extensive database and a web tool [46] that classifies the building typology based on the country of origin, year of construction, and building size class. In terms of this master thesis the described tool allowed for the selection of the building typology which best corresponds to the characteristics of the building of the Department of Applied Thermodynamics, but as if it were constructed in accordance with the standards applicable in the three countries analyzed in this thesis.

Based on the general data of the building located in Spain, it was found that the thermal transmittance (U-values) of the envelope and the windows correspond to a wall type "Wall 1" (the existing state) and a window type "Window 1" (usual refurbishment). Therefore, the U-value of the mentioned wall and window types determined in TABULA WebTool correspond respectively for each city identified in this study. Table 3.3 summarizes the U-values both for the building's envelope and the windows for three analyzed locations.

Table 3.3. The building's thermal parameters extracted from TABULA database.

Thermal parameter	Stockholm	Strasbourg	Athens
U-value envelope (W/m ² ·K)	0.41	0.78	2.20
U-value windows (W/m ² ·K)	0.90	1.40	3.20

3.1.3 Operating parameters

The following section summarizes the main operating parameters, which remain constant for each analyzed location. These parameters constrain the operation scheme of the DSHP.

- Schedule for air-conditioning: from 6 a.m. to 10 p.m., excluding weekends.
- Schedule for the DHW production: from 4 a.m. to 6 a.m., excluding weekends.
- Comfort temperature: 23°C, both for heating and cooling operation.
- Occupant capacity of air-conditioned spaces was established based on the real schedule of the professors working in the offices.
- Each office has a space capacity for 5 people, therefore the DHW demand profile is calculated correspondingly. The DHW thermal demand is further described in section 3.1.4.1.
- The water supply temperature is represented as a function of the annual average ambient temperature, and it is 20% larger in the summer and 20% lower in the winter season.
- As described in section 2.2.1, the system has the same components and their corresponding size: heat pump of nominal capacity 8 kW, hydraulic loops, 150 l buffer tank, 300 l DHW tank, and circulation pumps.

3.1.4 Thermal demands

3.1.4.1 DHW thermal demand

The DHW thermal demand is introduced in the DSHP model as input using an external file, but in this case, the demand profile is defined only for one day of operation. It means that during the whole year there is a demand for the DHW, regardless of the season. The only constrain on the production of the DHW is, therefore, the schedule of the DSHP (from 4 a.m. to 6 a.m., excluding the weekends), defined in the heat pump control macro. The following Figure 3.1 represents DHW daily demand profile that corresponds to one person in one office. The total daily DHW demand per one person is 7.49 l/d. In this study it is considered that 5 people are working per office (5 offices are considered), giving the total daily DHW consumption of around 187.25 l/d.

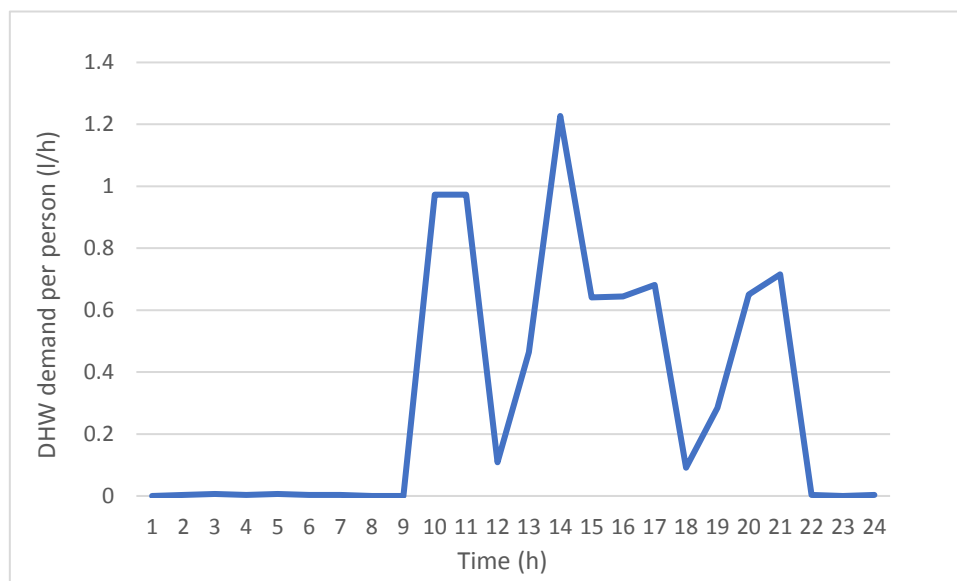


Figure 3.1. Hourly DHW demand per one person in an office.

3.1.4.2 User loop thermal demand

Similarly, the user thermal demand is modeled as a thermal load profile and can be introduced in the DSHP model in a form of an external file, without the necessity of additional building modeling. The process of thermal load extraction is described below.

As already mentioned, in the past, the heat distributed to the analyzed building used to be produced by a GSHP system. Moreover, previously the building was properly modeled in TRNSYS and the thermal loads for each specific location were extracted from the simulations. The thermal loads extracted from that GSHP system are therefore considered representative for this study. However, the GSHP installation at that time had a nominal capacity of 17 kW in heating and 14.7 kW in cooling, meanwhile, the DSHP system analyzed in this study has a significantly smaller nominal capacity (8 kW). As a result, in this study, only 30% of the surface of the offices is considered as a useful area for the air-conditioning using the DSHP system. Figure 3.2 represents the building thermal demand (expressed in kW) used for the analysis of the DSHP system in each city from the study. The first graph from Figure 3.2(a) describes the thermal demand used for the case of Stockholm, which is the only location where no cooling demand is considered. Strasbourg's thermal demand is displayed in the subsequent graph

(b), and the following (c) corresponds to Athens. Table 3.4 recaps the total and peak energy demands for both heating and cooling operation for the analyzed cities.

Table 3.4. Thermal energy demand in Stockholm, Strasbourg, and Athens.

Thermal energy demand	Stockholm	Strasbourg	Athens
Peak heating (kW)	11.7	9.2	6.1
Peak cooling (kW)	0	2.1	4.8
Heating demand (kWh)	11491	7766	3565
Cooling demand (kWh)	0	514	3262
Annual demand (kWh)	11491	8280	6827

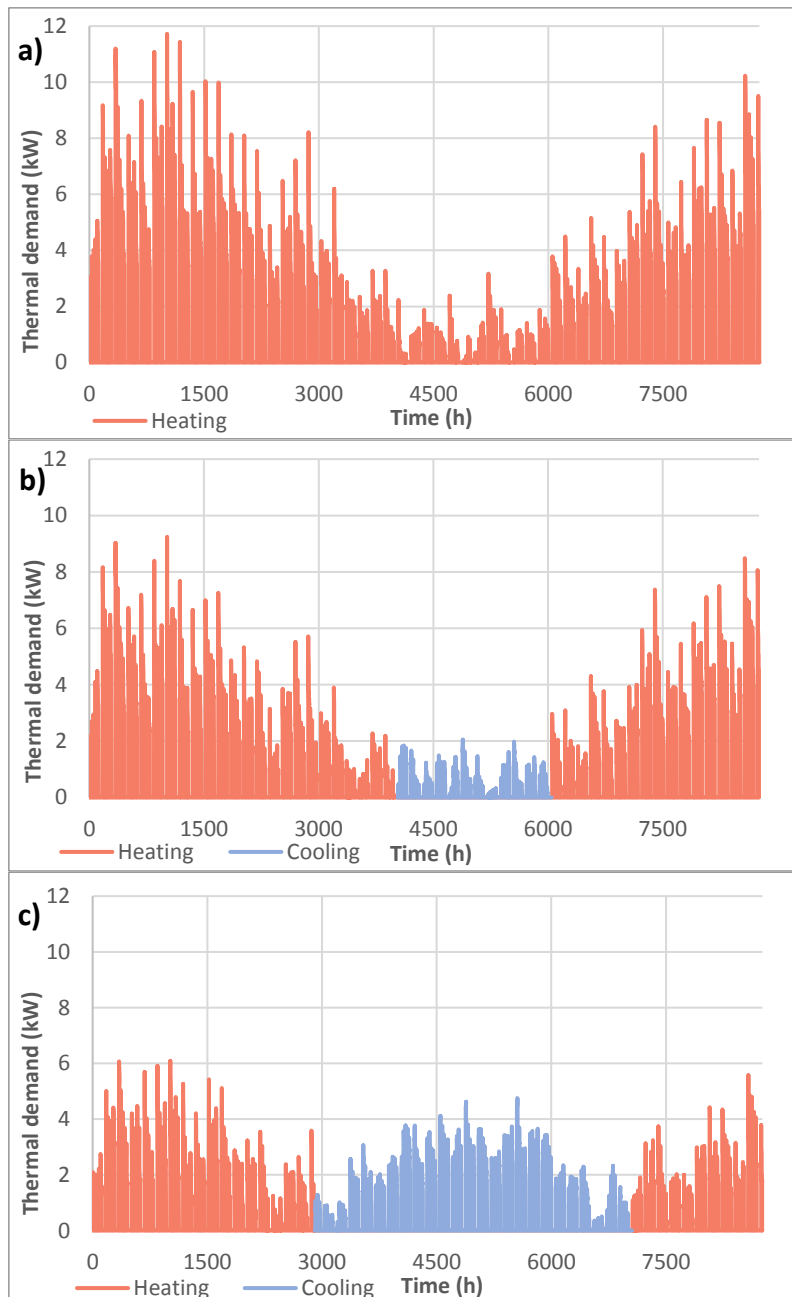


Figure 3.2. Thermal demand in kW, in Stockholm (a), Strasbourg (b), and Athens (c).

CHAPTER 4

4 The design of the BHE field

4.1 Introduction

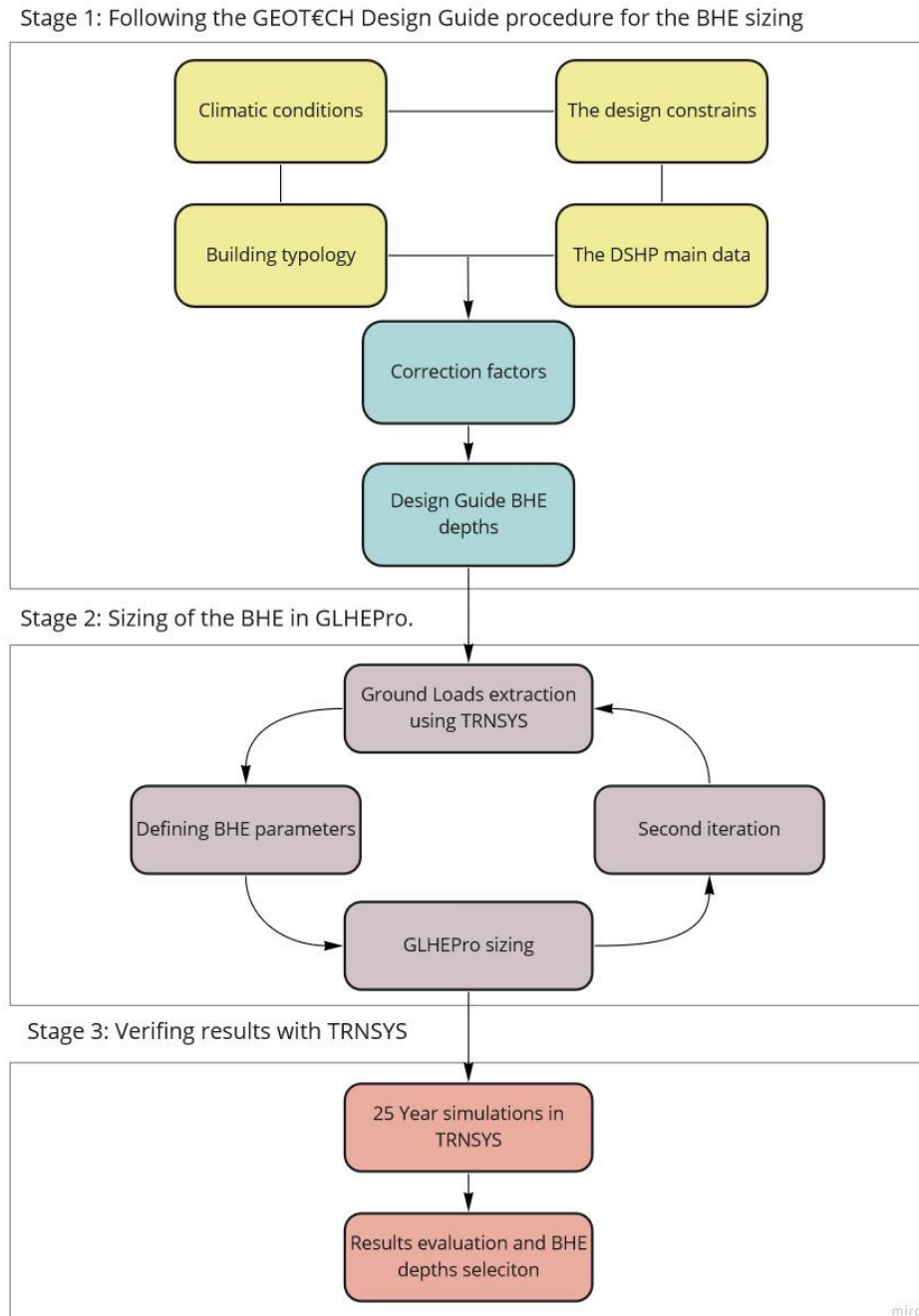
This chapter is dedicated to the design of the BHE depth for the three cities selected to represent different climatologies encountered in Europe. Both in the GSHP and DSHP systems, the GHE is the most expensive component mainly due to the costs associated with drilling and installation of the BHEs, therefore its optimal design is crucial for reducing the cost of the installation. On the other hand, the implementation of a deeper BHE often leads to the higher efficiency of the system, as the ground loop return temperatures are closer to the undisturbed ground temperature, and thus are more favorable. In this context, it is important to properly select the BHE depth, considering both the efficiency of the system and the cost associated with additional drilling.

Another factor that plays an important role in the BHE field design is the selection of an optimal configuration of the BHEs. There are many possibilities for the geometrical distribution of the boreholes on a surface, but often, it is the availability of the land area that constrains the selection of the final configuration of the ground heat exchangers. In earlier studies [34], [37], the configuration used for the energy simulations and assessment of the system was a rectangular 2 x 2 configuration. As described in the previous 3.1.2, it was related to the nominal capacity of the heat pump (8 kW) selected for the analysis. Moreover, each of the four BHEs in the rectangular field was separated by 3 meters. Following the methodology adopted in those studies, the BHE field configuration is kept the same in the first stage of the BHE field design process. However, a comparative analysis using other configurations is foreseen at a later stage of the project. Every configuration and depth-per-borehole are analyzed with respect to the design constraints for the DSHP systems, determined within the framework of the GEOTECH project. Additionally, the drilling technology developed in the course of this European project also establishes certain limits. All design constraints for the analysis of this chapter are further described in section 4.3.

4.1.1 Methodology

The methodology used in this chapter is divided into three consecutive stages, with an objective of the selection of the optimal BHE depth and configuration. The tools used in this section are the Design Guide (DG) for the plug & play DSHP systems (section 4.2), the TRNSYS model previously described in 2.3, and a computer program GLHEPro, used for the simulation and sizing of the GSHP systems.

As seen in Figure 4.1, the main tool used for the first stage of the methodology is the Design Guide for the plug & play systems, developed in the GEOTECH project. Following the instructions contained in the DG, the BHE depths for three analyzed locations are calculated.



The main objective of the second stage is to size the BHEs for every considered city using the GLHEPro simulation tool. GLHEPro is a program that offers the possibility of sizing the system using the ground thermal loads. Therefore, the first step consists of the ground thermal loads extraction using the TRNSYS model. For this purpose, the DG BHE depths from the first stage serve as an input for simulating the thermal loads in TRNSYS. The BHE field is considered properly sized if meets the

requirements determined by the DG. The main requirement constraining the design of these types of systems is to maintain certain temperature limits of the fluid that leaves the BHE field and enters the heat pump. These BHE outlet temperature limits should not be exceeded during a heat pump operating time of at least 25 years.

In the last stage of this chapter, the results obtained from the DG and GLHEPro are verified using the TRNSYS model. The DSHP model developed in TRNSYS is the most precise tool, as it includes the dynamic interaction of the integrated system components (DSHP, B2G model, building thermal loads, control board of the system, meteorological data, etc.), therefore it will be used to verify the results from GLHEPro and DG, by simulating them once again for 25 years. Using these simulation results the system will be evaluated for every BHE depth and configuration using the energy consumption data and outlet BHE fluid temperatures. Finally, the BHE depths for each city will be selected by analyzing the relation between the additional cost related to drilling and the energy savings associated with using a deeper BHE. The DSHP system with the selected BHE depth (and configuration) for each city will be used for the energy assessment in chapter 5.

4.2 BHE sizing with the Design Guide

One of the documents developed in the course of the GEOTeCH European project was the Design Guide for the plug & play DSHP systems. This GEOTeCH Deliverable 4.9 [38], redacted by the entities depicted in Figure 4.2 determines the guidelines for the design and selection of the required length of the BHE.



Figure 4.2. The GEOTeCH plug & play systems Design Guide consortium.

It is a compact set of instructions divided into two main parts. The first part instructs how to design the GHE for the DSHP installation by following four simple steps to identify the main characteristics of the system and the environment in which it is installed. These four steps of the GHE design process are displayed in Figure 4.3. The second part explains in detail how the methodology was defined. These design instructions were calculated using advanced simulation tools, such as Earth Energy Designer (for the ground heat exchanger), and TRNSYS model (for the building analysis).

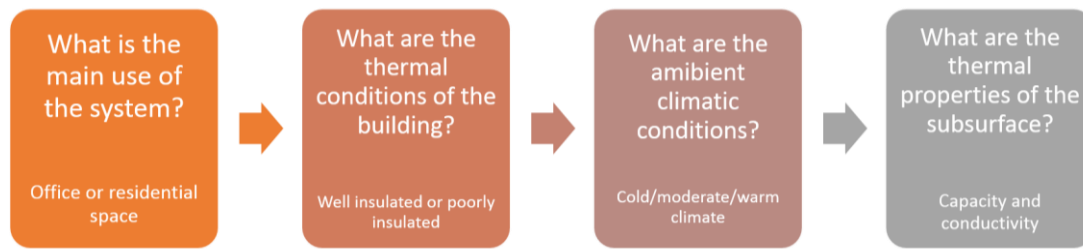


Figure 4.3. The steps of the GHE design process.

The main objective of the DG was to simplify the design process of the BHE by developing guidelines and design constraints so that the system could be easily adopted in different locations across Europe. For that reason, the simplified design is based on a reference situation, where two heat pump capacities are considered (8 kW and 16 kW). Additionally, three climate conditions are specified, cold, average, and warm. Each specific case, analyzed for different capacity and climate, corresponds to different reference loads, temperatures, ground properties, and BHE depths. The reference design for three climatic conditions and two different capacities is summarized below.

Table 4.1. Reference design (RD) for the two types of plug and play DSHP in different climates [38].

RD	cold climate		average climate		warm climate	
	8 kW	16 kW	8 kW	16 kW	8 kW	16 kW
Heat pump capacity	8 kW	16 kW	8 kW	16 kW	8 kW	16 kW
Reference max. load (heating or cooling, MWh)	5	10	5	10	5	10
Soil thermal conductivity (W/m·K)	1.75	1.75	1.75	1.75	1.75	1.75
Soil temperature (°C)	4.5	4.5	10.0	10.0	17.0	17.0
Borehole heat exchanger depth (m)	140	250	140	250	140	250
Design fluid temperature (heating and cooling operation, °C)	-5.5 17.0	-5.5 17.0	0.0 24.5	0.0 24.5	7.0 30.0	7.0 30.0
Frost protection (°C)	-10.0	-10.0	-5.0	-5.0	0.0	0.0

After defining the site-specific parameters (the HP capacity, climate, heating demand, and ground thermal properties) the user must apply several correction factors to arrive at the final size of the heat exchanger.

4.2.1 The correction factors

Using the site-specific parameters (defined by the user) and the reference design (defined in the DG) the correction factors can be applied for the calculation of the total BHE depth.

For each climate defined in Table 4.1, there are two heat pump capacities, 8 and 16 kW, which correspond to the borehole heat exchanger depth of 140 and 250 meters, respectively. In this project, the heating capacity of the DSHP prototype is 8 kW, therefore the reference BHE depth is 140 m. To calculate the final BHE size for each climate defined in the study, the reference BHE depth of 140 meters must be further multiplied by the correction factors that correspond to each climatology.

Table 4.2. Design correction factors for different governing parameters [38].

Design Correction Factor (DCF)	Value of the DCF			
DCF 1: Duration of maximum operation, cold climate	1.25			
DCF 2: Duration of maximum operation, building low insulation	1.25			
DCF 3: Total yearly energy demand (MWh) (if larger than the second row, apply the factor below)	8kW		16kW	
	8MWh	10MWh	16MWh	20MWh
	1.2	1.3	1.2	1.3
DCF 4: Soil thermal conductivity (W/m·K)	range		factor	
	<1.25		1.35	
	1.25 – 2.25		1.00	
	2.25 – 3.25		0.85	
	>3.25		0.75	

4.2.2 The Design Guide BHE depth calculation

As shown in Table 4.2, four different correction factors influence the size of the BHE. The first two (DCF 1 and DCF 2) are very subjective because their ranges are not defined in the DG. Regarding the first design correction factor (DCF 1), the document mentions that for a system installed in a cold climate the total duration of maximum capacity might be significantly larger than in the reference design. In the context of this master thesis, this situation might occur in the case of Stockholm, where the heat pump operates only in the heating mode throughout the year. Additionally, in terms of the DCF 2, the DG advises that for a badly insulated building the duration of maximum capacity may be larger, thus longer BHE would be necessary. This DCF 2 might be suitable for Athens, where the building's envelope and windows have high U-values of 2.2 and 3.2 W/m²·K, respectively. In both cases (DCF 1 and DCF 2) a 25% larger borehole heat exchanger is required.

On the other hand, the determination of the design correction factors DCF 3 and DCF 4 is more concise. Each is defined by a specified range, leaving no room for the user's interpretation. Regarding DCF 3, if the total energy demand (in an unbalanced energy design) is larger than the reference design, the system may be undersized. To prevent that from happening, in the case of an 8kW unit, the DCF 3 adds 20% or 30% to the final BHE depth if the yearly energy demand is larger than 8 MWh or 10 MWh, respectively. The last correction factor, DCF 4, assigns different multipliers (0.75 – 1.35) according to the soil thermal conductivity ranges.

To apply the correction factors correctly, the relevant site-specific parameters described in section 3.1, are summarized below.

Table 4.3. Site-specific parameters necessary for the correction factors determination.

Parameter	Stockholm	Strasbourg	Athens
Climate evaluation	cold	average	warm
Building insulation quality based on U-values	high	average	low
Annual demand (MWh)	11.5	8.3	6.8
Ground thermal conductivity (W/m·K)	3.75	2.25	3.75

***The climate and insulation quality are both evaluated subjectively, based on the available data.**

Using the information contained in Table 4.2 and Table 4.3 the correction factors are applied as follows for each city and its site-specific parameters.

Table 4.4. Selected design correction factors.

CITY	Demand correction factor	Soil thermal conductivity	Building low insulation	Cold climate operation
STOCKHOLM	1.3	0.75	1	1.25
STRASBOURG	1.2	1	1	1
ATHENS	1	0.75	1.25	1

To calculate the final BHE depth in each location, the design correction factors for every site-specific parameter are multiplied by the reference borehole heat exchanger depth (140 m):

$$BHE_{STO} = 140 * 1.30 * 0.75 * 1.00 * 1.25 = \mathbf{170.625\ m}$$

$$BHE_{SXB} = 140 * 1.20 * 1.00 * 1.00 * 1.00 = \mathbf{168\ m}$$

$$BHE_{ATH} = 140 * 1.00 * 0.75 * 1.25 * 1.00 = \mathbf{131.25\ m}$$

4.3 The design constraints

In this master thesis, two main parameters constrain the process of the BHE field design:

- The maximum drilling depth (m).
- The design fluid temperatures (°C).

The first design constraint is related to the drilling technology developed by GEOTECH. One of the main outcomes of this European project was the design, construction, and commercialization of a drill rig, Conrad Boxer 200 [47], capable of reducing the water consumption (dry drilling) and time of drilling in loose soils such as sand, gravel, or clays. Moreover, the cost of the rig was reduced by 70% in comparison with the conventional mud rotary rig, which brings down the overall cost of the drilling. The drill rig can be equipped with an auger drill head, which allows for integrating it with the coaxial spiral BHE used in this master thesis. Although according to the Boxer 200 specifications, the rig is capable of drilling up to 225 meters, the use of coaxial spiral BHE technology in this project limits the maximum drilling depth to 60 m. Moreover, the torque required to drill increases with thicker heat exchangers, and its maximum values are related to the selected drilling rig design, therefore the outer diameter of the coaxial BHE determines the maximum drilling depth. Table 4.5 shows the estimates for the maximum drilling depths according to different BHE diameters.

Table 4.5. Maximum drilling depths for different HE diameters according to drill rig capacity [38].

The heat exchanger diameter (mm)	Maximum drilling depth (m)
63	60
75	60
90	50
110	30
125	30
200	15

In this study, the selected BHE has an outer diameter of 63 mm thus, the corresponding maximum drilling depth is 60 meters. Although the maximum drilling depth depends on other factors related to local conditions such as the composition of the ground layers or the bedrock penetration [38], they are not considered in this project.

The second design constraint is related to the design fluid temperatures established by the DG. These are the maximum and minimum temperatures of the fluid at the outlet of the ground loop and thus, at the inlet of the heat pump unit. The DG determines the limits of the outlet fluid temperatures for three climatic conditions based on the reference design.

Table 4.6. Reference outlet fluid temperatures [38].

CLIMATE	Design fluid temperatures (°C)	
	Maximum	Minimum
Cold	17	-5.5
Average	24.5	0
Warm	30	7

As Table 4.6 indicates, the colder the climate, the lower the design fluid temperatures. It is of course dictated by the different ground temperatures encountered in each climate. By establishing different limits for every climatic condition, the HP is capable of providing the same power in each location using one size of the BHE (the reference design for BHE size is 140m in each climatic condition). Additionally, by constraining the outlet fluid temperature limit a certain operating regime is defined. In this regime, the depth of the BHE plays a crucial role in guaranteeing that the temperature range will be maintained for 25 years of operation considered in this study. This temperature limit is important from the point of view of the GLHEPro borehole sizing tool. A slight change in the temperature regime might result in a different BHE depth calculated by the software. In the following 4.4, the BHE sizing procedure using GLHEPro is described.

4.4 BHE sizing with GLHEPro

GLHEPro is the commercial tool for the design of vertical BHEs, developed by the School of Mechanical and Aerospace Engineering at Oklahoma State University. In this master thesis it is used to perform the two following actions:

- The action of “Sizing”. As stated before, GLHEPro allows the determination of the required depth of the BHE field in a user-specified temperature regime. By establishing the temperature regime (the desired minimum and maximum temperatures at the inlet of the heat pump) for the entire period of the simulation, the program computes the total BHE depth.
- The action of “Simulation”. This action allows simulating different BHE depths (specified by the user) to determine maximum and minimum fluid temperatures which flow from the BHE field to the HP unit. This method is used to simulate the DG depths to quickly verify the maximum and minimum fluid temperatures calculated by the software.

Both the simulation and sizing method allows for a simulation up to a maximum of 1200 months. In this master thesis, as mentioned before a simulation period of 25 years (300 months) is selected to analyze the configurations and depths of the BHE. The calculation methodology used by the program is based on Eskilson’s method for the design of the vertical GSHE [48]. Eskilson’s method uses “g-

functions”, which represent the temperature response of a given borehole configuration to a step-change in heat extraction or injection rate. In this program, the g-functions are calculated using a finite-difference model, developed by the authors of the software. As shown in Figure 4.1, the GLHEPro is used in the second stage of the methodology to size the borehole field. The BHE sizing process with GLHEPro used in this thesis consists of 3 following steps:

1. The first step is comprised of the description of the main borehole, ground, and fluid parameters (g-function parameters). Some of the examples are the type of BHE, pipe spacing, fluid, and ground thermal properties. These parameters are necessary to calculate the borehole thermal resistance. Additionally, the configuration must be defined, as it influences the final depth of the BHE. However, there are different possibilities regarding the distribution of the BHEs in the ground, therefore first a preliminary configuration study will be carried out (section 4.4.2) using the thermal loads from the following step.
2. In the second step, the thermal loads are defined. The program allows for the introduction of either the thermal loads on the heat pump or the ground thermal loads on the heat exchanger. In this project the second possibility is selected, therefore it is not necessary to define the HP parameters. The ground thermal loads used for the BHE sizing in three cities are extracted from TRNSYS simulations (using Design Guide BHE depths), which is further described in section 4.4.2.1.
3. In the last step, the period of the simulation and the desired outlet fluid temperature limit is defined to size the BHE. These outlet temperatures, defined by the DG, constrain the BHE sizing. Using the parameters from step 1, loads from step 2, and the temperature limits established in the DG, GLHEPro computes the final BHE size so that at the end of the simulation period, the temperature of the fluid entering the heat pump would not exceed the established range.

The main objective of this section is to compare the depths of the BHE calculated using the correction factors (DG BHE depths), with the BHE depths calculated in GLHEPro. The methodology used in this 4.4 follows an iterative design process, which means that once the total BHE depth is calculated for each location, the sizing is repeated. The design is done in this way because the ground thermal loads used in the first step are simulated in TRNSYS using the DG depths thus, the BHE fields from the first iteration may be over or undersized. In the second iteration, the ground thermal loads retrieved from TRNSYS are simulated using the BHE fields sized in the first iteration. In this manner, the second iteration results are more accurate.

4.4.1 Defining the G-function parameters

The g-function in GLHEPro is created by specifying the fluid, borehole, and ground parameters. These parameters are necessary for the calculation of the borehole thermal resistance. Considering, that there are three different locations, three different g-functions must be defined. However, most of the parameters regarding the fluid and borehole properties (including the calculated borehole thermal resistance) remain the same for every g-function. The parameters equal for every g-function are listed in Table 4.7.

Table 4.7. Ground loop parameters equal for every g-function.

Group	Parameter	Value
Fluid	Propylene glycol concentration	30%
	Average/freezing point temperature (°C)	6.38/-13.32
	Density (kg/m ³)	1034.51
	Volumetric heat capacity (kJ/°K· m ³)	3932.55
	Conductivity (W/m·°K)	0.43
	Viscosity (Pa·s)	0.00561
	Volumetric flow rate of the system (L/s)	0.6
BHE	Borehole spacing (m)	3
	Borehole diameter (mm)	88
	Inner tube diameters, inside/outside (mm)	28.5/44.5
	Outer tube diameters, inside/outside (mm)	57/63
	Grout's volumetric heat capacity (kJ/°K· m ³)	3500
	Grout's thermal conductivity (W/m·°K)	1.56
	Inner & outer pipe volumetric heat capacity (kJ/°K· m ³)	1542
	Inner/outer pipe thermal conductivity (W/m·°K)	0.20/0.42
	Borehole resistance (°K/(W/m))	0.2392

The parameters that differ between the analyzed cities are the ground thermal conductivity, ground volumetric capacity, and undisturbed ground temperature, all listed before, in Table 3.2. In this study, the only variable parameter of the g-function is the borehole configuration, and its analysis is described in further sections of the document. The rest of the parameters defined for three different g-functions is constant, meaning that once defined, they are not manipulated during the analysis.

4.4.1.1 Borehole field configurations

One of the main objectives of this study is to compare the energy performance of the DSHP between three analyzed cities, therefore, to minimize the number of variables, the same configuration of the borehole field is going to be selected for the system energy assessment in different locations. According to the DG, the available heating capacities (8 or 16 kW) with the integrated drilling technology would require a BHE field of between 4 and 8 heat exchangers. Additionally, the configurations suggested by the DG are: 4 x 1, 2 x 2, 2 x 3, or 2 x 4 layouts. Considering that the HP capacity is 8 kW, and the maximum drilling depth defined in the DG is 60 m, there are several possibilities for the BHE field configuration. The general principle is to use longer boreholes within the allowed limit, mainly to take advantage of more stable temperatures at higher depths. The total BHE lengths calculated in section 4.2.2, took values between 131 and 171 meters thus, the minimum possible number of boreholes in each case is 3. However, in the case of Stockholm and Strasbourg, the calculated depths are close to the maximum total of 180 meters (when 3 BHEs are considered), therefore it is possible, that after verifying the results with simulation software, longer BHEs will be required.

The preliminary analysis of the BHE configuration, optimal for every location, is executed in GLHEPro. In this software, many different configuration layouts are available, some of which are

presented in Figure 4.4. The following 4.4.2 describes both, the process of loads extraction which is necessary for the sizing of the BHEs, and preliminary analysis of the configuration.

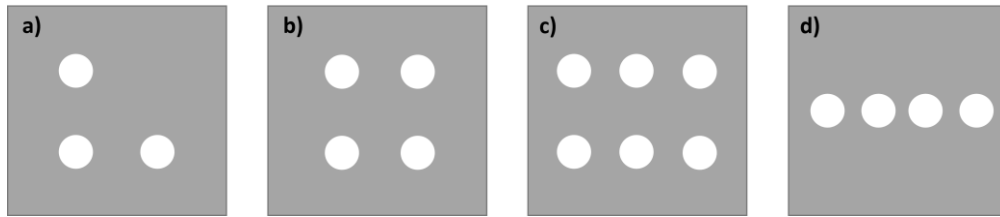


Figure 4.4. Configurations: a) L-configuration 2 x 2; b) Rectangular 2 x 2; c) Rectangular 2 x 3; d) Line 1 x 4.

4.4.2 Preliminary configuration analysis

To carry out the preliminary analysis of the BHE configurations, the ground thermal loads, including the heat extraction and injection, are necessary. As described before, the tool that is used for retrieving the ground thermal loads is the DSHP model developed in TRNSYS. The BHE depths which were calculated using the correction factors from the DG in section 4.2.2 are now used for the first iteration simulations. Following the methodology adopted in previous studies [34], [37], the configuration that will be first simulated is rectangular 2 x 2 (Figure 4.4 b), with 3 meters of spacing. By running the simulations in TRNSYS, the ground thermal loads are printed in an external file, which then is used for the peak load analysis, using the Peak Load Analysis Tool (an instrument provided in the GLHEPro package which in case of this master thesis uses the TRNSYS loads to calculate the peak loads that will serve as an input to the GLHEPro simulation tool). These loads will be used for the preliminary analysis. After executing the preliminary analysis, two configurations will be selected and studied in more detail.

4.4.2.1 Load's extraction

Although in the preliminary configuration analysis only one set of loads will be analyzed per each location, the overall loads' extraction procedure is equal also for the detailed analysis. The only difference between the preliminary and detailed configuration analysis is that in the detailed study the loads are extracted separately for each configuration. The load extraction procedure will be therefore described only for the initial configuration study. As stated before, the set of loads for the preliminary analysis will correspond to the rectangular 2 x 2 configuration with 3 m of spacing between the boreholes. As shown in Figure 4.5, the process of loads extraction consists of 4 steps. First, the DG depths must be divided by the number of boreholes selected for the preliminary analysis (4 BHEs). These depths per-borehole are simulated in TRNSYS to retrieve the hourly ground thermal loads during one year of operation.

Table 4.8. Design Guide depths per borehole for a field of 4 BHEs.

CITY	BHE depth per one borehole (m)
	2 x 2 configuration
STOCKHOLM (171.63 m)	42.66
STRASBOURG (168.00 m)	42.00
ATHENS (131.25 m)	32.81

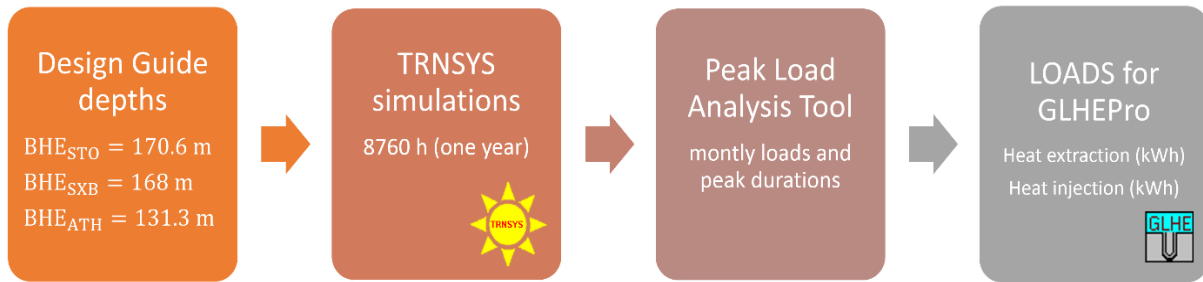


Figure 4.5. Steps of the process of load extraction.

4.4.2.2 Peak load analysis

In the following step, the loads are introduced to the Peak Load Analysis Tool which is an additional instrument provided in the GLHEPro package. Peak loads play an important role in determining the short-term temperature response of ground loop heat exchangers. This additional tool is used for two main tasks:

- It determines the daily peak load profile for heating and cooling operation.
- It allows determining the duration of peak loads (for heating and cooling day). The peak load duration is the number of peak heating and cooling hours during that specific day when the daily peak load occurred. Using these peak heating and cooling durations, the tool calculates the corresponding monthly peak loads.

The peak load analysis procedure is presented below using the example of Athens.

1. After importing the hourly ground thermal loads for one year of operation (printed with TRNSYS), days of maximum heating and cooling loads are encountered. The heating and cooling load profiles are generated for these days, as shown in Figure 4.6.

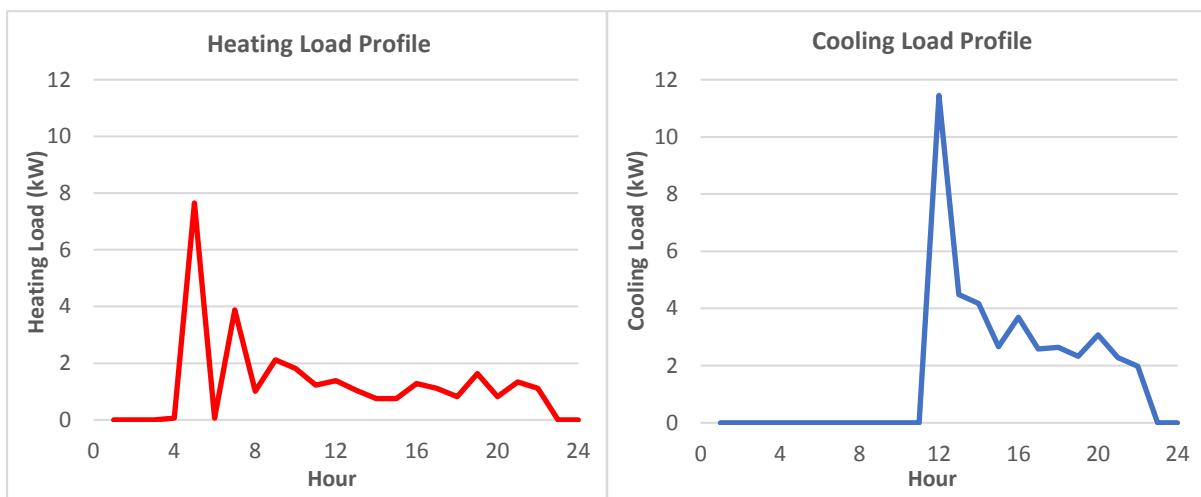


Figure 4.6. Heating and cooling maximum load profiles for Athens.

2. The primary and secondary parameters regarding the ground loop are defined. The primary parameters define the fluid factor (multiplier that gives the amount of fluid in the system relative to the amount of fluid in the GSHE tube, in the case of this project the fluid factor is 2) and one of the two available methods of peak load sampling:

- “Average over duration”, which determines the highest average value for the peak day over the peak duration and uses this value throughout the peak duration. In practice, it means that the program will look for the absolute maximum load during the analyzed day and apply it continuously for each hour of the peak duration.
- “Maximum over duration”, which analyzes the peak day to find the absolute maximum load during that day. Then, it uses this value throughout the peak duration by averaging this sum for the number of hours in the duration to determine the value of the peak load.

The secondary parameters are depicted in Figure 4.7.

System Sizing		U-Tube Size	
Borehole Depth [m]	32.81	Inner Diameter [mm]	44.5
Borehole Radius [mm]	88	Outer Diameter [mm]	63
Thermal Conductivities		Volumetric Heat Capacities	
Pipe [W/(m*K)]	0.42	Pipe [kJ/(m ³ *K)]	1542
Grout [W/(m*K)]	1.56	Grout [kJ/(m ³ *K)]	3500
Ground [W/(m*K)]	3.5	Ground [kJ/(m ³ *K)]	1250
		Fluid [kJ/(m ³ *K)]	3932
Convection Coefficient [W/(m ² *K)]			176
Borehole Thermal Resistance [(m*K)/W]			0.2392

OK

Figure 4.7. Secondary ground loop parameters for Athens (DG depth, 2 x 2 configuration).

3. In this step an iterative determination of heating and cooling peak load durations is carried out, using the heating and cooling day temperature responses. First, the program generates graphs representing the normalized ground temperature response in the day that corresponds to the heating and cooling load profiles from Figure 4.6. By establishing three different values of the peak durations, three different curves are displayed in the graph, and the one that best fits the curve with the hourly response is selected. According to the GLHEPro manual, for both, average and maximum methods, the best-adjusted solution (the one that best represents the peak duration related to the ground temperature response) is the one with the duration curve that reaches the peak value close to $\frac{\Delta T}{\Delta T_{max}} = 1$.

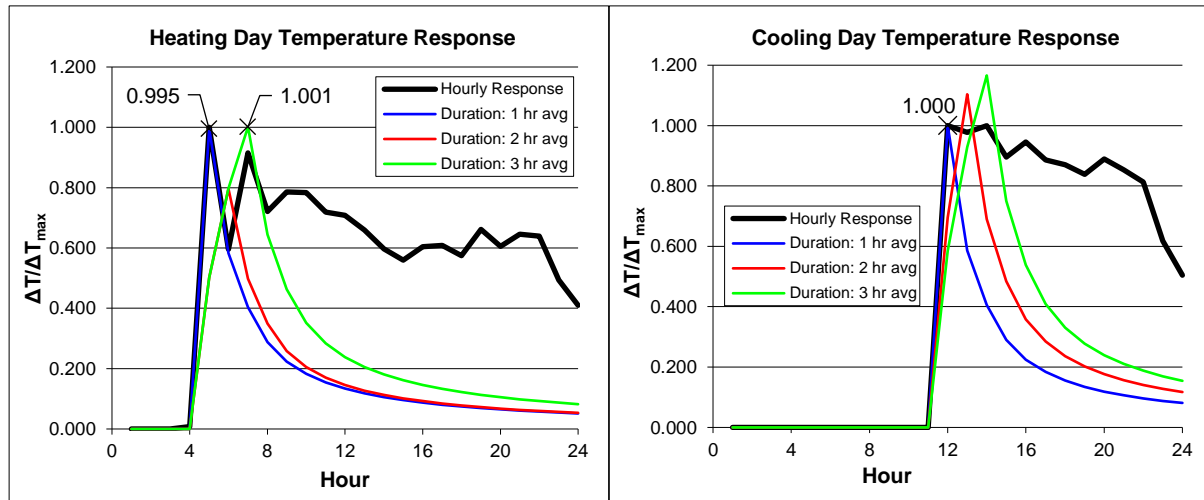


Figure 4.8. Heating and cooling day temperature response using the averaging method.

As seen in Figure 4.8, when the averaging method is considered, in the case of the heating day temperature response the peak duration that best matches the hourly response is 3 h duration (green curve), with $\frac{\Delta T}{\Delta T_{max}} = 1.001$. However, the peak duration of 1 h (blue curve), with $\frac{\Delta T}{\Delta T_{max}} = 1$, best represents the temperature response of the ground on a cooling day. Additionally, to compare the two methods of duration sampling (averaging and maximum), Figure 4.9 is shown below. The left-hand graph, representing the heating day temperature response with the maximum method, has the same value for the 1 h peak duration as with the averaging method. Although it would be the best pick among the three durations from the maximum sampling method, the averaging 3 h duration still best matches the hourly response. On the other hand, in the case of cooling day temperature response, both averaging and maximum method takes the same value for 1 h duration. It means that regardless of which method will be selected, both equally influence the peak loads. In conclusion, the averaging sampling method with durations of 3 h (heating day), and 1 h (cooling day), is selected in the case of Athens.

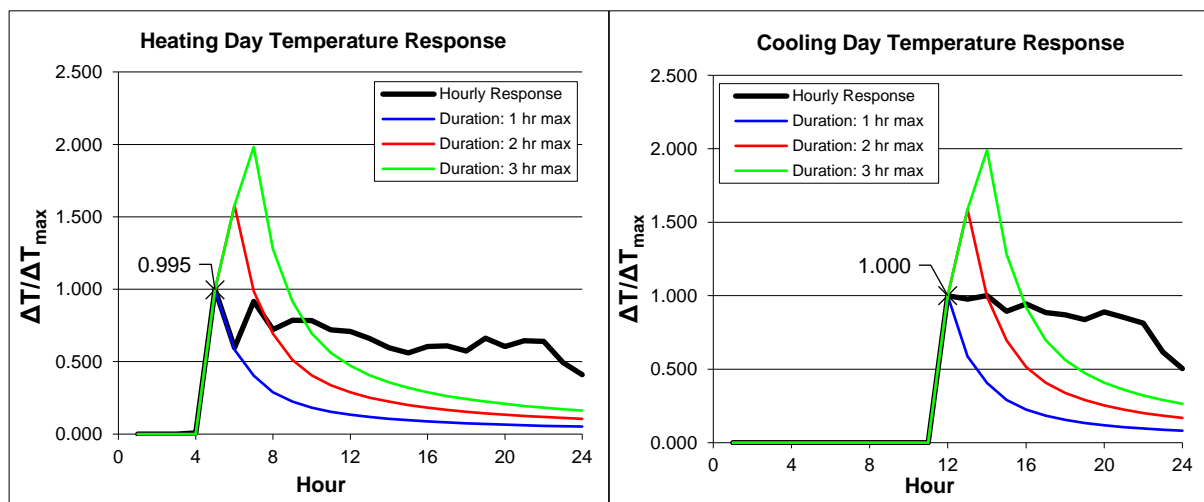


Figure 4.9. Heating and cooling day temperature response using the maximum method.

The procedure described above is repeated for the two remaining locations. Table 4.9 and Table 4.10 summarize the results of the monthly loads, monthly peak loads, and the peak load durations, for the three analyzed cities.

Table 4.9. Monthly loads (kWh) for the preliminary analysis.

Monthly loads (kWh)	STOCKHOLM		STRASBOURG		ATHENS	
	Heat extraction	Heat injection	Heat extraction	Heat injection	Heat extraction	Heat injection
January	1499.9	0	1236	0	839.2	0
February	1382.8	0	969.8	0	671.8	0
March	1283.5	0	655.4	0	560.4	0
April	757.1	0	344.3	0	246.3	0
May	241.4	0	72.8	0	12.5	303.5
June	12.1	0	14	126.2	1.7	669
July	0	0	0	221.2	0	968.3
August	14.3	0	0.8	177	0	947.4
September	99	0	44.5	38.9	4.2	485
October	491.7	0	346.5	0	118.4	116.5
November	789.7	0	810.2	0	410.6	0
December	1319.7	0	1054.7	0	661.4	0

Table 4.10. Peak monthly loads (kW), and peak durations (h) for the preliminary analysis.

Peak loads (kW)	STOCKHOLM		STRASBOURG		ATHENS	
	Heat extraction	Heat injection	Heat extraction	Heat injection	Heat extraction	Heat injection
January	8.8	0	8.7	0	3.9	0
February	7.9	0	7	0	4.4	0
March	7.3	0	5.8	0	4	0
April	6.4	0	4.6	0	2.3	0
May	5	0	3.2	0	0.8	3.6
June	2.9	0	3	3.1	0.3	4.5
July	0	0	0	2.2	0	5.5
August	2.9	0	0.8	2.2	0	11.5
September	3.7	0	3.1	1.7	0.8	4.2
October	6	0	5	0	1.9	2.7
November	6.6	0	6	0	3	0
December	7.2	0	6.7	0	4	0
Peak duration (h)	13	0	1	1	3	1

4.4.2.3 Preliminary configuration analysis results

As stated before, the objective of the preliminary analysis is to select two BHE field configurations that will be further analyzed with TRNSYS simulations. The simulations in GLHEPro of this section are done using one set of monthly and peak monthly loads per city (Table 4.9 and Table 4.10.) The only parameter that will change in this initial study is therefore the borehole configuration. The changes in the BHE field layout influence the total BHE depth. Considering that the DG depths vary between 131 and 171 meters, the configurations selected for the initial analysis are the L-configuration 2 x 2, Rectangular 2 x 2, Rectangular 2 x 3, and Line 1 x 4, previously depicted in Figure 4.4. The number of BHEs in these configurations varies from 3 to 6 BHEs. In this analysis, both actions described in section 4.4 (“sizing” and “simulation”) are used to carry out the simulations. First, the “sizing” action is used, therefore, the user-specified temperature regimes must be defined. The temperature regime for each location is the maximum heating and cooling outlet fluid temperatures specified by the DG (Table 4.6). Table 4.11 recaps the borehole sizing results from the preliminary configuration analysis.

When comparing the results from the preliminary configuration analysis, it is necessary to remark that the maximum achievable depth permitted by the drilling technology is 60 meters. According to this design constrain, the L-configuration with 3 BHEs is applicable only in the case of Athens (52.65 m). The remaining three configurations consist of either 4 or 6 BHEs. The rectangular 2 x 3 configuration composed of 6 BHEs complies with the allowed drilling depth in every city. However, it is at the expense of an increment in total borehole size (up to 4.3% compared to rectangular 2 x 2).

Table 4.11. BHE depths corresponding to each configuration from the preliminary sizing analysis in GLHEPro.

City	Stockholm		Strasbourg		Athens	
	Total size (m)	Size per BHE (m)	Total size (m)	Size per BHE (m)	Total size (m)	Size per BHE (m)
L-config. 2 x 2 (3 BHEs)	269.16	89.72	197.36	65.79	157.94	52.65
Rectangular 2 x 2 (4 BHEs)	277.63	69.41	202.23	50.56	160.25	40.06
Line 1 x 4 (4 BHEs)	269.16	68.38	198.38	49.59	158.26	39.57
Rectangular 2 x 3 (6 BHEs)	289.55	48.26	205.63	34.27	161.84	26.97

Finally, if 4 borehole fields are compared (Rectangular 2 x 2 and Line 1 x 4), the differences in the size of the BHE are relatively small, with a slight preference for the line configuration (up to 3.14% shorter BHE in case of line configuration). Nevertheless, line configurations are characterized by a higher surface requirement due to a less compact layout. Considering the comparison of this section, the two configurations discarded from the further analysis are the L-configuration 2 x 2, due to exceeded maximum drilling depth in every city, and line 1 x 4 configuration, due to disproportion between the additional space requirement versus insufficient BHE size reduction.

Overall, it can be observed that the total borehole depths calculated in GLHEPro are quite different from the BHE depths estimated by the DG. To additionally demonstrate the difference in results, the action of “simulation” is done for every city. The DG BHE sizes for each location are specified in GLHEPro and simulated to obtain the ranges of the outlet temperature. Table 4.12

represents the results of outlet fluid temperatures simulated for rectangular 2 x 2 configuration using the borehole depths suggested by the DG.

Table 4.12. Maximum and minimum outlet temperatures simulated in GLHEPro for the DG BHE depths.

City	Stockholm	Strasbourg	Athens
Simulated Design Guide depth per BHE (m)	42.66	42.00	32.81
Maximum/minimum design fluid temperature (°C)	17/-5.5	24.5/0	30/7
Maximum/minimum fluid temperature result (°C)	4.43/-28.17	10.2/-2.28	39.24/7.04

As Table 4.12 indicates, in the case of Stockholm and Strasbourg, the minimum temperature limits are overstepped, whereas in the case of Athens, the maximum. These results will be further analyzed and verified using simulations in TRNSYS. To conclude the findings from this section, according to GLHEPro, in every location the DG depths are insufficient to meet the design fluid temperatures. The preliminary analysis has shown that, among the analyzed configurations, the most appropriate solution would be the rectangular 2 x 3 configuration, as it meets the limits of the GEOTECH drilling technology. Additionally, the rectangular 2 x 2 configuration will be considered for the detailed analysis, mainly due to its more compact BHE layout which requires less surface and therefore can be applied in a higher variety of locations.

4.4.3 Detailed configuration analysis in GLHEPro

The main difference between the preliminary and detailed configuration analysis is that the detailed analysis considers a new set of loads for every configuration simulated for the different cities. Additionally, a second iteration is carried out, which allows for a more accurate estimation of the BHE size. However, the second iteration study requires previous verification of the results using TRNSYS, therefore it will be considered in the further section (4.5.1.2) of the study. The analysis from the prior section already explained the process of the loads' extraction (using TRNSYS simulations) and peak load analysis (using the Peak Load Analysis Tool); therefore, it will be not once again described.

4.4.3.1 First iteration sizing results

Table 4.13 recaps the first iteration results for both 2 x 2 and 2 x 3 configurations.

Table 4.13. First iteration sizing results with GLHEPro.

Configuration	2 x 2 (4 BHEs)		2 x 3 (6 BHEs)	
	Total size (m)	Size per BHE (m)	Total size (m)	Size per BHE (m)
Stockholm	277.74	69.44	288.68	48.11
Strasbourg	202.27	50.57	205.20	34.25
Athens	160.25	40.06	136.81	22.80

To compare not only the differences between the two configurations sized in GLHEPro but also the differences between the sizing from DG and GLHEPro, it is worth remarking the borehole depths calculated using the correction factors. The total DG depths along with their corresponding depths-per-borehole for two configurations are presented in Table 4.14.

Table 4.14. Total and per-borehole depth for two configurations using the Design Guide.

Configuration	Total size (m)	2 x 2; Size per BHE (m)	2 x 3; Size per BHE (m)
Stockholm	171.63	42.66	28.61
Strasbourg	168.00	42.00	28.00
Athens	131.25	32.81	21.875

Although there are significant differences between the DG and GLHEPro results for the total size of the BHE, it may be observed that the order of magnitude between the results for the three cities is maintained (Stockholm>Strasbourg>Athens). Additionally, in every city, and for each configuration, the GLHEPro results suggest using larger boreholes than the DG (4.1% to 40.5% of difference depending on city and configuration). The biggest difference in results is noticed in the case of Stockholm if a 2 x 3 configuration is used; over 117 meters of difference compared to the depth from the Design Guide. Moreover, comparing the two configurations sized in GLHEPro, it is seen that in Stockholm and Strasbourg the total borehole size is shorter for the fields with 4 BHEs. The main reason for this is that in the case of cold climates the ground at deeper layers offers more favorable temperatures, which are less influenced by the ambient temperature. In other words, if the total BHE depth for 2 x 2 configuration would be adopted to 2 x 3 configuration, likely, the design fluid temperatures would not be achieved. However, in the case of Athens, the results point to using a higher number of shorter boreholes to reduce the total BHE depth. The possible explanation for this circumstance is the different peak load duration in heating (1 hour instead of 3 hours) used in the case of 2 x 3 configuration. Although a 1-hour duration is more suitable for a field of 6 BHEs, to verify this event, a 3 h duration for heating day temperature response was used for the loads' calculation (the same as in Table 4.10). As a result, 141.49 meters of total borehole depth was obtained, thus only a small increase in BHE depth is noticed. Nevertheless, considering that not only the different peak durations were used, but also different loads were introduced in GLHEPro, this could be the cause for the resulting difference in size between the two configurations.

4.5 BHE sizing with TRNSYS

In this section, the results of BHE sizing done with the DG and GLHEPro are verified. The verification of the results is carried out in TRNSYS using the DSHP model. The DSHP model developed in TRNSYS is a very precise tool for the reproduction of the actual system performance, as it includes the dynamic interaction of the different system components (building thermal loads, DSHP, B2G model, control board, etc.), therefore it is likely that differences in results will appear. By simulating the different BHE depths the evolution of the maximum and minimum outlet fluid temperatures is captured and may be used to compare the results. Additionally, in case of a significant mismatch between the results, alternative BHE depths will be proposed to reach the temperature limits

established by the DG. In consequence, three different sources of results for the BHE depth will be analyzed:

- DG (BHE depths calculated with the correction factors),
- GLHEPro (BHE depths calculated using a commercial tool for GSHE systems),
- TRNSYS DSHP model (alternative BHE depths that meet the design fluid temperatures),

whereas the DSHP model developed in TRNSYS will be used to verify the results by simulating each corresponding borehole depth. These simulations from TRNSYS provide additional information regarding the heat pump operation (energy consumptions and percentage of operation beyond the design temperature limit), which will be used in the final stage of the design process to compare the three sources of results and to select the most suitable borehole depth for each city.

4.5.1 Outlet temperature verification

One of the main constraints for the design of the DSHP systems provided by the GEOTeCH guidelines is the design of fluid temperature at the outlet of the BHE field. This section is dedicated to the analysis of the long-term outlet fluid temperature evolution for the different BHE depths. It is expected that the BHE depths calculated with the DG and with GLHEPro, may be either exaggerated or insufficient to meet the required temperatures. The long-term analysis (25 years) will include:

- The evolution of the minimum and maximum peak outlet fluid temperatures.
- The evolution of lowest/highest average monthly outlet fluid temperature.

First, the DG depths for 2 x 2 configuration are simulated (Stockholm 42.66 m; Strasbourg 42 m; Athens 32.81 m). Figure 4.10 represents the evolution of the maximum, minimum, and average (minimum or maximum) monthly temperature for the three analyzed cities. The horizontal lines in the graph represent the design fluid temperatures established by the DG. The minimum and maximum outlet fluid temperatures found for each following year correspond to the blue and orange curves, respectively. In general, according to the temperature verification in TRNSYS, in none of the cities both temperature limits are met during the whole simulation period. It can be observed, that in the case of Stockholm (a) and Strasbourg (b) the problem occurs with the minimum outlet temperatures, whereas in Athens (c) with the maximum. Additionally, in the case of Stockholm and Strasbourg, the minimum outlet temperature exceeds the established limit every year, never meeting the minimum limit. In Athens, however, during the first 6 years of the simulation, the maximum outlet temperatures are within the desired range. Then, periodically (in 1 – 3 years intervals), the maximum temperature peaks over the allowed limit (30°C), however in the next year always returns below the horizontal line. Figure 4.10 shows, that in cold, heating-dominated climates, the minimum temperature limits are overstepped, and they tend to slightly decrease along the analyzed period (average annual decrease of 1.85% in Stockholm, and 4.5% in Strasbourg). This is due to the predominant heat extraction from the ground. In the case of Athens (warm climate), the maximum temperature limit is exceeded, however, the outlet temperatures are relatively constant (excluding the peaks of maximum temperature which will be further analyzed). The lack of increase or decrease in temperature is related to the balanced share of demand for heating and cooling. Considering that the tendencies for the three cities observed in Figure 4.10 are likely to repeat for other BHE sizes and that the DG depths are considered as a reference because they are the smallest of all analyzed results, further analysis will not include the graphs of the temperature evolution, but only summarized information regarding:

- The minimum and maximum peak outlet temperature noticed during the 25 years.

- The temperature of the coldest and warmest months during the period of analysis.

Table 4.15 and Table 4.16 summarize the outlet fluid temperatures (for 2 x 2 and 2 x 3 configuration respectively) corresponding to the analyzed borehole depths in different cities.

Table 4.15. Outlet fluid temperatures for 2 x 2 configurations from TRNSYS.

CITY	Stockholm		Strasbourg		Athens	
	DG	GLHEPro	DG	GLHEPro	DG	GLHEPro
Source of result	DG	GLHEPro	DG	GLHEPro	DG	GLHEPro
Total size (m)	171	278	168	204	131	160
Size per BHE (m)	43	69	42	51	33	40
Min. peak temp. (°C) at month/year	-10.8 Feb/21	-3.7 Feb/21	-4.3 Jan/19	-1.8 Jan/19	8.0 Feb/10	9.7 Feb/5
Max. peak temp. (°C) at month/year	9.8 Jul/1	10.0 Jul/1	14.0 Jul/1	14.1 Jul/1	38.5 Aug/14	34.9 Aug/14
Min. average temp. (°C) coldest month	-2.3 Feb/21	0.4 Feb/21	-0.2 Jan/25	1.9 Jan/25	13.8 Feb/3	14.4 Feb/3
Max. average temp. (°C) warmest month	5.3 Jul/1	5.5 Jul/1	10.6 Jul/1	10.5 Jul/1	22.3 Aug/14	21.5 Aug/14

Table 4.16. Outlet fluid temperatures for 2 x 3 configurations from TRNSYS.

CITY	Stockholm		Strasbourg		Athens	
	DG	GLHEPro	DG	GLHEPro	DG	GLHEPro
Source of result	DG	GLHEPro	DG	GLHEPro	DG	GLHEPro
Total size (m)	171	289	168	206	131	137
Size per BHE (m)	28	48	28	34	22	23
Min. peak temp. (°C) at month/year	-12.4 Feb/24	-4.1 Feb/21	-4.9 Jan/19	-2.3 Jan/19	7.7 Feb/10	8.0 Feb/5
Max. peak temp. (°C) at month/year	9.4 Jul/1	9.9 Jul/1	13.6 Jul/1	13.8 Jul/1	39.3 Aug/7	38.5 Aug/14
Min. average temp. (°C) coldest month	-2.7 Feb/21	-0.1 Feb/21	-0.4 Jan/25	1.5 Jan/25	13.6 Feb/2	13.8 Feb/2
Max. average temp. (°C) warmest month	5.0 Jul/1	5.4 Jul/1	9.6 Jul/1	10.2 Jul/1	22.5 Aug/16	22.3 Aug/14

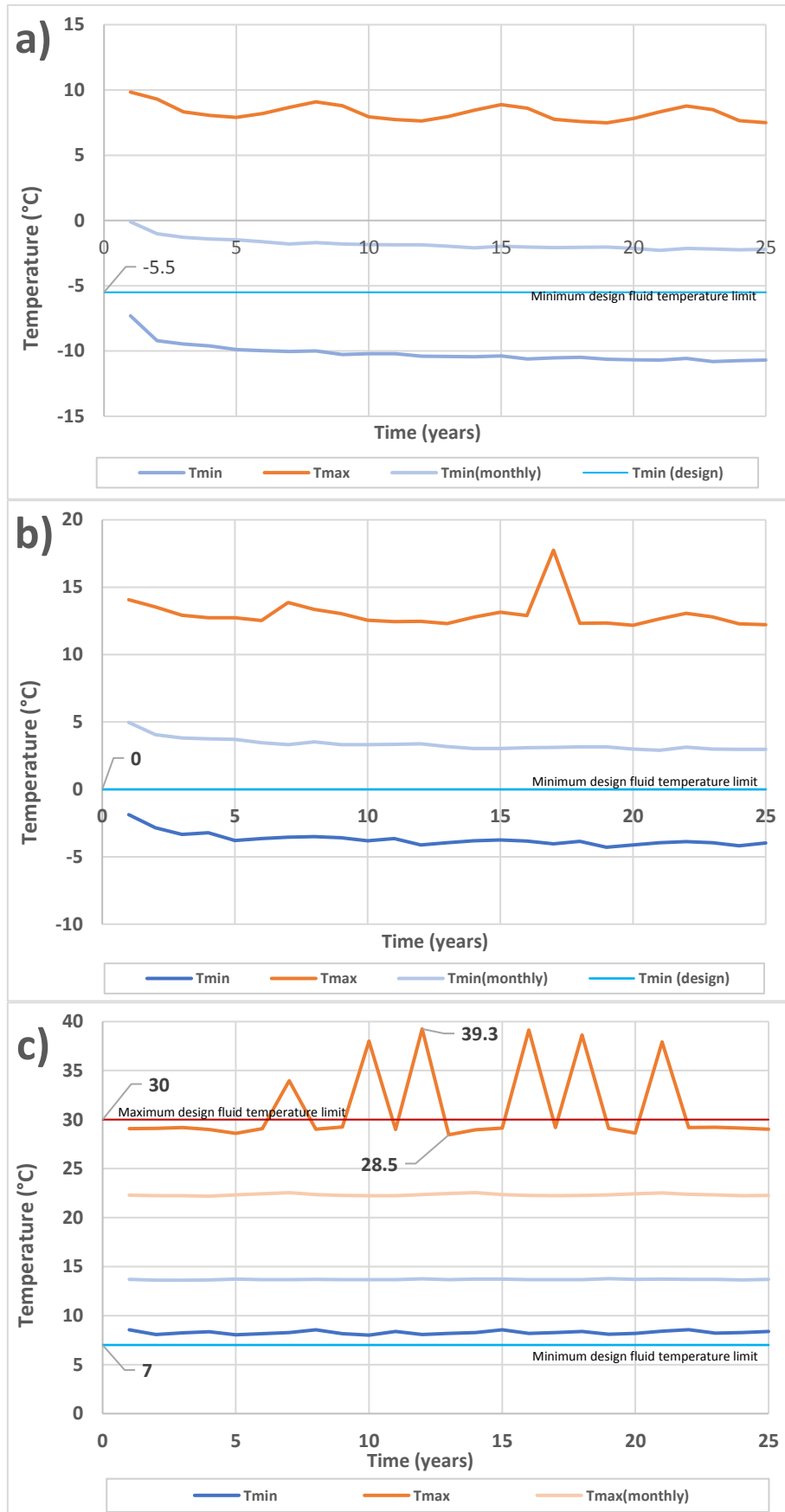


Figure 4.10. Outlet temperatures for 2 x 2 DG depths in: (a) Stockholm, (b) Strasbourg, (c) Athens.

First, it should be noticed, that in the case of the DG the total size of the borehole is kept the same for both configurations. This is because the Design Guide does not include any correction factor regarding the configuration. The verification in TRNSYS, however, points out that if the number of boreholes increase but the total size is kept equal, it has a negative impact on the outlet fluid temperatures. This might be observed in the example of the DG results when passing from 2 x 2 to 2 x 3 configuration; Stockholm’s and Strasbourg’s minimum peak temperatures get even lower, whereas the maximum peak temperature in Athens increases. In the case of Stockholm and Strasbourg, the tendency is therefore consistent with the results obtained from GLHEPro (section 4.4.3.1), however in Athens it is not (in GLHEPro, the design fluid temperatures for 2 x 3 configuration were achieved with a 23.2 m shorter borehole). Therefore, if only DG depths were considered, the 2 x 2 configuration should be selected over the 2 x 3 configuration. In this context it is worth reminding Table 4.12, with temperature results for DG depths directly simulated in GLHEPro, recalled below:

***Table 4.12’s fragment**

CITY	STOCKHOLM	STRASBOURG	ATHENS
Maximum/minimum fluid temperature result (°C)	4.43/-28.17	10.2/-2.28	39.24/7.04

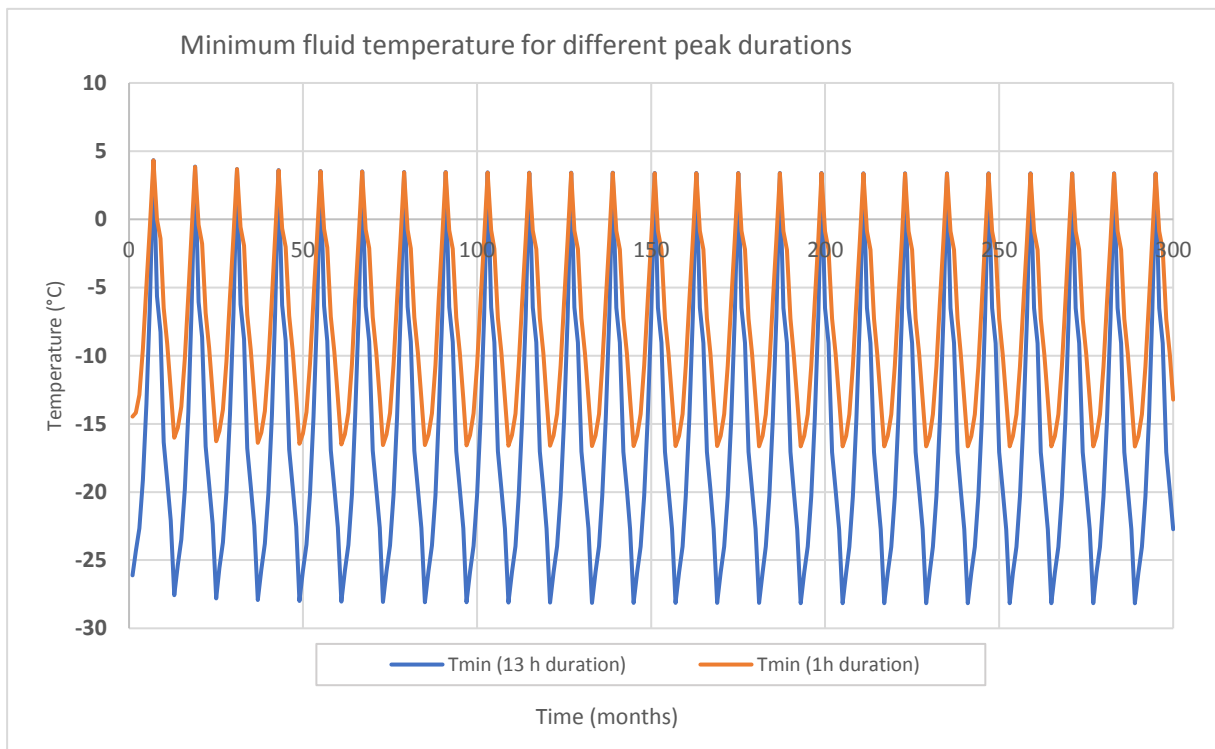


Figure 4.11. Minimum fluid temperature evolution in Stockholm using different peak durations.

Comparing the maximum and minimum fluid temperatures obtained in the GLHEPro simulation tool, with the temperatures obtained from the TRNSYS (both are simulations for the DG borehole depths using 2 x 2 configuration), it may be seen that GLHEPro minimum fluid temperatures are lower, especially in the case of Stockholm. In part, it is caused by the high number of peak duration hours (13 h) used to calculate peak heating loads (look Table 4.10). In fact, if a 1-hour duration is selected to

compute the loads for GLHEPro, the minimum fluid temperature increases from $-28.17\text{ }^{\circ}\text{C}$ to $-16.66\text{ }^{\circ}\text{C}$, which is much closer to the temperature obtained in TRNSYS ($-10.8\text{ }^{\circ}\text{C}$).

Nevertheless, the duration of 13 hours is determined following the instructions provided in the GLHEPro manual, and although one may argue on the accuracy of this peak load approximation method, this will not be questioned in the master thesis.

For Stockholm's 2×2 configuration, the GLHEPro sizing results suggested using a 69-meter-long borehole to meet the design temperatures. However, the TRNSYS verification points out that it is not necessary to drill a borehole that large, as the minimum peak temperature, never drops below $-3.7\text{ }^{\circ}\text{C}$ during the 25 years. Additionally, this drilling depth is not allowed according to the GEOTECH design constraints. In remaining locations (for both 2×2 and 2×3 configuration), according to TRNSYS, the increment in BHE size between DG and GLHEPro is not sufficient, because the temperature limits are not obeyed.

Considering the above, the assumption made at the beginning of this section is correct; the GLHEPro borehole depths are either exaggerated (Stockholm) or insufficient (Athens and Strasbourg) to meet the required temperatures. Additionally, based on the comparative analysis between the two configurations, more favorable results are achieved for the 2×2 than for the 2×3 configuration. Although, most of the tendencies are respected (i.e., the preference of the longer boreholes but lower in number, or the order of magnitude of the BHE size between the cities), so far, the analysis indicates that it is necessary to select alternative sizes of the BHE to meet the design fluid temperatures.

4.5.1.1 Alternative borehole depths

The following section aims to design an alternative BHE size using the minimum (Stockholm, Strasbourg) or the maximum (Athens) outlet fluid temperature as a design parameter. To accomplish this objective a parametric study is carried out by varying the values of borehole depth and using the design fluid temperature as a constraining factor in each location. Although the methodology and results provided in this section are brief, in practice it was one of the largest tasks to perform, due to the long duration of a single simulation in TRNSYS (over 12 hours). Figure 4.12 represents the outlet fluid temperature evolution for three different cities. In the case of Stockholm (a) and Strasbourg (b), the BHE depth is adjusted to reach the minimum design temperature. In both cases, the final borehole depth for which the desired temperature was achieved with approximately 60 meters. In Athens (c), the maximum temperature limit ($30\text{ }^{\circ}\text{C}$) is reached for a borehole size of 56 m. Following the same approach, the results for the 2×3 configuration were obtained. Table 4.17 recaps the alternative borehole sizes for both, 2×2 and 2×3 configurations, obtained from the TRNSYS simulations.

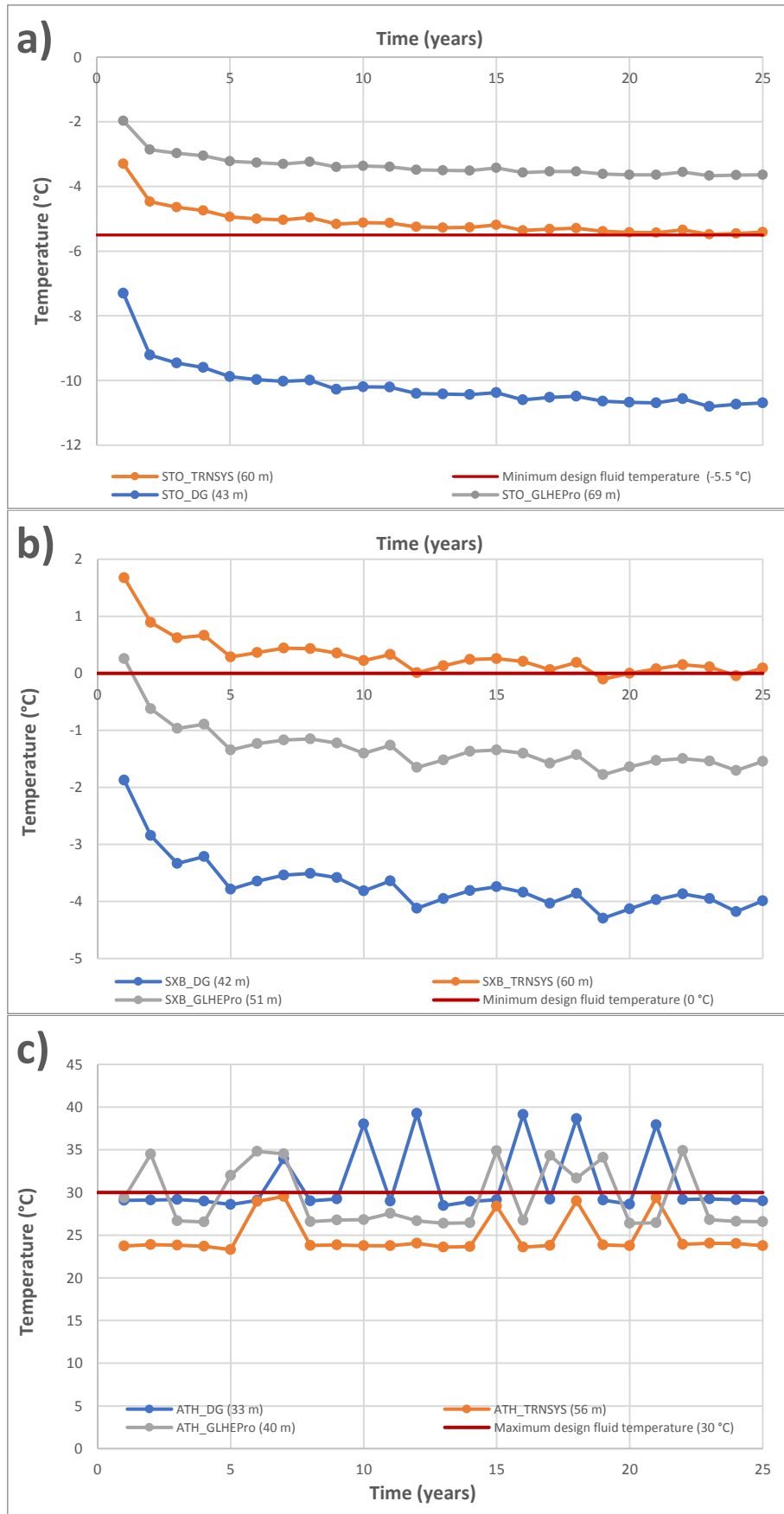


Figure 4.12. Peak fluid temperature for 2 x 2 configuration in (a) Stockholm, (b) Strasbourg, (c) Athens.

Table 4.17. Summary for the alternative BHE sizes.

CITY	Stockholm		Strasbourg		Athens	
Configuration	2 x 2	2 x 3	2 x 2	2 x 3	2 x 2	2 x 3
Total size (m)	238	258	240	270	224	224
Size per borehole (m)	59.5	43	60	45	56	37.3
Design fluid temperatures (°C)	Min. -5.5 Max. 17		Min. 0 Max. 24		Min. 7 Max. 30	
Min. or max peak temp. reached (°C)	-5.5	-5.5	-0.1	0	29.5	30.0

As it may be observed, in the case of 4 BHE configuration, in every city, the peak outlet temperatures are reached within the maximum 60 m of depth allowed by the GEOTECH drilling technology. It means that the 2 x 3 configuration may be discarded from the future analysis, as its use would present no benefits, and would create unnecessary expenditure due to the drilling of two additional boreholes.

4.5.1.2 The second iteration in GLHEPro

To complete the design process in GLHEPro described in section 4.4, second iteration sizing is carried out. The ground thermal loads used for the second iteration are simulated for the alternative borehole depths obtained with TRNSYS (Table 4.17). The purpose of this section is to verify if the newly used loads will influence the final BHE depth, making the GLHEPro sizes more consistent with the TRNSYS results. Table 4.18 summarizes not only the results for the first and second iteration in GLHEPro but also the sizes obtained with TRNSYS.

Table 4.18. The summary of borehole depths from TRNSYS, and both iterations from GLHEPro.

CITY	Stockholm			Strasbourg			Athens		
Iteration	1 st	TRNSYS	2 nd	1 st	TRNSYS	2 nd	1 st	TRNSYS	2 nd
Total BHE size (m)	277.7	238	263.4	202.3	240	206.9	160.3	224	206.6
Size per borehole (m)	69.4	59.5	65.9	50.6	60	51.7	40.1	56	51.7

As Table 4.18 indicates, the second iteration's boreholes sized in GLHEPro if compared with their first iteration's equivalents, take more similar values to the results from TRNSYS. The best convergence between TRNSYS and the 2nd iteration is achieved in the case of Stockholm and Athens, where differences in the size of a single borehole are 6.4 m (Stockholm) and 4.3 m (Athens), corresponding to 9.7% and 7.7%, respectively. For Strasbourg, the results slightly more deviate as there is a 13.8% difference between the borehole size from TRNSYS and the 2nd iteration. The second iteration indicates how the properly defined ground thermal loads can influence the BHE design process in GLHEPro.

4.6 Techno-economic analysis

In the previous sections of this chapter, two different sets of results for the BHE depth determination were analyzed (DG and GLHEPro), and third, an alternative set of results was proposed

using TRNSYS. However, the analysis of the different sets of results was mainly based on the outlet fluid temperature examination, which may be not sufficient to discard one option or another. In this section, a more detailed study will be carried out, including:

- The analysis of the percentage of operation beyond the temperature limit.
- The DSHP consumption analysis.
- The drilling cost analysis in different locations.

The first two analyses will be performed using the data retrieved from the TRNSYS simulations which were previously used to analyze the outlet fluid temperatures. The second study will examine the drilling cost in three different European locations, to provide data that will allow for comparison of the energy savings due to a longer BHE versus the additional cost related to the drilling. The main objective of this section is to understand the techno-economic consequences of using different BHE sizes in the DSHP system that will allow for the selection of the final BHE depth in each analyzed location. The simple way of describing the methodology used to select the final borehole depth can be depicted using Figure 4.13.

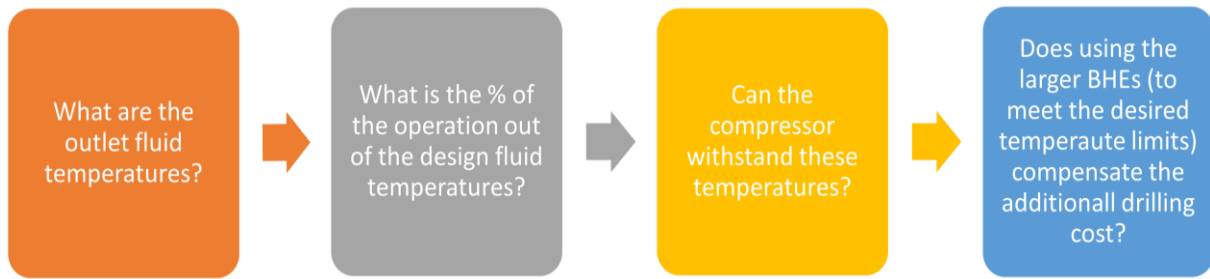


Figure 4.13. Methodology flux for the comparative BHE depth analysis.

4.6.1.1 The percentage of operation beyond the temperature limit

As shown in Figure 4.13, apart from identifying the outlet fluid temperatures, it is important to verify what is the share of occurrence of these temperatures in the 25 years operation period. This analysis is executed using the available data sets extracted from the TRNSYS simulations, and the DSHP operating time based on the schedule of the heat pump. The available data of the outlet fluid temperatures are registered at a timestep of 5 minutes (12 intervals per hour). To estimate the percentage of operation beyond the design guide limits it is assumed that the same temperature occurs throughout the whole duration of the time step. The 5-minute intervals are then summed during the whole period of analysis and divided by the number of intervals per hour. The calculation of the operating hours is done using both the DHW and air-conditioning schedules:

- Air-conditioning: from 6 a.m. to 10 p.m. (16 h).
- DHW production: from 4 a.m. to 6 a.m. (2 h).

Considering that there are no scheduled holidays, and the only period when the HP is off is on weekends, the estimated operating time is calculated as follows:

$$T_{\text{operation}} = 18 \left(\frac{\text{hour}}{\text{day}} \right) \cdot 5 \left(\frac{\text{day}}{\text{week}} \right) \cdot 52 \left(\frac{\text{week}}{\text{year}} \right) \cdot 25 \text{ (years)} = 117,000 \text{ hours}$$

The hours of operation when the outlet fluid temperature is below or above the design limit in Stockholm, Strasbourg, and Athens, along with the corresponding proportion during the whole time of operation (117,000 h), are summarized below.

Table 4.19. Percentage of operation of the DSHP out of the design temperature limits.

CITY	Stockholm			Strasbourg			Athens		
	DG	GLHE Pro	TRNSYS	DG	GLHE Pro	TRNSYS	DG	GLHE Pro	TRNSYS
Total BHE size (m)	170.6	277.7	238	168	202.3	240	131.3	160.3	224
Operation out of limit (h)	3050	0	0	5547	342	2	17	11	0
Operation out of limit (%)	2.61	0	0	4.74	0.29	0	0.01	0.01	0

As Table 4.19 indicates, in the case of boreholes sized with the design guide, which are the shortest among the 3 sources of result, the DSHP operates only in a small percentage of time beyond the established design temperatures (up to 4.74% in case of Strasbourg). Interestingly, in Athens, although the maximum outlet temperature was overstepped by a high value of around 9 °C, the registered peaks must have been momentary, because the outlet temperature exceeded the limit for only 17 hours during the entire system operation. Additionally, according to Figure 4.12(c), the instantaneous peaks have not even once occurred in 19 out of 25 years of the system simulation. Therefore, in the case of Athens, it is unnecessary to increase the BHE depth by 92.7 meters only to cover 17 hours of undesired operating conditions. In the case of the remaining two locations, the undesired outlet temperatures are registered each year, with an increasing annual rate, caused by predominant heat extraction from the ground. On the other hand, the overall percentage of the operation beyond the temperature range is low in both cases, therefore, at this point, they are not discarded from further analysis.

4.6.1.2 The compressor data

Once the number of hours and the corresponding percentage of operation beyond the established limits is assessed, the next step is to verify if the compressor can withstand these temperature regimes. The fluid leaving the borehole field enters the heat pump at the inlet of a heat exchanger. The pressure change between the evaporator and the condenser is driven by a compressor, which in the case of this DSHP is a variable speed compressor. The vapor compression cycle depends on the evaporation and condensation temperatures which react to a change in pressure driven by a compressor. As shown in the table below, the compressor used in this heat pump unit has an operating temperature range of -25 up to 65°C, whereas the minimum and maximum fluid temperatures registered in the simulations were -10.8°C (Stockholm) and 39.3°C (Athens), respectively. Assuming a 5-10°C difference between the outlet of the ground loop and the evaporation/condensation temperature in the refrigeration circuit, the compressor should not present any problems by operating in the design guide temperature regime in any of the analyzed locations.

Table 4.20. Data of the variable speed compressor of the DSHP unit [39].

General data	
Producent	Copeland
Model and type	XHV0251P – variable speed & inverter
Volume of displacement	25 cm ³ /rev
Refrigerant and oil	R32 - Copeland Ultra 32-3MAF
Frequency range	20-120 rps
Pressure limit (H/L)	43.3/28 bar
Temperatures of operation	
Condensation	≤ 65°C
Evaporation	-25/15°C

4.6.1.3 Consumption savings analysis

The previous analysis has shown that the temperature regime is not a sufficient factor to reject the borehole sizes calculated with the DG, which was additionally supported by verifying the evaporation and condensation temperature limits of the compressor. The following section intends to analyze the changes in the consumption of the DSHP caused by adopting different sizes of the borehole heat exchanger to the system. As a rule, the longer the BHE, the better the efficiency of the system, therefore, less energy is consumed by the heat pump. The total energy consumption of the system is calculated using the long-term simulation results. In the simulations the electrical energy use is registered by integrating the power input in the different system components listed below:

- The heat pump includes the consumption of the compressor and fan. Additionally, parasitic energy losses due to the consumption of the electronics (and energizing the solenoid valves) are involved in the heat pump consumption.
- The fan coils distribute the heat to the building. The total consumption is calculated as a sum of the individual fan coil consumptions, which depend on the time and speed of operation.
- Three circulation pumps, one per loop. Here, the important factor plays the pressure drop in each of the BPHE, which is necessary for calculating the electric consumption of the circulation pump in each loop.

These consumptions, together with the useful heat provided to the user in form of air-conditioning and DHW, can be used to calculate the SPF4 (4). However, the system efficiency and seasonal performance will be analyzed in section 5, dedicated to the energy assessment of the system. The following Table 4.21 recaps the energy consumption of the heat pump components during the 25 years of operation.

Table 4.21. The energy consumption of the HP components during 25 years of operation (in kWh).

CITY	Stockholm			Strasbourg			Athens		
	DG	GLHE Pro	TRNSYS	DG	GLHE Pro	TRNSYS	DG	GLHE Pro	TRNSYS
BHE size (m)	170.6	277.7	238	168	202.3	240	131.3	160.3	224
\dot{W}_{HP}	94088	91115	91952	67768	66707	66028	45484	44188	42967
\dot{W}_{FAN}	2316	2228	2273	1886	1795	1717	294	280	257
\dot{W}_{BHE}	3062	3656	3418	2327	2542	2700	2367	2534	2817
\dot{W}_{USER}	2325	2351	2344	1965	1981	1986	2417	2488	2492
\dot{W}_{DHW}	47	48	48	46	46	47	45	46	47
\dot{W}_{total} (kWh)	101838	99398	100034	74038	73071	72477	50607	49536	48580

The DG results are considered as a reference case for the comparison between the three sources of results. As anticipated, if the BHE is larger, the total energy consumption is lower in each analyzed city. This is due to the more favorable temperatures which leave the BHE field and enter the evaporator, creating a less demanding operational regime for the compressor, which consumption has the biggest share among other components of the system (c.a. 90%). It may be observed by analyzing the consumption of the heat pump (\dot{W}_{HP}), which decreases along with the increase in borehole depth. On the other hand, the consumptions of the circulation pumps tend to be higher for larger boreholes. It is caused by an increase in the amount of fluid that circulates in the system and needs to be pumped to flow back to the BHE field. However, in each city the energy consumed by the circulation pumps corresponds approximately to 5-6% of the total, thus has little impact on the overall energy consumption balance. Finally, it is possible to calculate the financial benefit related to the higher efficiency of the system with a larger borehole. It can be done, by simply applying the electricity cost in each location to the corresponding energy savings. The energy savings of the different options compared to the reference case, and their corresponding economic savings are presented below. The average electricity prices, calculated by Eurostat, include taxes, levies, and VAT for household consumers, and correspond to the second half of the year 2020 [49].

Table 4.22. Electrical energy and financial savings in reference to design guide result in 25 years.

Stockholm	Strasbourg	Athens
Electricity cost: 0.1718 €/kWh	Electricity cost: 0.1958 €/kWh	Electricity cost: 0.1641 €/kWh
DG vs GLHEPro	DG vs GLHEPro	DG vs GLHEPro
$\begin{array}{r} 101,838 \\ - 99,398 \\ \hline 2440 \text{ kWh} \end{array}$	$\begin{array}{r} 74,038 \\ - 73,071 \\ \hline 967 \text{ kWh} \end{array}$	$\begin{array}{r} 50,607 \\ - 49,536 \\ \hline 1071 \text{ kWh} \end{array}$
Savings: <u>419.2 €</u>	Savings: <u>189.3 €</u>	Savings: <u>175.8 €</u>
DG vs TRNSYS	DG vs TRNSYS	DG vs TRNSYS
$\begin{array}{r} 101,838 \\ - 100,034 \\ \hline 1804 \text{ kWh} \end{array}$	$\begin{array}{r} 74,038 \\ - 72,477 \\ \hline 1561 \text{ kWh} \end{array}$	$\begin{array}{r} 50,607 \\ - 48,580 \\ \hline 2027 \text{ kWh} \end{array}$
Savings: <u>309.9 €</u>	Savings: <u>305.6 €</u>	Savings: <u>332.6 €</u>

4.6.1.4 Drilling cost study

One of the main barriers to the widespread application of the vertical GSHP systems is the high cost of the GSHE, which is mainly related to the drilling, grouting, purchasing, and installing of the BHE. According to a German study by Blum et. al., the capital cost of a single GSHP system with about 200 meters of total depth and 2 BHEs, can cost between 23,500 € ± 6800 €, whereas approximately 51% of the capital costs correspond to the vertical GSHE [50]. The share of the BHE and drilling-related costs increase even more if a higher number of boreholes were installed. Moreover, many studies point out that the local market dynamics and economy of scale play a crucial role in establishing the drilling cost, which differs from one country to another [31], [50]. Additionally, factors such as the ground lithology and type of BHE have a great impact on the excavation cost, as they often imply the use of a different type of drilling technology [51]. This project considers three cities located in different countries (Sweden, France, and Greece); therefore, three costs related to drilling are determined. Presumably, the drilling cost will differ between the analyzed countries; mainly due to GSHP systems deployment in the market, but also due to the ground composition factors involved. Considering the above, the drilling cost study provides only an estimation for the excavation cost, used to compare the additional cost of the installation (due to the drilling) versus the generated energy savings (due to using larger BHEs).

Sweden (Stockholm)

Sweden is a country that has a long history of geothermal energy utilization, which starts in the 1970s when nationwide efforts were undertaken to achieve an oil-independent energy system. Since the 1990s, geothermal energy use in Sweden is almost entirely based on shallow geothermal applications [52]. In 2013, more than 350,000 shallow geothermal heat pumps have been installed (mainly in the residential sector), covering approximately 10% of Swedish heat demand [53]. Moreover, according to the World Geothermal Congress Proceedings, in 2019 the shallow GSHP systems provided approximately 17.1 TWh of heating energy, while the total installed heating capacity was 6,680 MW_{th}

[54]. With around 27,000 units installed each year, Sweden is one of the European leaders in the GSHP market. Such a great GSHP deployment in the market not only influences the drilling price but also makes the costs more available and easier to retrieve.

The drilling cost used in the case of Sweden is determined using the report “*Deep Boreholes for Ground-Source Heat Pumps*”, by research program Effsys Expand, which was funded by the Swedish Energy Agency [55]. The data collected in this Swedish study were retrieved from a survey run during a reunion of Swedish driller associations. The questions asked in the survey were for a BHE diameter of 115 mm, the prices were given for ranges of depth (50-150; 150-250; 250-350) and did not specify the drilling precision. Regarding this master thesis, the range of depth applicable for the calculated BHE sizes is 150-250 meters. As may be seen in Figure 4.14, the answers given for this range indicated prices between 130 and 150 SEK/m (13 – 25 €/m), excluding VAT. However, this price does not consider other costs related to drilling such as the establishment and removal of the drill rig, manifolds, trench digging for pipe connection to the heat pump, or the BHE itself. Additionally, one of the findings of the survey was that the number of boreholes in the ground loop does not have a significant impact on the price per meter of drilling.

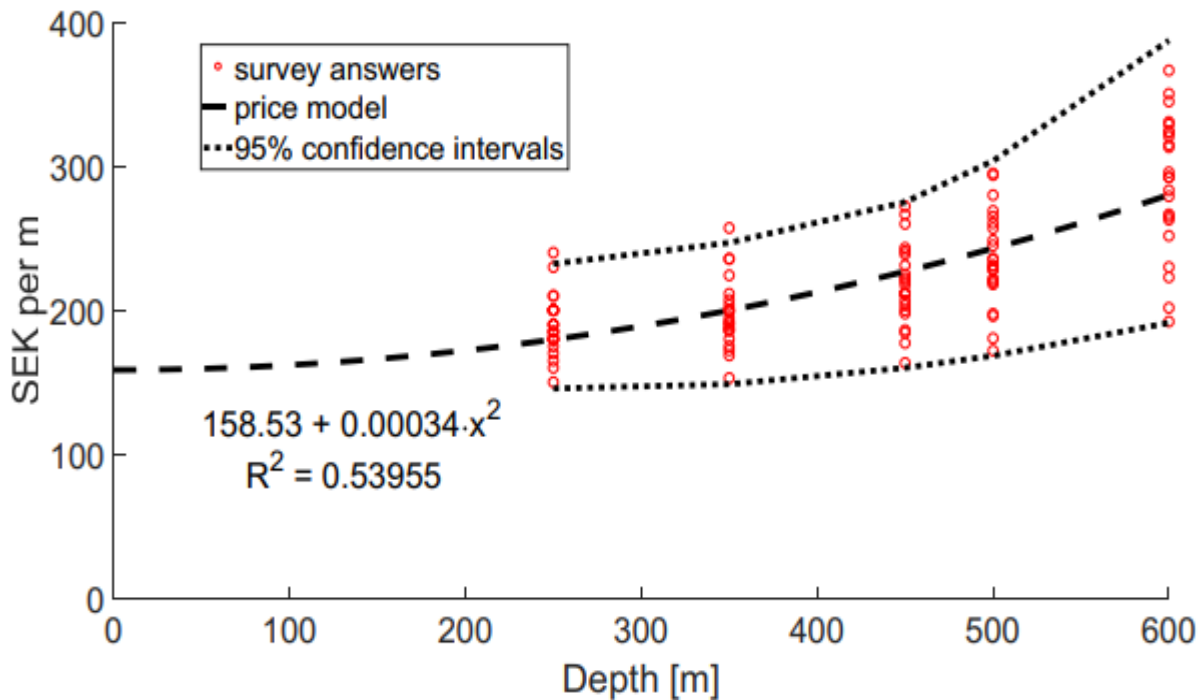


Figure 4.14. Depth-averaged drilling prices per meter for different borehole depths [55].

Considering that the borehole depths calculated for the case of Stockholm, take higher values from the range in the survey (150-250 meters of drilling depth), the final price per meter of drilling selected in the case of Sweden is 25 €/m*.

* Provisional data based on estimations.

France (Strasbourg)

According to the study by the French Association of Geothermal Professionals (2016), the geothermal market in France has a total installed capacity of 2500 MW_{th} for heating and cooling [56]. Although an increasing part of that market is formed by shallow geothermal applications, these new installations mainly feed collective housing areas, residential blocks, and offices. On the other hand,

the single housing geothermal market has decreased by 87.5% between the years 2010 to 2018, due to the vast competition with natural gas (tax credit at 30% for geothermal probes), and lack of governmental support [56]. One of the main barriers identified by the REGEOCITIES project for the shallow geothermal systems deployment in the French market is the high drilling cost [57]. On the other hand, Strasbourg is a bordering city with Germany, where the GSHP market is better developed, meaning that not only the price of drilling is more attractive but also easier to estimate thanks to the available data. Considering the above, in the case of Strasbourg, it is assumed, that the drilling services are provided by France's eastern neighbor.

For the drilling price estimation in Strasbourg, an earlier mentioned work by Blum et. al. is used. The study analyzes the German geothermal market and estimates the cost of drilling and purchasing the BHE with respect to the total length of the BHE [50]. The total borehole sizes designed for Strasbourg have an average value of about 200 meters, which according to the study would have a cost of approximately 13,000 €. Now, by simply dividing these values the price per meter is obtained (65 €/m). This, however, includes the price of the BHE, which usually corresponds to approx. 40% [55] of the total cost (BHE + drilling), thus the final drilling price used for the case of Strasbourg is 39 €/m*.

* Provisional data based on estimations.

Greece (Athens)

According to the Greek Ministry of Energy and Environment at the end of 2018, the total installed capacity of GSHPs installations was estimated to approximately 175 MW_{th}, with more than 3300 operating units. If compared with Sweden, the geothermal market in Greece is over 97% smaller, meaning that the cost of drilling must be significantly higher. However, due to the lack of available data in the case of Greece, the cost of drilling was estimated using findings from a study by Perego et. al. [51], developed within the framework of the European project Cheap-GSHP[58]. The study analyzed the feasibility of different types of geothermal probes (double-U or "Cheap-GSHP coaxial") in different locations, using techno-economic maps that represented the cost of drilling of the BHE with respect to the heating capacity in kW. One of the locations in which the techno-economic feasibility was mapped is Valencia (Spain), which similarly to Athens, is a Mediterranean city sharing comparable climate and ground composition. Additionally, the deployment of the shallow GSHP systems in Spain is similar (estimated total heating capacity of 289 MW_{th} [59]). For the double-U technology, the cost per kW installed, mapped in the coastal areas, is 1800 €/kW on average. However, if the Cheap-GSHP coaxial drilling was adopted, the savings per kW could be approximately 150 €/kW, meaning that the overall cost for drilling for 8 kW installation would be about 13200 €. Similarly, as in other cases, a total borehole size of 200 meters is considered, thus the drilling price per meter used for Athens is 66 €/m*.

* Provisional data based on estimations.

Table 4.23. Additional drilling costs related to the borehole depth increment.

Stockholm	Strasbourg	Athens
Drilling cost: 25 €/m	Drilling cost: 39 €/m	Drilling cost: 66 €/m
DG vs GLHEPro	DG vs GLHEPro	DG vs GLHEPro
277.7	205.5	160.2
<u>- 170.6</u>	<u>- 168.0</u>	<u>- 131.3</u>
107.1 m	37.5 m	28.9 m
Drilling cost:	Drilling cost:	Drilling cost:
<u>2677.5 €</u>	<u>1462.5 €</u>	<u>1907.4 €</u>
DG vs TRNSYS	DG vs TRNSYS	DG vs TRNSYS
238.0	240.0	224.0
<u>- 170.6</u>	<u>- 168.0</u>	<u>- 131.3</u>
67.4 m	72.0 m	92.7 m
Drilling cost:	Drilling cost:	Drilling cost:
<u>1685 €</u>	<u>2808 €</u>	<u>6118.2 €</u>

4.6.1.5 Energy savings vs the drilling cost

To select the most economic option among the DG, GLHEPro, and TRNSYS results, it is necessary to compare the energy savings and additional drilling cost, generated by the use of larger boreholes. Following the same principle as in sections 4.6.1.3 and 4.6.1.4, the DG results are considered as a reference case. The results regarding the additional drilling cost related to the borehole depth increment, and the electrical energy and financial savings in 25 years are represented in Table 4.23 and Table 4.22, respectively. However, the easiest way to compare these results is by establishing the profitability value for the borehole size expressed in €/m and contrasting it with the drilling cost for each city. It is done by simply verifying what are the financial savings generated in 25 years (due to lower HP consumption) per one meter of additional drilling. Table 4.24 represents the profits generated in 25 years per meter of additional drilling.

Table 4.24. The savings per meter generated in 25 years.

City	Stockholm		Strasbourg		Athens	
	DG vs GLHE	DG vs Final	DG vs GLHE	DG vs Final	DG vs GLHE	DG vs Final
Borehole drilling cost (€/m)	25		39		66	
25y Consumption savings (€)	419.2	309.9	189.3	305.6	175.8	332.6
Additional drilling depth (m)	107.1	67.4	37.5	72.0	28.9	92.7
25y Savings per meter (€/m)	3.9	4.6	5.0	4.2	6.1	3.6

Using this method, the GLHEPro and TRNSYS savings per meter (€/m) would have to be higher than the borehole drilling cost (in a given city) in order to be economically beneficial. Therefore, the lowest profitability value is the borehole drilling cost in each city. As seen in the table above, in none of the cases the 25-year savings per meter are higher than the lowest profitability value. Concluding,

for every city the increase in efficiency (corresponding to the increase in the borehole depth) is insufficient to compensate for the cost related to the additional drilling. Considering the above, the borehole sizes calculated by the Design Guide present the best economic balance among the analyzed options.

4.6.1.6 Final BHE depths selection

The techno-economic study carried out in section 4.6 proves that the borehole depths calculated using the methodology described in the DG for the plug-and-play DSHPs are well estimated. Although the outlet fluid temperatures exceeded the limits established by the DG, the analysis indicated that the percentage of the operation beyond the design fluid temperature is fairly low in the case of Stockholm and Strasbourg (2.61% and 4.74%, respectively), whereas in Athens these temperatures rarely occur. Moreover, the temperatures which are entering the heat pump are far below the evaporation and condensation temperature limits, therefore, the compressor will withstand the operational temperature regime in each city during the entire period of analysis. Finally, both the drilling cost study and the consumption analysis have indicated that drilling deeper than the Design Guide borehole size, will not provide any economic benefits during the 25 years, because the cost related to excavation of a deeper borehole is higher than the savings generated due to better efficiency of the system. Considering all the above, the total borehole sizes selected for the system energy assessment are the Design Guide depths in a field of 4 BHEs and a 2 x 2 rectangular configuration:

- Stockholm: $BHE_{STO} = 170.6$ m
- Strasbourg: $BHE_{SXB} = 168$ m
- Athens: $BHE_{ATH} = 131.3$ m

CHAPTER 5

5 The energy assessment in different locations

5.1 Introduction

In the previous chapter, the BHE depths for the three different European locations were determined and validated using the simulation results from the Dual-Source Heat Pump TRNSYS model. The results obtained from the energy simulations in each city are used for the energy analysis of the system under different climatic conditions. Previous sections 4.5.1.1 and 4.6.1.3, already included some of the aspects related to the energy assessment (the outlet fluid temperatures and the DSHP electrical consumption analysis), necessary for the proper design of the borehole depth. This chapter completes the energy assessment by analyzing these remaining segments:

- The ground thermal energy balance, using the thermal loads on the ground which includes the amount of energy extracted and injected during the operation of the system.
- The total energy production analysis, including the study of energy produced in each operating mode.
- The heat pump energy efficiency analysis in different seasons, using the SPFs calculated with the SEPOMO definitions described in section 2.2.4.

5.1.1 Methodology

The simulations for the energy assessment were executed with a time of 219000 hours (equivalent to 25 years of operation). Setting a long simulation time is a common practice for analyzing the ground loop outlet temperatures entering the heat pump [60], [61], and in a wider spectrum, for evaluating the long-term performance of the GSHP systems [62]. To take advantage of the long period of analysis, in this work, the energy performance of the DSHP will be evaluated not only in the 1st but also in the 15th and 25th years of operation. However, in this chapter, only the results for the 15th year are presented, while the results of the 1st and 25th year will be analyzed briefly in the annexes, by pointing out the differences in the system performance. Thereby, the 15th year of operation is considered as the reference case used for the comparison between the border years of the simulation. The 15th year was chosen for the analysis of this section because the actual system performance is more representative after some time of operation of the installation.

5.2 The ground energy balance

First, the ground energy balance is assessed. The DSHP can operate reversibly, for heating or cooling, which in terms of the use of ground means, that the energy is either extracted from or rejected into the ground. By comparing these two values it might be deduced if the ground temperature is

gradually (year-to-year) increasing or decreasing. The ground energy balance is a complementary analysis for the outlet temperature analysis carried out in section 4.5.1. As stated before, this section provides results for the 15th year of operation of the system, whereas the results for the first, and the last year is presented in annexes, along with the remarks regarding the differences between the analyzed years.

Table 5.1. Ground thermal balance in 15th year of the system operation.

City	Stockholm	Strasbourg	Athens
Extraction (kWh)	7922	5138	3449
Injection (kWh)	0	546	3483
Balance (kWh)	-7922	-4592	34

In the case of Stockholm and Strasbourg, the ground thermal balance is negative, meaning that in both cities there is a higher need for heating than for cooling. In fact, in the case of Stockholm the entire thermal demand corresponds to heating (Table 3.4), reflecting in lack of heat injection to the ground, whereas in Strasbourg, the ground thermal load in cooling mode is over 9 times smaller than in the heating mode. On the other hand, in Athens, the proportion between the extraction and injection is well balanced, with a slightly higher cooling load. In this regard, it is worth remarking that in Athens there was a higher demand for heating than for cooling, which may be explained in many different manners, for example, the SPF in winter mode is lower than in summer mode or that significant part of the demand is covered by the air coil during the winter. However, these aspects will be further investigated in the operating mode analysis. Before that, the temperatures leaving the ground loop in the analyzed year are summarized below, together with the number of hours when the outlet fluid exceeded the DG temperature limits.

Table 5.2. Outlet ground loop temperatures in the 15th year of analysis.

City	Stockholm	Strasbourg	Athens
Maximum temperature (°C)	8.9	13.2	29.1
Minimum temperature (°C)	-10.4	-3.7	8.6
DG temperature limits (°C)	17/-5.5	24/0	30/7
Average temperature (°C)	1.2	6.3	17.5
Hours below the DG limit (h)	138	264.8	0
Hours below the DG limit (%)	1.59	3.02	0

Additionally, as stated before, the annexes provide the comparison of the 15th year with the first and the last year of simulation.

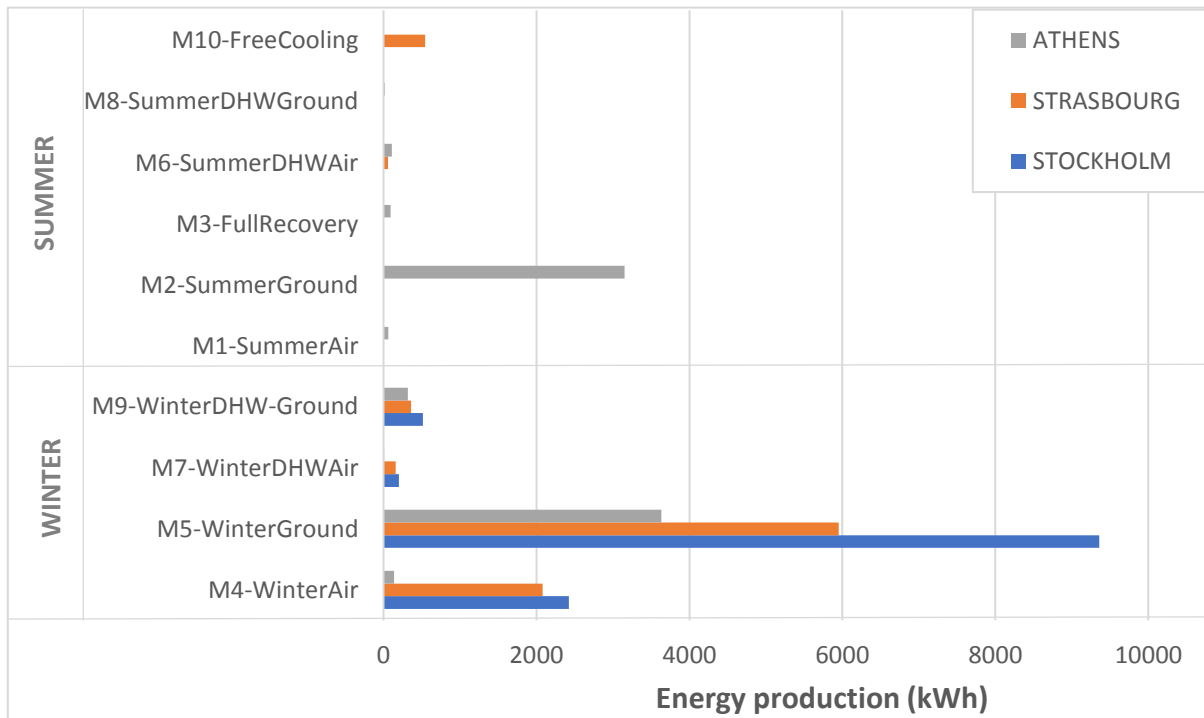
5.3 The energy production analysis

As described in section 2.2.2, the heat pump can work in 11 individual operating modes. This section intends to verify what is the proportion of usage of each mode during one year of operation (15th year of simulation). First, to verify what are the losses of the system, the total amount of energy produced by the DSHP is compared with the demands introduced to the model. Table 5.3 represents the energy demand for air-conditioning, related to the produced energy. Additionally, the last verse of the table includes the total DHW production, however, it is not possible to compare it directly with the DHW demand, as it was defined as a daily profile in l/d.

Table 5.3. Energy demand vs energy production (15th year of operation).

City	Stockholm	Strasbourg	Athens
Air-conditioning demand (kWh)	11491	8280	6827
Air-conditioning production (kWh)	11784	8579	6985
DHW production (kWh)	715	580	546

The highest energy loss through piping and thermal buffer occurs in Strasbourg reaching 3.5%, followed by Stockholm with 2.5%, whereas in Athens, only 2.3% of excess energy is produced to meet the thermal demand. Considering the DHW, it is worth remarking that the same thermal demand defines each city. The differences in DHW production between the analyzed locations result from a diversified temperature of the water entering the heat pump. In colder locations the water has a lower temperature, thus more energy will be used to heat it to maintain the required temperature in the tank. Figure 5.1 presents the share of each mode in the total energy production.

**Figure 5.1. The energy produced in different operating modes (15th year of operation).**

As indicated, the most utilized winter mode in each city is the M5-Winter Ground. It is the mode defined for heating of the offices in form of air-conditioning. The air component is not as often used for this purpose, which may be seen in the share of M4-Winter Air mode. In fact, in Athens the M4 is seldom selected by the heat pump, meaning that almost the entire air-conditioning demand in winter is covered by the borehole field. Stockholm and Strasbourg share quite similar energy production in M4-Winter Air mode, with over 2000 kWh in both cases. However, considering that in Stockholm the energy demand is for heating is over 30% higher than in Strasbourg (Table 3.4), it might be deduced that M4 has a higher share in Strasbourg's total energy production compared to Stockholm. For all cities, similar tendencies occur in the case of DHW production in winter (ground mode is preferred over air mode).

The cooling demand is defined only for Strasbourg and Athens therefore, the blue bar for Stockholm is not present in the summer modes (Figure 5.1). It may be observed that almost entire cooling production in Strasbourg corresponds to M10-Free-cooling mode, whereas in Athens to M2-Summer Ground. Some of the described tendencies can be observed in the figure below, which integrates operating modes in both the winter and summer seasons.

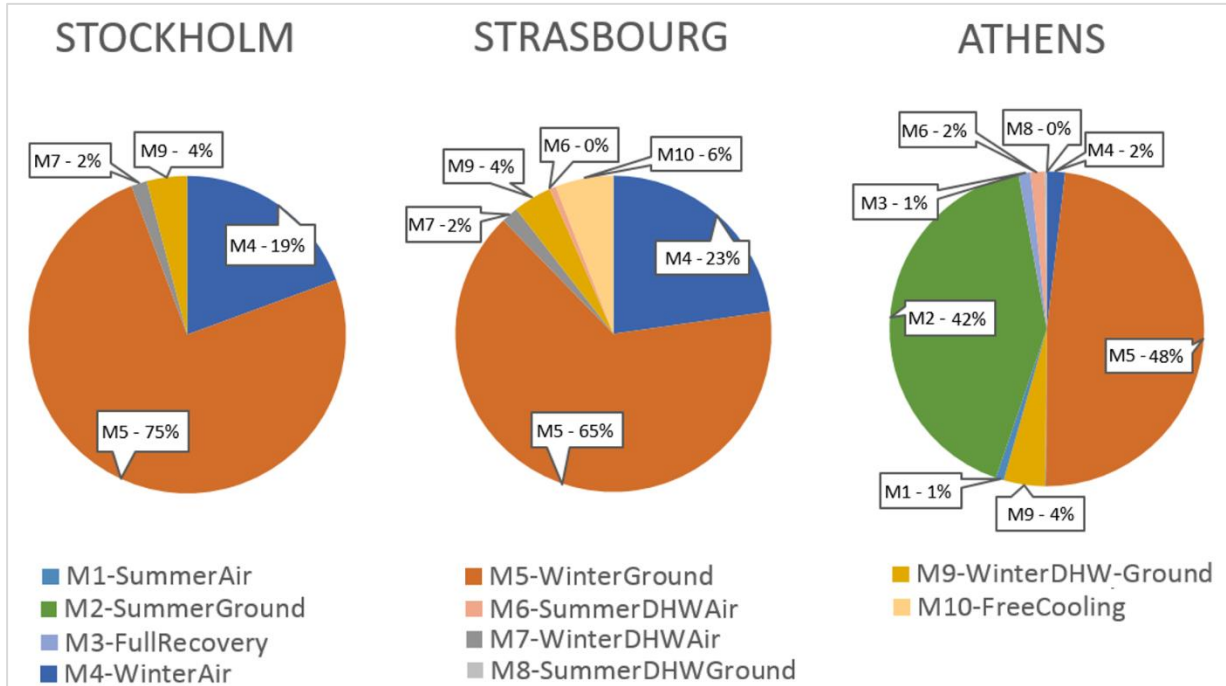


Figure 5.2. Percentage of energy production in each operating mode (year 15th).

Table 5.4. Percentage of ground and air used for each city (year 15).

City	Stockholm	Strasbourg	Athens
Ground usage (%)	79.0%	74.9%	95.8%
Air usage (%)	21.0%	25.1%	4.2%

Considering the above Stockholm and Strasbourg are locations with the most balanced share between ground and air usage. However, in every city, the ground modes are more frequently selected throughout the year. It is especially notable in Athens where ground usage corresponds to 95.8% of the total. Additionally, in this city, the ground is the most evenly shared source/sink between the two seasons. It may be observed by comparing the energy produced in modes M2-Summer Ground (green) and M5-Winter Ground (orange) with 42% and 48%, respectively. Athens owes such a well-distributed ground thermal balance to its warmer climate, where in summer the temperature of the air is higher than the ground, whereas in winter it is lower. Only in some periods like spring, where there is a small need for heating, the air temperatures might be more advantageous than the ground temperatures. However, the thermal energy demand of the building is low compared to winter and summer, thus the percentage of operation in air modes is almost negligible. Ultimately, the heat pump compares these source/sink temperatures, and mainly selects the ground as it is closer to the comfort temperature, thereby less energy is consumed.

Strasbourg is the only location where the free-cooling BPHE is used. In fact, the whole air-conditioning demand in summer is covered by the mode M10-Free-cooling. Due to the relatively short summer period and low cooling demand, the fluid coming from the ground loop can bypass the heat pump, as it is sufficiently cold (6.3°C on average) to handle the cooling demand.

The ground/air usage proportion, along with the energy produced in every mode will be compared for the remaining years (1st and 25th) in annexes in form of tables.

5.4 The energy efficiency analysis

This section of the energy assessment describes the system efficiency in the 15th year of analysis. The system efficiency is evaluated using the SPF4s for the summer and winter periods. Additionally, yearly SPF will be included. In conventional GSHPs the SPF values tend to decrease significantly during the long-term operation of the system, mainly due to the temperature degradation in the borehole surrounding caused by continuous heat extraction. However, in this reversible dual heat pump concept, the HP can not only extract/inject the heat using the ground as a thermal source/sink (providing thermal balance to the ground) but also take advantage of an additional thermal source, air, which is available to take over a part of the load. Those two aspects combined enhance the heat pump efficiency and prevent the excessive decrease of the SPF values over time. As described in section 2.2.4, SPF is the ratio between the useful heat provided by the system related to the energy consumption of the heat pump. The SPF 4 includes the consumptions of all the components of the DSHP system, thus evaluates the system performance in the most objective way.

Figure 5.3 represents the SPF4 values in the 15th year of analysis for Stockholm, Strasbourg, and Athens. First, it is important to remark on the lack of summer SPF4 for Stockholm. It is absent because only the winter season was defined. For that reason, in Stockholm, the winter SPF4 takes the same value as yearly SPF4. The remaining cities (Strasbourg and Athens) are characterized by higher summer SPF4 values and lower winter SPF4 values. The highest summer SPF4 corresponds to Athens, which is mainly due to higher return temperatures and a high proportion of ground use. In Strasbourg due to the colder climate, the summer SPF4 is 26% lower than in Athens. Additionally, Strasbourg is the only city with lower thermal conductivity compared to other locations ($2.25\text{ W/m}\cdot\text{K}$ instead of $3.75\text{ W/m}\cdot\text{K}$), which according to Tang et. al., has a significant influence on the return ground temperatures and thus, in the heat pump's performance factor [29]. It may be observed by comparing Strasbourg's and Stockholm's winter SPF4s. Stockholm has a colder climate, and higher heating demand compared to Strasbourg, yet the winter SPF4 has the same value in both cities. Again, in Athens, due to a warmer winter and more favorable return temperatures, the SPF4 is slightly higher than in the rest of the cities (7.3% of the difference).

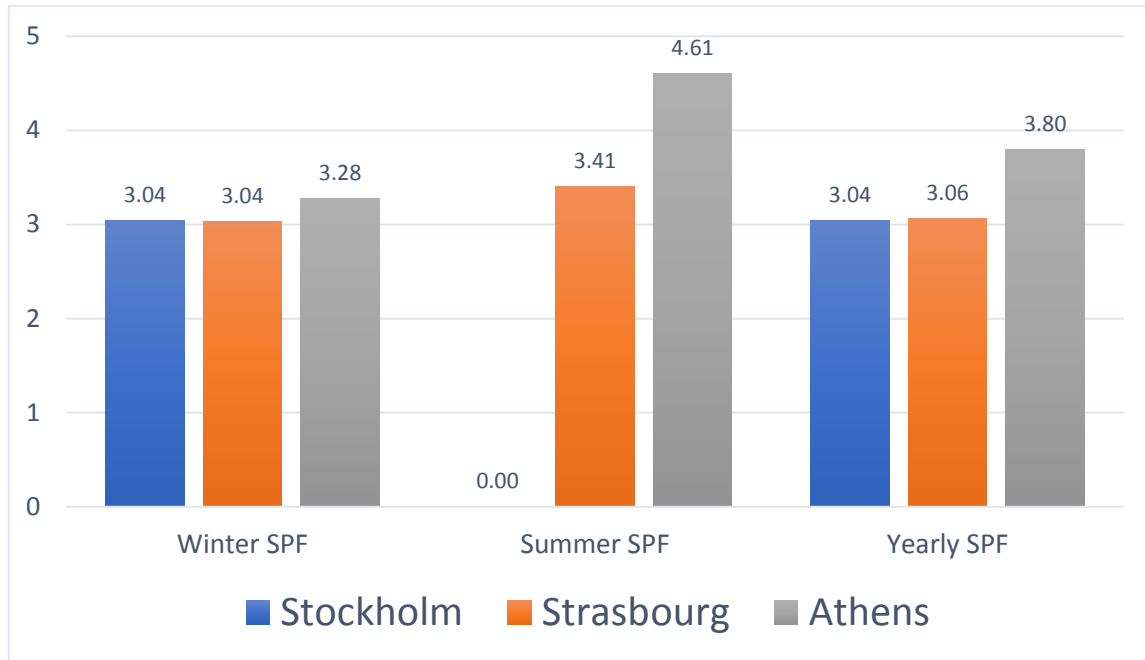


Figure 5.3. Winter, summer, and yearly SPF4 in three analyzed cities (year 15th).

Considering the high use of free cooling mode in Strasbourg the summer SPF4 in this city is surprisingly low. This can be explained by the fact that apart from the use of the free-cooling mode, additionally the DHW is produced using the air in summer, which may have a negative impact on the efficiency of the DSHP system. To further analyze this event, the summer SPF4 in Strasbourg is verified including and excluding the free cooling mode. Table 5.5 below represents the consumption of each component of the heat pump in the summer operation.

Table 5.5. Useful heat and consumption of the DSHP in summer in the 15th year (Strasbourg).

Useful heat (kWh)		Consumption of the components (kWh)				
\dot{Q}_{USER}	\dot{Q}_{DHW}	\dot{W}_{HP}	\dot{W}_{FAN}	\dot{W}_{BHE}	\dot{W}_{USER}	\dot{W}_{DHW}
545.55	59.75	148.27	4.93	16.74	7.31	0.39

To assess the SPF4 of the heat pump with and without the free cooling mode, first, the modes that provide useful heat in the summer must be identified. In the case of Strasbourg, there are only 2 modes in which the energy is produced in the summer season: M10-Free cooling, and M6-DHW Air (look Figure 5.2). In this context, the entire useful heat for the user in summer is provided with the M10-Free cooling mode, whereas the entire useful heat for the DHW is provided using the M6-DHW Air mode. Thereby using the elements identified in Table 5.5 to assess the SPF4 in summer both for the M10 and M6 modes, the following equations are used:

$$SPF4_{M10} = \frac{\dot{Q}_{USER}}{\dot{W}_{BHE} + \dot{W}_{USER}} \quad (5)$$

$$SPF4_{M6} = \frac{\dot{Q}_{DHW}}{\dot{W}_{HP} + \dot{W}_{FAN} + \dot{W}_{DHW}} \quad (6)$$

where \dot{Q} corresponds to the useful heat in the user loop and DHW loop (\dot{Q}_{USER} and \dot{Q}_{DHW} , respectively); and \dot{W} is the power consumption of each component of the system (ground loop circulation pump \dot{W}_{BHE} , user circuit circulation pump \dot{W}_{USER} , heat pump \dot{W}_{HP} , fan \dot{W}_{FAN} , DHW loop circulation pump \dot{W}_{DHW}).

Using these definitions, the SPF4s calculated for both summer operating modes (in 15th year) are as follows:

$$SPF4_{M10} = \frac{545.55}{16.74 + 7.31} = 22.69$$

$$SPF4_{M6} = \frac{59.75}{148.27 + 4.93 + 0.39} = 0.39$$

As indicated, the SPF4 of the HP for the free cooling mode is remarkably higher than the SPF4 for the DHW Air mode in summer. It is due to the high electrical energy consumption of the heat pump necessary for the DHW production during the periods when the BHE is used only for the free cooling of the offices. During these summer periods, the air temperature must be very high, and therefore the HP's compressor consumes high portions of electricity in order to satisfy the DHW demand. These two SPF4s combined result in a fairly low Strasbourg's summer SPF4 which is equal to $SPF4_{SUMMER} = 3.41$.

Lastly, if the yearly SPF4 is considered, the highest value corresponds to Athens (3.80). The winter and summer seasons have similar durations which result in a yearly SPF4 close to the mean average of the winter and summer SPF4s. In Strasbourg, the summer duration is short (less than 3 months), thus the summer SPF4 has a low impact on the yearly efficiency factor of the DSHP.

Overall, the values of the SPF4 presented in Figure 5.3 are not as high as the efficiencies of the commercially available heat pumps. This topic has been previously mentioned in the work by Cazorla-Marín [37], where the unoptimized compressor was identified as the major factor limiting the heat pump's efficiency.

Additionally, although the SPF4 value is higher in Athens than in Strasbourg and Stockholm, it is mainly due to a warmer climate where the use of the ground is predominant (>95%). For that reason, hybridizing the ground with the air might not be the most beneficial solution for warm climatologies, like Athens, where the air coil does not operate during most of the year. On the other hand, in colder climates (Stockholm, Strasbourg) the air component is more frequently used (over 20%), which may lead to a significant borehole size reduction, and thus decrease the investment cost. Additionally, further cost reduction may be achieved by implementing the free-cooling BPHE which is more recommended in cold/moderate climates, where during the summer the ground temperature is sufficiently cold to cover the cooling needs of the building.

Apart from the ground thermal balance and the energy production long-term analysis, annex A also includes the long-term efficiency assessment of the heat pump using the SPF4s calculated for the first and the last years of the simulation. One of the outcomes of the long-term SPF4 analysis (annex A.1) is that the DSHP has the ability to maintain efficiency during the 25 years of operation. A slight degradation in the SPF4 over the years is related to the decrease in the heat extraction from the ground, and increased proportion in the air use (annex A.1). In terms of source control optimization, the results of the SPF4 for the first year of the system operation will be used for the analysis of the last chapter, where different source control parameters are tested to enhance the system performance.

CHAPTER 6

6 The source control optimization

6.1 Introduction

The following chapter analyzes the different source control parameters used to optimize the performance of the DSHP. As described in section 2.2.3, the principle of the selection of the thermal source or sink relies on the current season (heating or cooling) and the source/sink temperature (of the air and ground). Depending on a given season, the heat pump compares the air and the ground temperatures, selecting the most favorable. A method used to prevent the HP from alternating between the two sources too frequently is the hysteresis band which establishes the upper and lower temperature limits (with respect to the ground temperature) in which the selected source is maintained until it crosses the limit. Following the methodology adopted in earlier studies [34], [37], in this master thesis the hysteresis band used for the source control in all the previous simulations (which were carried out to select the most optimal BHE size for all locations) was ± 2 K. However, different deadband values may likely be more adequate for the source control in one location or another. To verify the above, the source control optimization consists of a parametric study where different hysteresis bands are used. Additionally, the analysis involves different offsets adopted to the hysteresis band. Thereby, the parametric study comprises another parameter that might bias the controller of the heat pump towards selecting one source or another. Ultimately, as different parameters of the source control affect the rate of the “ground/air” use, they should likewise influence the heat pump consumptions and thereby, in the system efficiency.

6.1.1 Methodology

In contrast to the analyses from the previous chapters, source control optimization does not include a long-term approach. Instead, the energy simulations are carried out for 1 year (8760 hours), which is sufficient for assessing the heat pump operation in different seasons.

While the same DSHP system model developed in TRNSYS is used for the analysis, a small improvement is adopted in the HP control macro (look Table 2.2), facilitating the simulation process. In brief, the adopted feature allows to easily test the different offsets by simply changing the value of a parameter (offset or hysteresis band) in the Control Cards (a section in TRNSYS mainly used for setting simulation time and different constants in the model).

Three different values for the hysteresis band are tested (± 1 K; ± 2 K and ± 3 K) for each city. Additionally, for each value of the hysteresis band 5 different offsets are examined (-2K; -1K; 0K; 1K and 2K), where the negative offsets prioritize the use of the air and positive offsets prioritize the use of the ground. Considering the above a total of 45 simulations (15 per location) are executed.

To select the set of parameters that best enhances the heat pump operation in a given city the following items are compared:

- Rate of ground/air use (for summer and winter seasons).
- The winter, summer, and yearly SPF4.

6.2 The optimization methods

6.2.1 Using different hysteresis bands

As described before, three different hysteresis bands are tested ($\pm 1 - 3$ K). Figure 6.1 depicts the principle of source selection according to the different deadband values.

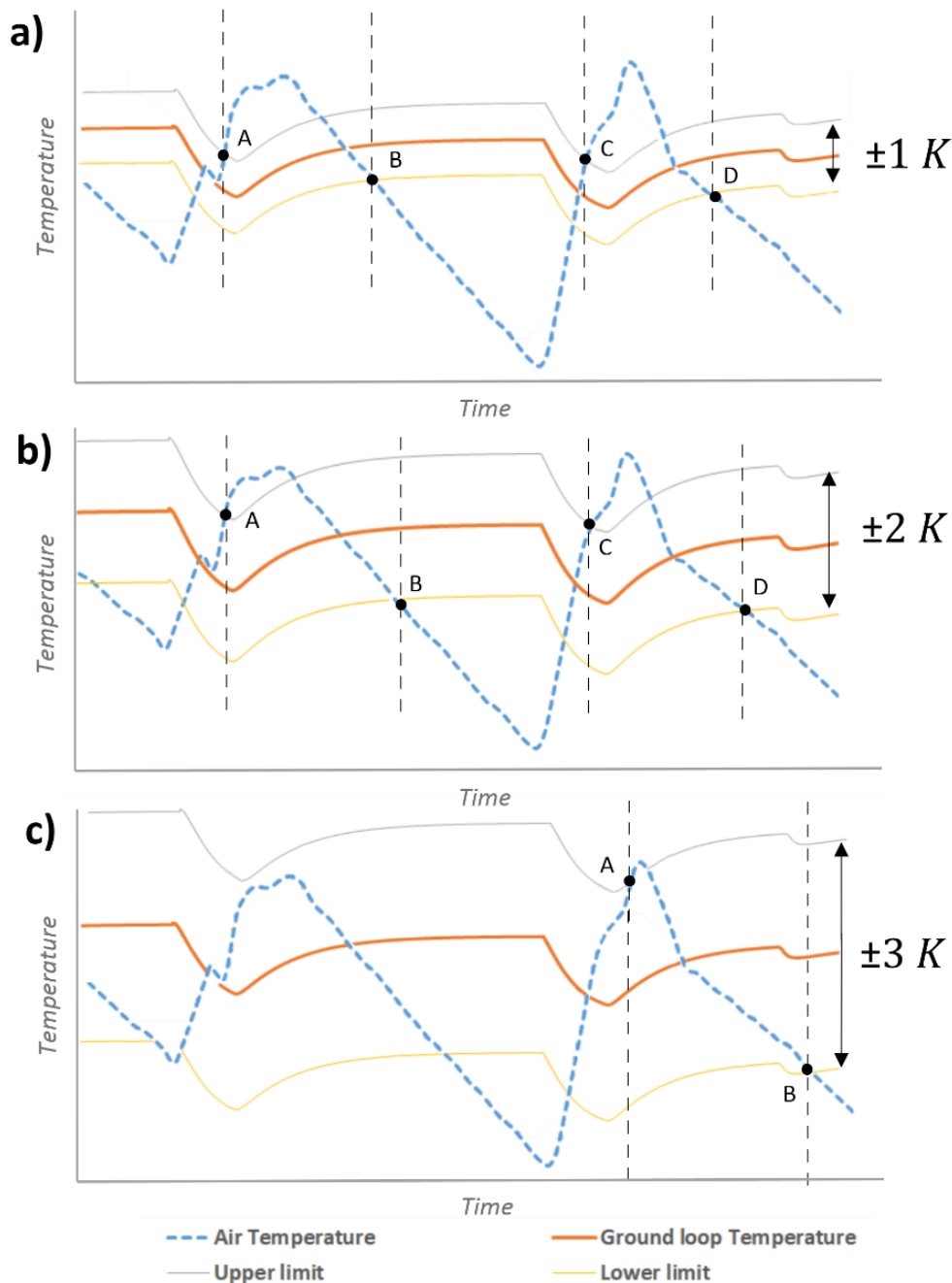


Figure 6.1. Deadbands used for the source control analysis: a) ± 1 K; b) ± 2 K; c) ± 3 K.

The hysteresis band used for the source selection is adopted to the ground loop fluid temperature, as it is more stable throughout the year. The smaller the deadband, the narrower the temperature range in which the given source withholds, meaning that the heat pump alternates between the sources more frequently. Ideally, the best system efficiency with the DSHP model should be reached without implementing the hysteresis band, allowing the HP's controller to respond more accurately to the changes in the source temperature. On the other hand, setting upper and lower temperature limits prevents too frequent source switching and thus, has a positive impact on the heat exchangers in the refrigeration circuit. In order to allow for the change of the source, the compressor has to reduce the speed to the minimum which leads to a certain efficiency loss. In this context, various deadbands are tested, to compare the differences in the system efficiency and verify the sensitivity of this parameter.

Figure 6.1 a), b) and c) represent the same distribution of ground and air temperatures. The only difference between these graphs is the upper and lower temperature limit. Assuming that the heat pump operates in the winter season (heating), it will select the source with the higher temperature. If Figure 6.1 a) is considered, the air is selected by the controller between points A and B. Once the ambient temperature goes below the lower deadband limit (point B) the heat pump switches to the ground thermal source. The air is selected again when the ambient temperature crosses the upper deadband limit (point C).

In Figure 6.1 b) a different $\pm 2\text{K}$ deadband is selected. Comparing the two graphs a certain delay in the source selection can be observed (especially in points B and D). It is of course due to the use of a wider hysteresis band which allows for a longer operation with the selected source.

The last c) graph represents a source control where a $\pm 3\text{K}$ deadband is used. As indicated, the source is now switched only in A and B points which are considerably shifted towards the right-hand side. In heating, the air would be now selected between points A and B, whereas before point A, the ground would serve as a thermal source.

It is worth remarking that for a cooling operation, the controller of the heat pump obeys the opposite rule of the source selection, meaning that the source with a lower temperature is preferred.

6.2.2 Testing different offsets

The next parameter used for the parametric analysis is the offset of the hysteresis band. The offset does not influence the range of the deadband, only shifts it towards higher or lower temperature. There are 5 tested offsets: -2K, -1K, 0K, 1K, and 2K (negative offsets prioritize the air and positive offsets prioritize the ground). Each offset is checked for every selected hysteresis band, which gives 15 simulations per city (45 in total). Figure 6.2 represents the principle of adopting an offset to a deadband.

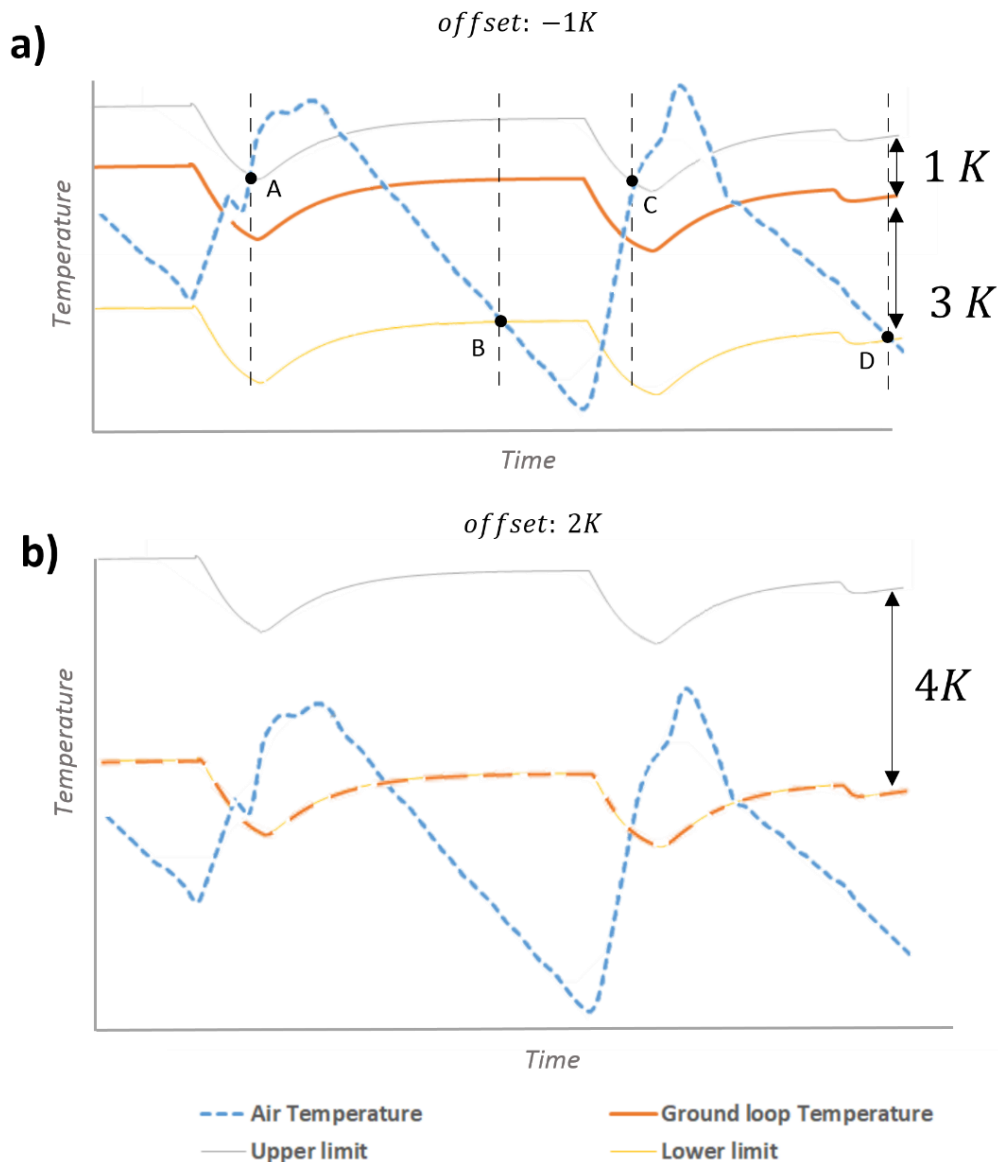


Figure 6.2. Two different offsets adopted to a $\pm 2K$ deadband: a) offset $-1K$, b) offset $2K$.

Both offsets shown in Figure 6.2 are adopted to a $\pm 2K$ hysteresis band (or a $4K$ hysteresis band). Using these two examples it can be seen how different offsets can influence the selection of the thermal source/sink. In the first graph (a) the deadband is shifted by an offset of $-1K$. The source is changed 4 times as the air temperature intersects four times with the lower and upper limits of the deadband. On the other hand, if (b) graph is considered the selected offset is $2K$, thus the ground loop temperature is now the lower limit of the hysteresis band. In this example, during the represented period there would not be a single change of the source. It is because the blue line (air temperature) would have to cross both the lower and the upper limits of the hysteresis band to switch to the air source. In practice, considering graph (b) and assuming the operation in heating mode, the heat pump would only use the ground throughout that period. On the other hand, in cooling, during the whole period, it would only select the air. The given examples indicate how impactful can be the use of different offsets, especially in shifting the proportion of the ground/air use.

6.3 Results of the analysis

As stated before, the parametric study includes a total of 45 simulations. Each simulation is executed for 8760 hours (entire year), using a time step of 1 minute (the result is printed in each minute). The set of parameters that best enhances the heat pump operation in a given city will be selected by analyzing and comparing the following aspects:

- Rate of ground/air use (for summer and winter seasons).
- The winter, summer, and yearly SPF4.

The energy assessment was carried out (section 5) using a deadband of $\pm 2\text{K}$, and an 0K offset, therefore the same set of source control parameters is considered a reference case for comparing the results.

6.3.1 Stockholm

Stockholm is the only city where the cooling demand is not defined. Thereby, the winter SPF4 takes the same values as the yearly SPF4, whereas the summer SPF4 and source use in summer is not considered. The reference case (deadband of $\Delta T_g = \pm 2\text{K}$, and an 0K offset) is presented in the middle row of Table 6.1. It is the only row where the SPF4 is given using the original (unitless) value of the Seasonal Performance Factor 4. The differences in SPF4 between other tested deadbands and offsets are shown in form of an efficiency gain (positive values) or loss (negative values) which are calculated with respect to the reference case.

Table 6.1. Efficiency gains and the rate of ground/air use for both seasons in Stockholm.

STOCKHOLM							
ΔT_g (K)	Offset (K)	Efficiency gain or loss ($\pm\%$)			Source use (%)		
		Winter SPF4	Summer SPF4	Yearly SPF4	Ground/air winter (%)	Ground/air summer (%)	Ground/air yearly (%)
± 1	-2	+0.11%	-	+0.11%	75/25	-	75/25
	-1	+0.06%	-	+0.06%	76/24	-	76/24
	0	+0.01%	-	+0.01%	77/23	-	77/23
	1	-0.08%	-	-0.08%	80/20	-	80/20
	2	-0.23%	-	-0.23%	82/18	-	82/18
± 2	-2	+0.09%	-	+0.09%	75/25	-	75/25
	-1	+0.07%	-	+0.07%	76/24	-	76/24
	0	3.149	-	3.149	77/23	-	77/23
	1	-0.12%	-	-0.12%	79/21	-	79/21
	2	-0.15%	-	-0.15%	80/20	-	80/20
± 3	-2	+0.09%	-	+0.09%	75/25	-	75/25
	-1	+0.07%	-	+0.07%	76/24	-	76/24
	0	+0.01%	-	+0.01%	77/23	-	77/23
	1	-0.07%	-	-0.07%	79/21	-	79/21
	2	-0.15%	-	-0.15%	80/20	-	80/20

The general remarks regarding Stockholm's results are presented below:

- The best results are obtained for $\Delta T_g = \pm 1\text{K}$ and offset -2K (air prioritized), where the efficiency gain is 0.11% compared to the reference case.
- For all ΔT_g values used in the analysis, better results are obtained for negative offsets.
- For the positive offsets, the higher the offset the lower the efficiency. The rule applies to every considered hysteresis band (2K the lowest SPF4, 0K medium SPF4, -2K the highest SPF4).
- For the negative offsets, the higher the offset the higher the use of the air source. Moreover, better efficiency is reached when the air is used at a higher percentage.
- For the different hysteresis bands, when no offset is adopted, the results are practically the same for each value of the tested deadband (for the SPF there is a 0.01% difference, while the ground/air use remains the same).

6.3.2 Strasbourg

Similarly, the efficiency gain and the percentage of source use is assessed in Strasbourg for the different hysteresis bands (ΔT_g) and offsets.

Table 6.2. Efficiency gains and the rate of ground/air use for both seasons in Strasbourg.

STRASBOURG							
ΔT_g (K)	Offset (K)	Efficiency gain or loss ($\pm\%$)			Source use (%)		
		Winter SPF4	Summer SPF4	Yearly SPF4	Ground/air winter (%)	Ground/air summer (%)	Ground/air yearly (%)
± 1	-2	+0.09%	+0.10%	+0.09%	70/30	92/8	72/28
	-1	+0.12%	+0.02%	+0.11%	74/26	91/9	75/25
	0	+0.13%	+0.04%	+0.12%	77/23	90/10	78/22
	1	+0.07%	-0.06%	+0.07%	81/19	90/10	82/18
	2	-0.04%	-0.04%	-0.04%	84/16	90/10	84/16
± 2	-2	-0.00%	+0.08%	+0.00%	70/30	91/9	71/29
	-1	+0.04%	+0.05%	+0.04%	74/26	90/10	76/24
	0	3.138	3.467	3.158	78/22	90/10	79/21
	1	-0.09%	-0.41%	-0.11%	82/18	90/10	82/18
	2	-0.21%	-0.13%	-0.21%	85/15	90/10	85/15
± 3	-2	-0.02%	-0.05%	-0.02%	69/31	90/10	71/29
	-1	-0.02%	+0.14%	-0.01%	74/26	90/10	75/25
	0	-0.14%	+0.03%	-0.13%	79/21	90/10	80/20
	1	-0.26%	-0.03%	-0.24%	83/17	90/10	83/17
	2	-0.39%	+0.01%	-0.37%	86/14	90/10	86/14

The general remarks regarding Strasbourg's results are presented below:

- The best results are obtained for $\Delta T_g = \pm 1\text{K}$ and offset 0K, where the yearly SPF4 is 0.12% higher compared to the reference case.
- For $\Delta T_g = \pm 3\text{K}$ none of the offsets would enhance the yearly SPF4 value.

- The two parameters combined have a relatively small sensitivity in terms of yearly SPF4 (maximum efficiency gain is 0.12% and the maximum loss is 0.37%).
- The more negative the offset the higher the air use, however it does not always translate to higher SPF4 values.
- In terms of the source use, changes in the analyzed parameters mainly influence the winter ground/air balance, without much impact on the summer ground/air proportion.

6.3.3 Athens

Similar to the analysis from previous sections the same sets of parameters are tested for Athens, while the reference case is presented in the middle row of the table.

Table 6.3. Efficiency gains and the rate of ground/air use for both seasons in Athens.

ATHENS							
ΔT_g (K)	Offset (K)	Efficiency gain or loss ($\pm\%$)			Source use (%)		
		Winter SPF4	Summer SPF4	Yearly SPF4	Ground/air winter (%)	Ground/air summer (%)	Ground/air yearly (%)
± 1	-2	-0.54%	-0.09%	-0.38%	86/14	94/6	90/10
	-1	-0.27%	-0.40%	-0.32%	91/9	95/5	93/7
	0	-0.01%	+0.34%	+0.12%	95/5	96/4	95/5
	1	+0.11%	+0.55%	+0.27%	97/3	96/4	97/3
	2	+0.17%	+0.64%	+0.34%	99/1	96/4	97/3
± 2	-2	-0.48%	-0.44%	-0.47%	88/12	93/7	90/10
	-1	-0.18%	-0.12%	-0.16%	93/7	94/6	94/6
	0	3.243	4.826	3.830	96/4	95/5	96/4
	1	+0.11%	-1.01%	-0.31%	98/2	96/4	97/3
	2	+0.17%	+0.58%	-0.32%	99/1	96/4	98/2
± 3	-2	-0.36%	-2.88%	-1.33%	92/8	92/8	92/8
	-1	-0.09%	-1.54%	-0.64%	96/4	94/6	95/5
	0	+0.04%	+0.40%	+0.17%	97/3	95/5	96/4
	1	+0.13%	+0.54%	+0.28%	99/1	96/4	97/3
	2	+0.18%	+0.45%	+0.28%	99/1	96/4	98/2

The general remarks regarding Strasbourg's results are presented below:

- The best results are obtained for $\Delta T_g = \pm 1K$ and offset 2K (ground prioritized), where the yearly SPF4 is 0.34% higher compared to the reference case. In this configuration, the summer SPF4 is 0.64% higher than the reference.
- The highest efficiency loss is observed for $\Delta T_g = \pm 3$ and an offset of -2K, were (compared to the reference case) the yearly SPF4 is 1.33% lower, while the summer SPF4 even 2.88% lower.
- For positive offsets, the higher it is the higher the efficiency in general, which also translates to an increment in the use of the ground as a thermal source.

- The tested sets of parameters influence more in the summer SPF4 than in the winter SPF4. Additionally, different sets of parameters have a higher impact on winter ground/air use balance than in summer ground/air proportion.
- Using negative offsets in winter significantly shifts the ground/air use balance towards more frequent air selection.

6.4 Discussion of results

First, the overall sensitivity of the optimization method in the values of the SPF4 is evaluated. The overall sensitivity is considered the sum of maximum efficiency gain and maximum efficiency loss, where both are absolute values. In this context, the overall sensitivity of the optimization method is treated as a total impact of varying the source control parameters on the SPF4 values. Figure 6.3 represents the sensitivity of the optimization method on the SPF4, with respect to the reference case (deadband of $\Delta T_g = \pm 2K$, and an 0K offset) in each city.

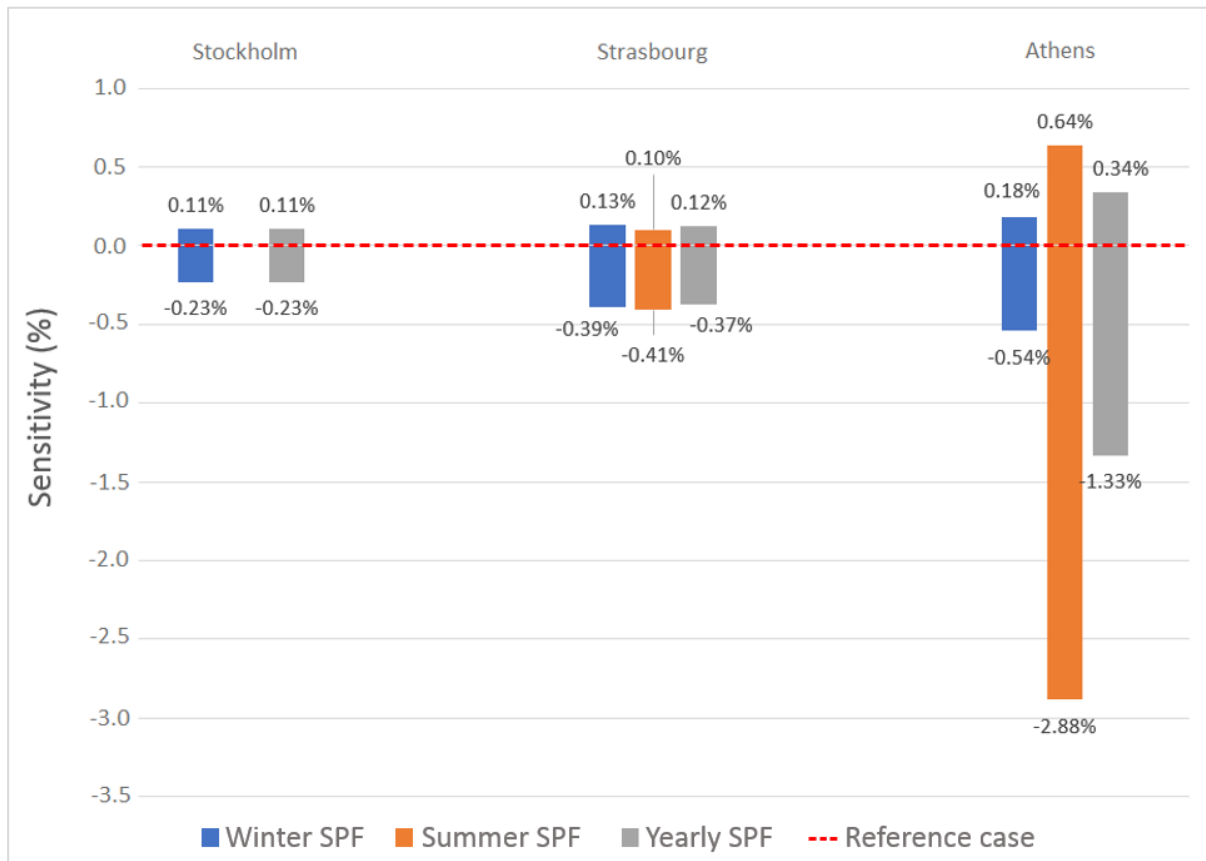


Figure 6.3. The sensitivity of the optimization method on the SPF4, with respect to the reference case in each city (overall sensitivity is the sum of efficiency gain and efficiency loss, both in absolute values).

In general, the highest overall sensitivity is observed in Athens, where using different sets of parameters has a total impact of 3.52% on the summer SPF4, 0.72% on the winter SPF4, and 1.67% on the yearly SPF4. Athens is the city, where combining different deadbands and offsets may result in the highest efficiency gains (+0.64% in the case of summer SPF4), but also the highest efficiency loss (-2.88% also in the case of summer SPF4). Strasbourg and Stockholm present lower sensitivity to change

in the optimization parameters. In these cities, the different source control parameters influenced the yearly SPF4 values by only 0.49% and 0.34%, respectively.

For each city, the hysteresis band for which the best results are achieved is $\Delta T_g = \pm 1\text{K}$. Nevertheless, the offset that best enhances the efficiency of the heat pump is different in every location (-2K in Stockholm, 0K in Strasbourg, and 2K in Athens). In general, the impact of the source control optimization method in increasing the efficiency of the DSHP is very small. If these deadbands and offsets were used, on a scale of one year the maximum consumption savings in Stockholm, Strasbourg, and Athens would correspond to 4.6 kWh (0.11%), 3.6 kWh (0.12%), and 7 kWh (0.34%), respectively. Using the same electricity costs as defined in Table 4.22, the economic savings in the scale of one year would correspond to 0.8€ in Stockholm, 0.7€ in Strasbourg, and 1.1€ in Athens, which is a negligible financial benefit.

On the other hand, choosing different deadbands and offsets has a significant impact on shifting the proportion between the use of ground and air as the thermal source. For example, in Stockholm, applying negative offsets favors the use of the air, additionally increasing the efficiency of the heat pump. In Strasbourg and Athens similar tendency occurs – the more negative the offset the higher the air use – however, it does not always translate to higher SPF4 values, especially in Athens, where during most of the year the ground has a more favorable temperature than the ambient, thus using the air as a thermal source in Athens leads to lower efficiency.

The results present higher sensitivity to change in the optimization parameters when the source use is considered. In the case of the yearly ground/air balance, the use of the two sources might be shifted by a total of 5% in Stockholm, 14% in Strasbourg, and 8% in Athens. In the case of Stockholm and Strasbourg, it is more recommended to shift the source towards selecting the air, as it has a positive or neutral impact on the efficiency, but it may significantly reduce the size of the BHE. On the other hand, in Athens, it is not recommended to shift the heat pump towards selecting the air as it harms the efficiency of the heat pump.

The fact that prioritizing the air in Stockholm leads to higher efficiency, whereas in Athens to the lower, is related to the difference between the ground thermal balance in the two cities. Stockholm is a city with continuous heat extraction, thus prioritizing the air enhances the heat pump's efficiency because less heat is extracted from the ground. In this way, the ground temperatures decrease at a lower degree, thus more favorable ground temperatures are conserved for the periods when the air is colder. Athens is a contrasting city to Stockholm, where the balance between heat extraction and injection is shared at the same proportion. This fairly shared ground thermal balance has a positive effect on maintaining the ground temperature during the year, which leads to higher SPF4 values for when the ground use is prioritized.

CHAPTER 7

7 Conclusions

The present master thesis was a complementary investigation for the studies developed in the framework of the GEOTECH project, mainly focused on the optimal design of the borehole field for the Dual Source Heat Pump system in three different European locations. The European cities selected to represent the distinctive climate types defined in the European regulation EU Reg. 811/2013 (average, colder, and warmer conditions) were Strasbourg, Stockholm, and Athens, respectively. The methodology developed for the design of the BHE field was based on GEOTECH's Deliverable 4.9, which determines the guidelines for the design and selection of the required length of the BHE for DSHP systems. To verify the calculations from the D4.9 and to determine the most adequate configuration of the BHE field an iterative process was followed using GLHEPro software. Finally, the optimal configuration and size of the BHE were determined using a TRNSYS model developed in the framework of the GEOTECH project, validating the Deliverable 4.9 calculations. The final borehole sizes were used for the long-term energy performance assessment where the energy production and efficiency of the system were evaluated. In the last stage of the master thesis, the control system of the DSHP was optimized by carrying out an analysis where two parameters responsible for the source selection were modified (hysteresis band and offset).

Concerning the design of the BHE field, the Design Guide for the plug and play systems (D4.9) proved to be a good instrument for the design and selection of the BHE size. Although the return ground fluid periodically exceeded the allowed temperature limit, it occurred in a very low proportion in the case of Stockholm and Strasbourg (2.61% and 4.74%, respectively), whereas in Athens these temperatures were rarely encountered (only several hours in the frame of 25 years). Moreover, examining the cost-effectiveness of the alternative BHE sizes which consisted of a detailed electrical energy consumption analysis, followed by a drilling cost study explicitly pointed out towards using shorter BHEs; the energy savings would have to be from 6 to 18 times higher in order to compensate the additional drilling costs. In this context, it is worth remarking that the main objective of the D4.9 was to derive simple tools and methods to minimize the complexity of the design. Using simple instructions contained in the Design Guide has its limitations, as the entire process of the BHE design comes down to the application of several correction factors. Considering the above, the plug-and-play packaged solution comes at the price of a slight result divergence if compared with a highly precise tool such as the DSHP model in TRNSYS.

Regarding the energy assessment in different cities, although the yearly SPF_s of the DSHP were not as attractive (SPF_{STO} = 3.04, SPF_{SXB} = 3.06, SPF_{ATH} = 3.80), and fairly low if compared to

the commercially available GSHPs, the DSHP developed in the GEOTECH project is still a prototype and at the time of its construction, the available compressor was still not optimized for the used refrigerant (R32), which explains the lower efficiency. On the other hand, the long-term SPF4 analysis indicated only a slight variation in the SPF4 values, meaning that the DSHP system can maintain efficiency throughout the years. Regarding the dual-source concept, hybridizing the ground with the air was found to be most beneficial in colder climates (Stockholm, Strasbourg) where the ground/air use ratio (in %) was more balanced; approximately 75/20 in Stockholm and Strasbourg vs 95/5 in Athens. Such a fairly shared use of two thermal sources can lead to a significant borehole size reduction, and thus decrease the investment cost. Additionally, further cost reduction may be achieved by implementing the free-cooling BPHE which according to the energy production analysis is more recommended in moderate climates (the only city where the free cooling mode was used was Strasbourg), where during the summer the ground temperature is sufficiently cold to cover the cooling needs of the building.

With regard to the source control optimization, the parametric study comprised of 45 TRNSYS simulations did not present a significant potential for increasing the HP's efficiency (maximum yearly SPF4 gain observed in Athens was +0.34%). On the other hand, it was found that the source control optimization method has a greater impact on shifting the proportion of the ground/air use. In a cold climate (Stockholm) where the heat is continuously extracted from the ground, it is more recommended to shift the source towards selecting the air (using positive offsets), as it can lead to the BHE size reduction and additionally, may have a positive impact on the HP's efficiency. In warm climates with a balanced proportion between the extraction and injection (Athens), shifting the source selection control towards prioritizing the air is not recommended, as it has a negative impact on the efficiency of the heat pump.

This study proved the Deliverable 4.9, a simple and user-friendly design guide, to be a good and effective tool for the design of the BHE size for the DSHP installations. Although as seen in this master thesis, the cost of the drilling of the BHE is still elevated, the key component necessary for its reduction will be the pace of the deployment of these systems in the market, where such simple, plug-and-play packaged solutions will play an important role in shaping its future. In addition, considering the great potential of the DSHP and GSHP technologies for the reduction of the environmental costs related to the heating, cooling, and DHW, the EU and state member policies should further promote their use, guaranteeing further deployment of the shallow geothermal applications in the market.

REFERENCES

- [1] Intergovernmental Panel on Climate Change, "Climate Change 2014: Synthesis Report," Geneva, Switzerland, 2014. [Online]. Available: https://www.ipcc.ch/site/assets/uploads/2018/02/SYR_AR5_FINAL_full.pdf.
- [2] Intergovernmental Panel on Climate Change, "Climate change 2007 Synthesis Report," 2007. [Online]. Available: https://www.ipcc.ch/site/assets/uploads/2018/02/ar4_syr_full_report.pdf.
- [3] Intergovernmental Panel on Climate Change, "Global Warming of 1.5°C. Chapter 1: Framing and Context," 2018. [Online]. Available: https://www.ipcc.ch/site/assets/uploads/sites/2/2019/05/SR15_Chapter1_Low_Res.pdf.
- [4] European Commission, "Energy efficiency targets," 2020. https://ec.europa.eu/energy/topics/energy-efficiency/targets-directive-and-rules/eu-targets-energy-efficiency_en.
- [5] International Energy Agency, "World Energy Outlook 2020: Overview and key findings," 2020. <https://www.iea.org/reports/world-energy-outlook-2020/overview-and-key-findings#abstract>.
- [6] European Parliament and The Council, "Directive 2018/2002/EU," *Off. J. Eur. Union*, vol. 328, p. L 328/211, 2018, [Online]. Available: <https://eur-lex.europa.eu/legal-content/EN/TXT/PDF/?uri=CELEX:32018L2002&from=EN>.
- [7] International Energy Agency, "Total final consumption (TFC) by sector, World 1990-2018." 2020, [Online]. Available: <https://www.iea.org/data-and-statistics>.
- [8] European Commission, "Energy consumption and use by households." 2020, [Online]. Available: <https://ec.europa.eu/eurostat/web/products-eurostat-news/-/DDN-20200626-1>.
- [9] IEEE European Public Policy Committee, "Heating and Cooling Future of Europe and Interactions with Electricity," p. 2, 2018, [Online]. Available: https://www.ieee.org/content/dam/ieee-org/ieee/web/org/about/heating_and_cooling_future_of_europe_25_january_2018.pdf.
- [10] European Commission, "EnE-HVAC – a comprehensive approach to HVAC system efficiency," *SETIS Magazine*, 2016. <https://setis.ec.europa.eu/publications/setis-magazine/low-carbon-heating-cooling/ene-hvac—comprehensive-approach-hvac-system>.
- [11] European Commission, "Horizon 2020 programme." <https://ec.europa.eu/programmes/horizon2020/en/what-horizon-2020>.
- [12] A. Kujbus *et al.*, "Strategic research innovation agenda for geothermal technologies," Brussels, 2020. [Online]. Available: <https://www.rhc-platform.org/content/uploads/2020/09/Geothermal-SRIA-2020-v.3-FINAL.pdf>.
- [13] European Commission, "Geothermal Technology for Economic Cooling and Heating (H2020-LCE-2014-2, GEOTECH-656889)," 2015. <http://www.geotech-project.eu/>.

-
- [14] European Geothermal Energy Council, "Geothermal Market Report 2015," 2016. [Online]. Available: <https://www.egec.org/wp-content/uploads/2017/05/EGEC-market-report-preview-version.pdf>.
- [15] European Geothermal Energy Council, "Geothermal Market Report 2019 Key Findings," 2020. [Online]. Available: https://www.egec.org/wp-content/uploads/2020/06/MR19_KeyFindings_new-cover.pdf.
- [16] P. Christodoulides, L. Aresti, and G. Florides, "Air-conditioning of a typical house in moderate climates with Ground Source Heat Pumps and cost comparison with Air Source Heat Pumps," *Appl. Therm. Eng.*, vol. 158, pp. 1–6, Jul. 2019, doi: 10.1016/j.applthermaleng.2019.113772.
- [17] F. Alshehri, S. Beck, D. Ingham, L. Ma, and M. Pourkashanian, "Techno-economic analysis of ground and air source heat pumps in hot dry climates," *J. Build. Eng.*, vol. 26, pp. 1–9, 2019, doi: 10.1016/j.jobe.2019.100825.
- [18] P. Farzanehkhameh, M. Soltani, F. M. Kashkooli, and M. Ziabasharhagh, "Optimization and energy-economic assessment of a geothermal heat pump system," *Renew. Sustain. Energy Rev.*, vol. 133, pp. 1–15, 2020, doi: 10.1016/j.rser.2020.110282.
- [19] I. Grossi, M. Dongellini, A. Piazzini, and G. L. Morini, "Dynamic modelling and energy performance analysis of an innovative dual-source heat pump system," *Appl. Therm. Eng.*, 2018, doi: 10.1016/j.applthermaleng.2018.07.022.
- [20] S. Marinelli, F. Lolli, M. A. Butturi, B. Rimini, and R. Gamberini, "Environmental performance analysis of a dual-source heat pump system," *Energy Build.*, vol. 223, pp. 4–13, 2020, doi: 10.1016/j.enbuild.2020.110180.
- [21] S. Rayegan, S. Motaghian, G. Heidarinejad, H. Pasdarshahri, P. Ahmadi, and M. A. Rosen, "Dynamic simulation and multi-objective optimization of a solar-assisted desiccant cooling system integrated with ground source renewable energy," *Appl. Therm. Eng.*, vol. 173, 2020, doi: 10.1016/j.applthermaleng.2020.115210.
- [22] S. Kaviani, C. Aghanajafi, J. H. Mosleh, A. Nazari, and A. Nazari, "Exergy, economic and environmental evaluation of an optimized hybrid photovoltaic-geothermal heat pump system," *Appl. Energy*, vol. 279, pp. 1–14, 2020, doi: 10.1016/j.apenergy.2020.115469.
- [23] R. Lazzarin and M. Noro, "Photovoltaic/Thermal (PV/T)/ground dual source heat pump: Optimum energy and economic sizing based on performance analysis," *Energy Build.*, vol. 211, 2020, doi: 10.1016/j.enbuild.2020.109800.
- [24] M. Abu-Rumman, M. Hamdan, and O. Ayadi, "Performance enhancement of a photovoltaic thermal (PVT) and groundsource heat pump system," *Geothermics*, vol. 85, 2020, doi: 10.1016/j.geothermics.2020.101809.
- [25] R. Lazzarin, "Heat pumps and solar energy: A review with some insights in the future," *Int. J. Refrig.*, vol. 116, pp. 146–159, 2020, doi: 10.1016/j.ijrefrig.2020.03.031.
- [26] A. G. Olabi, M. Mahmoud, B. Soudan, T. Wilberforce, and M. Ramadan, "Geothermal based hybrid energy systems, toward eco-friendly energy approaches," *Renew. Energy*, vol. 147, pp. 2003–2012, 2020, doi: 10.1016/j.renene.2019.09.140.
- [27] D. Qi, L. Pu, Z. Ma, L. Xia, and Y. Li, "Effects of ground heat exchangers with different connection configurations on the heating performance of GSHP systems," *Geothermics*, vol. 80, p. 22, 2019, doi: 10.1016/j.geothermics.2019.02.002.
- [28] P. Hein, O. Kolditz, U. J. Görke, A. Bucher, and H. Shao, "A numerical study on the sustainability

- and efficiency of borehole heat exchanger coupled ground source heat pump systems,” *Appl. Therm. Eng.*, 2016, doi: 10.1016/j.applthermaleng.2016.02.039.
- [29] F. Tang and H. Nowamooz, “Factors influencing the performance of shallow Borehole Heat Exchanger,” *Energy Convers. Manag.*, vol. 181, pp. 581–582, 2019, doi: 10.1016/j.enconman.2018.12.044.
- [30] M. Rivoire, A. Casasso, B. Piga, and R. Sethi, “Assessment of energetic, economic and environmental performance of ground-coupled heat pumps,” *Energies*, 2018, doi: 10.3390/en11081941.
- [31] G. R. Aditya, O. Mikhaylova, G. A. Narsilio, and I. W. Johnston, “Comparative costs of ground source heat pump systems against other forms of heating and cooling for different climatic conditions,” *Sustain. Energy Technol. Assessments*, vol. 42, 2020, doi: 10.1016/j.seta.2020.100824.
- [32] J. M. Corberán, A. Cazorla-Marín, J. Marchante-Avellaneda, and C. Montagud, “Dual source heat pump, a high efficiency and cost-effective alternative for heating, cooling and DHW production,” *Int. J. Low-Carbon Technol.*, 2018, doi: 10.1093/ijlct/cty008.
- [33] A. Cazorla-Marin, C. Montagud, J. M. Corberán, and J. Marchante-Avellaneda, “TRNSYS modelling and energy assessment of a dual source heat pump system,” in *IX Congreso Ibérico y VII Congreso Iberoamericano de Ciencias y Técnicas del Frío - CYTEF2018, 2018*, 2018.
- [34] A. Cazorla-Marin, C. Montagud, J. M. Corberán, and J. Marchante-Avellaneda, “Seasonal performance assessment of a Dual Source Heat Pump system for heating, cooling and domestic hot water production,” in *IGSHPA Research Track 2018*, 2018, pp. 180–188.
- [35] A. Cazorla-Marín, C. Montagud-Montalvá, F. Tinti, and J. M. Corberán, “A novel TRNSYS type of a coaxial borehole heat exchanger for both short and mid term simulations: B2G model,” *Appl. Therm. Eng.*, vol. 164, 2020, doi: 10.1016/j.applthermaleng.2019.114500.
- [36] A. Cazorla-Marin, C. Meeng, C. Montagud, and J. M. Corberán, “Energy assessment and optimization of a dual source heat pump system located in Amsterdam,” *CYTEF 2020 – X Congr. Ibérico | VIII Congr. Iberoam. las Ciencias y Técnicas del Frío*, pp. 1–7, 2020.
- [37] A. Cazorla Marín, “Modelling and Experimental Validation of an Innovative Coaxial Helical Borehole Heat Exchanger for a Dual Source Heat Pump System,” no. June, 2019, [Online]. Available: <https://riunet.upv.es/handle/10251/125696>.
- [38] GEOTECH, “Deliverable 4.9 Plug & Play system design, selection and installation guidelines,” 2018.
- [39] J. Marchante-Avellaneda, J. M. Corberán, A. Cazorla-Marín, and C. Montagud-Montalvá, “Diseño y ensayos de puesta a punto de una bomba de calor de 8 kW con foco de calor dual: aerotermia y geotermia,” pp. 19–21, 2017.
- [40] SEPAMO-Build, “SEasonal PERformance factor and MOnitoring for Heat Pump Systems in the Building Sector. (IEE/08/776/SI2.529222),” 2012. .
- [41] Meteotest, “Meteonorm,” 1981, [Online]. Available: <https://meteonorm.com/>.
- [42] M. Gwadera, B. Larwa, and K. Kupiec, “Undisturbed ground temperature-Different methods of determination,” *Sustain.*, 2017, doi: 10.3390/su9112055.
- [43] F. Tinti, S. Kasmaee, M. Elkarmoty, S. Bonduà, and V. Bortolotti, “Suitability evaluation of specific shallow geothermal technologies using a GIS-Based multi criteria decision analysis implementing the analytic hierarchic process,” *Energies*, 2018, doi: 10.3390/en11020457.

- [44] European Comission, "GeoCool 'Geothermal Heat Pump for Cooling and Heating along European coastal Areas,'" 2003, [Online]. Available: <https://cordis.europa.eu/project/id/13548>.
- [45] Intelligent Energy Europe, "TABULA (Typology Approach for Building Stock Energy Assessment)," 2009, [Online]. Available: <https://episcopes.eu/iee-project/tabula/>.
- [46] Intelligent Energy Europe, "TABULA WebTool," 2009, [Online]. Available: <https://webtool.building-typology.eu>.
- [47] Conrad, "Drill rig Boxer 200." [Online]. Available: https://conrad-stanen.nl/assets/pdf/boxer_200_EN.pdf.
- [48] P. Eskilson, "Thermal Analysis of Heat Extraction Boreholes," University of Lund, 1987.
- [49] Eurostat, "Electricity price statistics," 2021. https://ec.europa.eu/eurostat/statistics-explained/index.php?title=Electricity_price_statistics.
- [50] P. Blum, G. Campillo, and T. Kölbl, "Techno-economic and spatial analysis of vertical ground source heat pump systems in Germany," *Energy*, 2011, doi: 10.1016/j.energy.2011.02.044.
- [51] R. Perego *et al.*, "Economic, geological and technical potential mapping test for GSHP systems in Europe," no. June, p. 10, 2019.
- [52] S. Gehlin and O. Andersson, "Geothermal Energy Use, Country Update for Sweden," *Media.Geoenergicentrum.Se*, 2019.
- [53] World Energy Council, "World Energy Resources: Geothermal," in *Energy resources in New Mexico: oil and gas, coal, electrical generation, uranium, and geothermal energy, (New Mexico Energy & Minerals Department, Santa Fe, Energy & Minerals Department)*, 2013.
- [54] O. Andersson, S. Gehlin, and J.-E. Rosberg, "Country Update for Sweden," *Proc. World Geotherm. Congr.*, 2020.
- [55] W. Mazzotti, J. Acuña, A. Lazzarotto, and B. Palm, "Deep Boreholes for Ground-Source Heat Pump - Effsys Expand Final Report," 2018.
- [56] C. Boissavy, R. Vernier, and P. Laplaige, "Geothermal Energy Use, Country Update for France," *Eur. Geotherm. Congr. 2019*, p. 18, 2019.
- [57] J. Florence *et al.*, "Overview of shallow geothermal legislation in Europe," no. D2.2 General Report of the current situation of the regulative framework for the SGE systems, p. 50, 2013, [Online]. Available: <http://regeocities.eu/wp-content/uploads/2012/12/D2.2.pdf>.
- [58] European Comission, "Cheap-GSHP Project." <https://cheap-gshp.eu/> (accessed Jun. 05, 2021).
- [59] A. Iñigo, M. De Gregorio, C. De Santiago, C. García de la Noceda, P. Perez, and J. F. Urchueguia, "Geothermal Energy Use, Country Update for Spain," *Eur. Geotherm. Congr.*, p. 9, 2019, [Online]. Available: <https://europeangeothermalcongress.eu/wp-content/uploads/2019/07/CUR-27-Spain.pdf>.
- [60] S. Javed, "Design of ground source heat pump systems - Thermal modelling and evaluation of boreholes," *Chalmers Univ. Technol.*, 2010, [Online]. Available: <http://publications.lib.chalmers.se/records/fulltext/122101/122101.pdf>.
- [61] J. A. Pérez, "Understanding numerically generated g-functions: A study case for a 6x6 borehole field," p. 63, 2013.
- [62] E. Mands, M. Sauer, E. Grundmann, and B. Sanner, "Optimisation of industrial size cold production from a ground source heat pump plant using borehole heat exchangers," *Eur. Geotherm. Congr. 2013*, pp. 1–6, 2013.

ANNEXES

A. Long-term energy assessment

This annex describes the long-term energy performance of the DSHP, analyzing the same segments as in section 5. Results are presented for years 1, 15, and 25. The differences are briefly summarized in form of bullet points.

A.1 Ground thermal balance and outlet temperatures

Stockholm

Table A. 1. Long-term outlet temperature and thermal balance results in Stockholm.

OUTLET FLUID TEMPERATURES			
Year	1st	15th	25th
Maximum temperature (°C)	9.8	8.9	7.5
Minimum temperature (°C)	-7.3	-10.4	-10.7
DG temperature limits (°C)	17/-5.5		
Average temperature (°C)	2.7	1.2	1.0
Hours below the DG limit (h)	33	138	162
Hours below the DG limit (%)	0.38	1.59	1.85
GROUND THERMAL BALANCE			
Extraction (kWh)	8082	7922	7672
Injection (kWh)	0	0	0
Balance (kWh)	-8082	-7922	-7672
AIR VS. GROUND USAGE			
Ground usage (%)	80.0	79.0	76.4
Air usage (%)	20.0	21.0	23.6

Observations:

- Both peak and average temperatures decrease over time.
- Between the 1st and 15th years, the minimum fluid temperature decreases at a higher rate than between the 15th and 25th years (the temperatures tend to stabilize with time). The maximum temperature decreases gradually, at a similar annual proportion.

- Between the 1st and 15th years the heat extraction from the ground decreases at a slower rate than between years 15 and 25, which is caused by less favorable return temperatures. As a result, the air is used at a higher proportion which is observed in the last part of Table A. 1 (where the use of the air as a ground source increased by 3.6% during the 25 years).

Strasbourg

Table A. 2. Long-term outlet temperature and thermal balance results in Strasbourg.

OUTLET FLUID TEMPERATURES			
Year	1 st	15 th	25 th
Maximum temperature (°C)	14.1	13.2	12.2
Minimum temperature (°C)	-1.9	-3.7	-4.0
DG temperature limits (°C)	24/0		
Average temperature (°C)	7.8	6.3	6.1
Hours below the DG limit (h)	36.2	264.8	312.0
Hours below the DG limit (%)	0.41	3.02	3.56
GROUND THERMAL BALANCE			
Extraction (kWh)	5470	5138	5028
Injection (kWh)	553	546	567
Balance (kWh)	-4917	-4592	-4462
AIR VS. GROUND USAGE			
Ground usage (%)	78.6	74.9	73.6
Air usage (%)	21.4	25.1	26.4

- Regarding the outlet fluid temperatures, the same tendencies occur as for Stockholm.
- The difference between the heat extraction and injection is decreasing over time (9% in the 25 years), improving the thermal balance of the ground. In small part, it is caused by the increase in the heat injection (in 25th year 14 kWh more are injected compared to the 1st year levels), however mainly it occurs due to the increment in the air usage (5% between year 1 and 25).

Athens

Table A. 3. Long-term outlet temperature and thermal balance results in Athens.

OUTLET FLUID TEMPERATURES			
Year	1 st	15 th	25 th
Maximum temperature (°C)	29.1	29.1	29.0
Minimum temperature (°C)	8.5	8.6	8.4
DG temperature limits (°C)	30/7		
Average temperature (°C)	17.6	17.5	17.5
Hours below the DG limit (h)	0	0	0
Hours below the DG limit (%)	0	0	0
GROUND THERMAL BALANCE			
Extraction (kWh)	3459	3449	3298
Injection (kWh)	3476	3483	3454
Balance (kWh)	17	34	156
AIR VS. GROUND USAGE			
Ground usage (%)	95.8	95.8	93.0
Air usage (%)	4.2	4.2	7.0

- The outlet fluid temperatures have very similar values in each analyzed year, which is caused by a fairly shared extraction/injection rate.
- Both the ground thermal balance and the air/ground usage proportion is maintained in the first and 15th year, whereas in the last year of analysis the heat extraction in the winter season is lower by around 4.5% causing the overall increment in the air usage (2.8% approx.).

A.2 Energy production in different operating modes

Table A. 4. The energy produced (in kWh) in summer and winter modes for 3 different cities.

City		STOCKHOLM			STRASBOURG			ATHENS		
Year		1 st	15 th	25 th	1 st	15 th	25 th	1 st	15 th	25 th
Winter	M4-Air	2306	2425	2737	1778	2082	2200	141	140	319
	M5-Ground	9486	9359	9058	6259	5951	5829	3635	3632	3470
	M7-DHWAir	200	202	212	131	158	167	7	7	17
	M9-DHWGround	521	513	501	395	362	352	325	320	305
Summer	M1-Air	0	0	0	0	0	0	66	62	79
	M2-Ground	0	0	0	0	0	0	3146	3151	3124
	M3-FullRecovery	0	0	0	0	0	0	95	93	89
	M6-DHWAir	0	0	0	56	60	57	100	108	113
	M8-DHWGround	0	0	0	0	0	0	21	17	17
	M10-FreeCooling	0	0	0	553	546	567	0	0	0
Total (kWh)		12513	12499	12508	9173	9159	9171	7536	7531	7534

- Most of the energy is produced in the winter M3-Air and winter M5-Ground modes. Additionally, the main differences in the energy production between the analyzed years occur for these two modes, which means that they have the greatest impact on the rate of the air/ground source use.
- Interestingly, although the energy production in summer M2-Ground mode is significant, less fluctuation in the energy production is observed between the analyzed years (less impact in the proportion between the use of the air and ground).

A.3 The long-term SPF4 analysis

Table A. 5. SPF4 values calculated for different cities in each analyzed year.

STOCKHOLM			
Year	1st	15th	25th
Winter SPF	3.09	3.04	3.05
Summer SPF	-	-	-
Yearly SPF	3.09	3.04	3.05
STRASBOURG			
Winter SPF	3.10	3.04	3.05
Summer SPF	3.46	3.41	3.43
Yearly SPF	3.12	3.06	3.07
ATHENS			
Winter SPF	3.28	3.28	3.29
Summer SPF	4.62	4.61	4.59
Yearly SPF	3.80	3.80	3.79

- If the first and the last year's SPF4 values are compared, the smallest differences in yearly SPF4 occur in Athens (less than 0.3%), whereas the biggest in Stockholm and Strasbourg (1.3% and 1.6%, respectively).
- Overall, the SPF4 results for different cities indicate that the DSHP presents the ability to maintain system efficiency.

